

*Midwest States' Regional Pooled Fund Research Program
Fiscal Year 1999-2000 (Year 10)
Research Project Number SPR-3(017)
NDOR Sponsoring Agency Code RFPF-00-04*

NCHRP 350 DEVELOPMENT AND TESTING OF A GUARDRAIL CONNECTION TO LOW-FILL CULVERTS

Submitted by

Karla A. Polivka, M.S.M.E., E.I.T.
Research Associate Engineer

Dean L. Sicking, Ph.D., P.E.
Professor and MwRSF Director

John D. Reid, Ph.D.
Associate Professor

Ronald K. Faller, Ph.D., P.E.
Research Assistant Professor

John R. Rohde, Ph.D., P.E.
Associate Professor

James C. Holloway, M.S.C.E., E.I.T.
Research Associate Engineer

MIDWEST ROADSIDE SAFETY FACILITY

University of Nebraska-Lincoln
1901 "Y" Street, Building "C"
Lincoln, Nebraska 68588-0601
(402) 472-6864

Submitted to

MIDWEST STATES' REGIONAL POOLED FUND PROGRAM

Nebraska Department of Roads
1500 Nebraska Highway 2
Lincoln, Nebraska 68502

MwRSF Research Report No. TRP-03-114-02

November 1, 2002

Technical Report Documentation Page

1. Report No. SPR-3(017)	2.	3. Recipient's Accession No.	
4. Title and Subtitle NCHRP 350 Development and Testing of a Guardrail Connection to Low-Fill Culverts		5. Report Date November 1, 2002	
		6.	
7. Author(s) Polivka, K.A., Faller, R.K., Sicking, D.L., Rohde, J.R., Reid, J.D., and Holloway, J.C.		8. Performing Organization Report No. TRP-03-114-02	
9. Performing Organization Name and Address Midwest Roadside Safety Facility (MwRSF) University of Nebraska-Lincoln 1901 Y St., Bldg. C Lincoln, NE 68588-0601		10. Project/Task/Work Unit No.	
		11. Contract © or Grant (G) No. SPR-3(017)	
12. Sponsoring Organization Name and Address Midwest States' Regional Pooled Fund Program Nebraska Department of Roads 1500 Nebraska Highway 2 Lincoln, Nebraska 68502		13. Type of Report and Period Covered Final Report 1999-2002	
		14. Sponsoring Agency Code RPFP-00-04	
15. Supplementary Notes Prepared in cooperation with U.S. Department of Transportation, Federal Highway Administration			
16. Abstract (Limit: 200 words) A W-beam guardrail system was developed for installation with the steel posts attached to the top of a low-fill concrete culvert. The guardrail system was constructed with a 2.66-mm (12-gauge) thick W-beam rail totaling 53.34 m in length. The W-beam rail was supported by twenty-four W152x13.4 by 1,829-mm long steel posts and thirteen W152x13.4 by 946-mm long steel posts. The post spacing was 1,905-mm on center for post nos. 1 through 9 and 33 through 41, while the post spacing for post nos. 9 through 33 was 952.5-mm on center. Two full-scale vehicle crash tests, using ¾-ton pickup trucks, were performed on the W-beam guardrail system. One test was successfully conducted on the guardrail system with the backside of the posts positioned 457 mm from the front face of the culvert's headwall. The second test was unsuccessfully performed on the guardrail system with the backside of the posts positioned 25 mm from the front face of the headwall. The tests were conducted and reported in accordance with the requirements specified in the National Cooperative Highway Research Program (NCHRP) Report No. 350, <i>Recommended Procedures for the Safety Performance Evaluation of Highway Features</i> . The safety performance of the W-beam guardrail system attached to the top of a low-fill concrete culvert was determined to be acceptable according to the Test Level 3 (TL-3) evaluation criteria specified in NCHRP Report No. 350. From an analysis of the crash test results, it is recommended that the backside face of the steel posts can be positioned a minimum of 254 mm away from the front face of the culvert's headwall and still maintain acceptable barrier performance.			
17. Document Analysis/Descriptors Highway Safety, Guardrail, Longitudinal Barrier, Box Culvert, Roadside Appurtenances, Crash Test, Compliance Test		18. Availability Statement No restrictions. Document available from: National Technical Information Services, Springfield, Virginia 22161	
19. Security Class (this report) Unclassified	20. Security Class (this page) Unclassified	21. No. of Pages 205	22. Price

DISCLAIMER STATEMENT

The contents of this report reflect the views of the authors who are responsible for the facts and the accuracy of the data presented herein. The contents do not necessarily reflect the official views nor policies of the State Highway Departments participating in the Midwest States' Regional Pooled Fund Research Program nor the Federal Highway Administration. This report does not constitute a standard, specification, or regulation.

ACKNOWLEDGMENTS

The authors wish to acknowledge several sources that made a contribution to this project: (1) the Midwest States' Regional Pooled Fund Program funded by the Connecticut Department of Transportation, Iowa Department of Transportation, Kansas Department of Transportation, Minnesota Department of Transportation, Missouri Department of Transportation, Montana Department of Transportation, Nebraska Department of Roads, Ohio Department of Transportation, South Dakota Department of Transportation, Texas Department of Transportation, and Wisconsin Department of Transportation for sponsoring this project and (2) MwRSF personnel for constructing the barrier and conducting the crash tests.

A special thanks is also given to the following individuals who made a contribution to the completion of this research project.

Midwest Roadside Safety Facility

E.A. Keller, B.S.M.E., Research Associate Engineer
K.H. Addink, B.S.C.E., Research Associate Engineer
R.W. Bielenberg, M.S.M.E., Research Associate Engineer
K.L. Krenk, B.S.M.A., Shop Manager
A.T. Russell, Laboratory Mechanic II
M.L. Hanau, Laboratory Mechanic I
G.L. Schmutte, Laboratory Mechanic I
Undergraduate and Graduate Assistants

Connecticut Department of Transportation

Dionysia Oliveira, Transportation Engineer 3

Iowa Department of Transportation

David Little, P.E., Assistant District Engineer
Will Stein, P.E., Design Methods Engineer

Kansas Department of Transportation

Ron Seitz, P.E., Road Design Squad Leader
Rod Lacy, P.E., Road Design Leader

Minnesota Department of Transportation

Jim Klessig, Implementation Liaison
Mohammad Dehdashti, P.E., Design Standards Engineer
Ron Cassellius, Former Research Program Coordinator
Andrew Halverson, P.E., Former Assistant Design Standards Engineer

Missouri Department of Transportation

Daniel Smith, P.E., Research and Development Engineer

Montana Department of Transportation

Susan Sillick, Research Bureau Chief

Nebraska Department of Roads

Leona Kolbet, Research Coordinator
Mark Traynowicz, P.E., Transportation Planning Manager
Phil Tenhulzen, P.E., Design Standards Engineer

Ohio Department of Transportation

Monique Evans, P.E., Administrator
Dean Focke, Roadway Safety Engineer

South Dakota Department of Transportation

David Huft, Research Engineer
Bernie Clocksin, Lead Project Engineer
Kelly VanDeWiele, P.E., Road Design Engineer

Texas Department of Transportation

Mark Bloschock, P.E., Supervising Design Engineer
Mark Marek, P.E., Design Engineer

Wisconsin Department of Transportation

Peter Amakobe, Standards Development Engineer
William Anderson, P.E., Standards Development Engineer
Beth Cannestra, P.E., Chief in Roadway Development

Federal Highway Administration

John Perry, P.E., Nebraska Division Office
Frank Rich, P.E., Nebraska Division Office

Dunlap Photography

James Dunlap, President and Owner

TABLE OF CONTENTS

	Page
TECHNICAL REPORT DOCUMENTATION PAGE	i
DISCLAIMER STATEMENT	ii
ACKNOWLEDGMENTS	iii
TABLE OF CONTENTS	vi
List of Figures	ix
List of Tables	xiii
1 INTRODUCTION	1
1.1 Problem Statement	1
1.2 Objective	2
1.3 Scope	2
2 LITERATURE REVIEW	4
3 TEST REQUIREMENTS AND EVALUATION CRITERIA	7
3.1 Test Requirements	7
3.2 Evaluation Criteria	7
4 TEST CONDITIONS	10
4.1 Test Facility	10
4.2 Vehicle Tow and Guidance System	10
4.3 Test Vehicles	10
4.4 Data Acquisition Systems	13
4.4.1 Accelerometers	13
4.4.2 Rate Transducers	18
4.4.3 High-Speed Photography	18
4.4.4 Pressure Tape Switches	20
5 GENERAL DESIGN CONSIDERATIONS	23
5.1 Culvert Geometry	23
5.2 Depth of Soil Fill	24
5.3 Guardrail Post Attachments and Locations	25
6 TEST SITE PREPARATION	26
6.1 Culvert Construction	26
6.1.1 Test Pit	26
6.1.2 Culvert Substructure	26
6.1.3 Culvert Top Slab and Curb	28

7 DEVELOPMENT OF POST-TO-CULVERT SLAB ATTACHMENT	43
7.1 Design Considerations	43
8 DYNAMIC POST TESTING	45
8.1 Test Matrix	45
8.2 Test Conditions	46
8.2.1 Bogie Vehicle	46
8.2.2 Bogie Tow and Guidance System	46
8.2.3 Post Installation Procedure	49
8.2.4 Data Acquisition Systems	49
8.2.4.1 Accelerometer	49
8.2.4.2 High-Speed Photography	50
8.2.4.3 Pressure Tape Switches	50
8.3 Test Results	51
9 COMPUTER SIMULATION	59
9.1 Background	59
9.2 Design Alternatives	60
9.3 Barrier VII Results	61
10 W-BEAM GUARDRAIL SYSTEM DESIGN DETAILS (OPTION NO. 1)	64
11 CRASH TEST NO. 1 (OPTION NO. 1)	75
11.1 Test KC-1	75
11.2 Test Description	75
11.3 Barrier Damage	77
11.4 Vehicle Damage	78
11.5 Occupant Risk Values	79
11.6 Discussion	79
12 W-BEAM GUARDRAIL SYSTEM DESIGN DETAILS (OPTION NO. 2)	107
13 CRASH TEST NO. 2 (OPTION NO. 2)	116
13.1 Test KC-2	116
13.2 Test Description	116
13.3 Barrier Damage	117
13.4 Vehicle Damage	119
13.5 Occupant Risk Values	119
13.6 Discussion	120
14 SUMMARY AND CONCLUSIONS	140
15 RECOMMENDATIONS	142

16 REFERENCES	143
17 APPENDICES	145
APPENDIX A - Bogie Vehicle Design and Fabrication Details	146
APPENDIX B - Force-Deflection Behavior of Bogie Tests	151
APPENDIX C - BARRIER VII Computer Models	159
APPENDIX D - Typical BARRIER VII Input File	163
APPENDIX E - Occupant Compartment Deformation Data, Test KC-1	174
APPENDIX F - Accelerometer Data Analysis, Test KC-1	176
APPENDIX G - Rate Transducer Data Analysis, Test KC-1	183
APPENDIX H - Occupant Compartment Deformation Data, Test KC-2	185
APPENDIX I - Accelerometer Data Analysis, Test KC-2	187
APPENDIX J - Rate Transducer Data Analysis, Test KC-2	194
APPENDIX K - Accelerometer Data Analysis Comparison, Tests KC-1 and KC-2 ..	196
APPENDIX L - Rate Transducer Data Analysis Comparison, Tests KC-1 and KC-2 ..	204

List of Figures

	Page
1. Test Vehicle, Test KC-1	11
2. Vehicle Dimensions, Test KC-1	12
3. Test Vehicle, Test KC-2	14
4. Vehicle Dimensions, Test KC-2	15
5. Vehicle Target Locations, Test KC-1	16
6. Vehicle Target Locations, Test KC-2	17
7. Location of High-Speed Cameras, Test KC-1	21
8. Location of High-Speed Cameras, Test KC-2	22
9. Concrete Culvert Substructure Details	30
10. Concrete Culvert Substructure Details - Outside Culvert Wall	31
11. Concrete Culvert Substructure Details - Inside Culvert Wall	32
12. Concrete Culvert Substructure Details - Soil Retaining Wall For Test Purposes Only	33
13. Concrete Culvert Top Slab and Curb Details – Plan, End, and Side Views	34
14. Concrete Culvert Top Slab and Curb Details - Side View	35
15. Concrete Culvert Top Slab and Curb Details - End View	36
16. Concrete Culvert Top Slab and Curb Details - Plan View	37
17. Concrete Culvert Steel Reinforcement Details	38
18. Concrete Culvert Walls and Top Slab Formwork	39
19. Concrete Culvert Top Slab Formwork (continued)	40
20. Concrete Culvert Curb Construction	41
21. Concrete Culvert Substructures, Top Slab, and Curb	42
22. Large Bogie Design Details	47
23. Large Bogie Vehicle	48
24. Post and Plate Damage, Bogie Test KCB-1b	52
25. Post and Plate Damage, Bogie Test KCB-2	53
26. Post and Plate Damage, Bogie Test KCB-3	54
27. Post and Plate Damage, Bogie Test KCB-4	55
28. Post and Plate Damage, Bogie Test KCB-5	56
29. Post and Plate Damage, Bogie Test KCB-6	57
30. Post and Plate Damage, Bogie Test KCB-7	58
31. W-Beam Guardrail Attached to a Low-Fill Culvert (Option No. 1)	66
32. W-Beam Guardrail Attached to a Low-Fill Culvert Post Nos. 15 through 27 (Option No. 1)	67
33. W-Beam Guardrail Attached to a Low-Fill Culvert (Option No. 1)	68
34. W-Beam Guardrail Attached to a Low-Fill Culvert (Option No. 1)	69
35. W-Beam Guardrail Attached to a Low-Fill Culvert (Option No. 1)	70
36. W-Beam Guardrail Attached to a Low-Fill Culvert (Option No. 1)	71
37. Typical Post for W-Beam Guardrail Attached to a Low-Fill Culvert (Option No. 1)	72
38. Steel Post Connection Details on Bottom Side of Culvert's Top Slab	73
39. End Anchorage Systems	74
40. Summary of Test Results and Sequential Photographs, Test KC-1	81

41. Additional Sequential Photographs, Test KC-1	82
42. Additional Sequential Photographs, Test KC-1	83
43. Documentary Photographs, Test KC-1	84
44. Documentary Photographs, Test KC-1	85
45. Documentary Photographs, Test KC-1	86
46. Impact Location, Test KC-1	87
47. Vehicle Final Position and Trajectory Marks, Test KC-1	88
48. W-Beam Guardrail System Damage, Test KC-1	89
49. W-Beam Guardrail System Damage, Test KC-1	90
50. W-Beam Guardrail System Damage, Test KC-1	91
51. W-Beam Guardrail System Damage, Test KC-1	92
52. Post Nos. 18 and 19 Damage, Test KC-1	93
53. Post Nos.18 and 19 Damage, Test KC-1	94
54. Post Nos. 20 and 21 Damage, Test KC-1	95
55. Post Nos. 20 and 21 Damage, Test KC-1	96
56. Post Nos. 22 and 23 Damage, Test KC-1	97
57. Post Nos. 22 and 23 Damage, Test KC-1	98
58. Post Nos. 24 and 25 Damage, Test KC-1	99
59. Post Nos. 24 and 25 Damage, Test KC-1	100
60. Culvert's Top Slab Damage, Test KC-1	101
61. Culvert's Top Slab Damage, Test KC-1	102
62. End Anchorage Permanent Set Deflection, Test KC-1	103
63. Vehicle Damage, Test KC-1	104
64. Vehicle's Right-Side Damage, Test KC-1	105
65. Occupant Compartment Deformations, Test KC-1	106
66. W-Beam Guardrail Attached to a Low-Fill Culvert (Option No. 2)	108
67. W-Beam Guardrail Attached to a Low-Fill Culvert Post Nos. 15 through 17, 21, and 23 through 27 (Option No. 2)	109
68. W-Beam Guardrail Attached to a Low-Fill Culvert Post Nos. 18 through 20 and 22 (Option No. 2)	110
69. W-Beam Guardrail Attached to a Low-Fill Culvert (Option No. 2)	111
70. W-Beam Guardrail Attached to a Low-Fill Culvert (Option No. 2)	112
71. Typical Posts for W-Beam Guardrail Attached to a Low-Fill Culvert (Option No.2)	113
72. Steel Washer Plate Connection Details on Bottom Side of Culvert's Top Slab	114
73. End Anchorage Systems	115
74. Summary of Test Results and Sequential Photographs, Test KC-2	121
75. Additional Sequential Photographs, Test KC-2	122
76. Additional Sequential Photographs, Test KC-2	123
77. Additional Sequential Photographs, Test KC-2	124
78. Documentary Photographs, Test KC-2	125
79. Documentary Photographs, Test KC-2	126
80. Impact Location, Test KC-2	127
81. Final Vehicle Position and Trajectory Marks, Test KC-2	128
82. W-Beam Guardrail System Damage, Test KC-2	129

83. W-Beam Guardrail System Damage, Test KC-2	130
84. W-Beam Guardrail System Damage, Test KC-2	131
85. Post Nos. 18 and 19 Damage, Test KC-2	132
86. Post Nos. 20 and 21 Damage, Test KC-2	133
87. Post Nos. 22 and 23 Damage, Test KC-2	134
88. Post Nos. 24 and 25 Damage, Test KC-2	135
89. End Anchorage Permanent Set Deflections, Test KC-2	136
90. Vehicle Damage, Test KC-2	137
91. Vehicle Right-Front Corner Damage, Test KC-2	138
92. Undercarriage Vehicle Damage, Test KC-2	139
A-1. Bogie Vehicle Details	147
A-2. Bogie Vehicle Details	148
A-3. Bogie Vehicle Tube Fabrication Details	149
A-4. Bogie Vehicle Gusset Plate Details	150
B-1. Graph of Force-Deflection Behavior, Test KCB-1b	152
B-2. Graph of Force-Deflection Behavior, Test KCB-2	153
B-3. Graph of Force-Deflection Behavior, Test KCB-3	154
B-4. Graph of Force-Deflection Behavior, Test KCB-4	155
B-5. Graph of Force-Deflection Behavior, Test KCB-5	156
B-6. Graph of Force-Deflection Behavior, Test KCB-6	157
B-7. Graph of Force-Deflection Behavior, Test KCB-7	158
C-1. Model of the Post-to-Culvert Guardrail System, Full-Post Spacing	160
C-2. Model of the Post-to-Culvert Guardrail System, Half-Post Spacing	161
C-3. Idealized Finite Element, 2 Dimensional Vehicle Model for the 1,996-kg Pickup Truck	162
E-1. Occupant Compartment Deformation Data, Test KC-1	175
F-1. Graph of Longitudinal Deceleration Test KC-1	177
F-2. Graph of Longitudinal Occupant Impact Velocity, Test KC-1	178
F-3. Graph of Longitudinal Occupant Displacement, Test KC-1	179
F-4. Graph of Lateral Deceleration, Test KC-1	180
F-5. Graph of Lateral Occupant Impact Velocity, Test KC-1	181
F-6. Graph of Lateral Occupant Displacement, Test KC-1	182
G-1. Graph of Roll, Pitch, and Yaw Angular Displacements, Test KC-1	184
H-1. Occupant Compartment Deformation Data, Test KC-2	186
I-1. Graph of Longitudinal Deceleration, Test KC-2	188
I-2. Graph of Longitudinal Occupant Impact Velocity, Test KC-2	189
I-3. Graph of Longitudinal Occupant Displacement, Test KC-2	190
I-4. Graph of Lateral Deceleration, Test KC-2	191
I-5. Graph of Lateral Occupant Impact Velocity, Test KC-2	192
I-6. Graph of Lateral Occupant Displacement, Test KC-2	193
J-1. Graph of Roll, Pitch, and Yaw Angular Displacements, Test KC-2	195
K-1. Comparison Graph of Longitudinal Decelerations, Tests KC-1 and KC-2	197
K-2. Comparison Graph of Lateral Decelerations, Tests KC-1 and KC-2	198
K-3. Comparison Graph of Vertical Decelerations, Tests KC-1 and KC-2	199

K-4. Comparison Graph of Resultant Decelerations, Tests KC-1 and KC-2	200
K-5. Comparison Graph of Longitudinal Velocity Change, Tests KC-1 and KC-2	201
K-6. Comparison Graph of Lateral Velocity Change, Tests KC-1 and KC-2	202
K-7. Comparison Graph of Vertical Velocity Change, Tests KC-1 and KC-2	203
L-1. Comparison Graph of Roll, Pitch, and Yaw Angular Displacements, Tests KC-1 and KC-2	205

List of Tables

	Page
1. NCHRP Report No. 350 Test Level 3 Crash Test Conditions	8
2. NCHRP Report No. 350 Evaluation Criteria for Crash Tests	9
3. Steel Post Bogie Impact Test Matrix	45
4. Steel Post Bogie Test Results	51
5. Computer Simulation Results	63
6. Summary of Safety Performance Evaluation Results	141

1 INTRODUCTION

1.1 Problem Statement

The current long-span guardrail design allows for an open span of 7.6 m, utilizes nested W-beam for 11.4 m on either side of the culvert, and has three CRT posts adjacent to the culvert on either side to aid in the transition back to the standard longitudinal barrier (1-3). This unsupported length is about the longest span that can be accommodated with a W-beam system while maintaining reasonable stability, tensile capacity, and deflection limits. In order to accommodate larger spans over low fill culverts, it becomes necessary to provide intermediate posts attached to the top of the culvert. This type of design was originally developed at the Texas Transportation Institute (TTI) during the mid-1980's (4), and it was successfully tested according to the evaluation criteria of National Cooperative Highway Research Program (NCHRP) Report No. 230, *Recommended Procedures for the Safety Performance Evaluation of Highway Appurtenances* (5).

Two different configurations have been utilized for rigidly attaching the steel posts to the culvert surface (4, 6). In general, attachment options have varied based on the proximity of the posts to the ends of the transverse culvert section or headwall. In some applications, steel guardrail posts have been positioned nearly 580 mm away from the front face of the culvert headwall, as measured to the back-side face of the posts. For other situations, the steel posts have been positioned adjacent to the culvert headwall, with only 25 mm of clear distance between the headwall and the back-side face of the posts. In addition to differences in post locations, post embedment depths have also varied. For example, prior crashworthy guardrail systems were developed with either 229 mm or 457 mm of soil fill placed above the top surface of the concrete box culvert. In actual field

installations, the soil embedment depth on the culvert surface and near the guardrail face can be even more variable, approaching zero at the lower limit and nearly 1,090 mm for an upper limit.

Although crashworthy W-beam guardrail systems have been developed for use as a rigid attachment to reinforced concrete box culverts, none of the existing systems have been shown to meet current impact safety standards. Therefore, a need exists to develop a strong-post, W-beam guardrail system that can be rigidly attached to the surface of concrete culverts and that which will meet the safety performance criteria found in NCHRP Report No. 350, *Recommended Procedures for the Safety Performance Evaluation of Highway Features* (7).

1.2 Objective

The objective of the research project were to develop a strong-post, W-beam guardrail system that can be rigidly attached to the surface of concrete box culverts and evaluate its safety performance through the use of full-scale vehicle crash testing. The guardrail system was to be evaluated according to the Test Level 3 (TL-3) safety performance criteria set forth in NCHRP Report No. 350.

1.3 Scope

The research objective was achieved by performing several tasks. First, a design review of the Midwest Pooled Fund States' standard plans and other publications was undertaken in order to determine a representative culvert configuration for use in the crash testing program. This review included an investigation of typical culvert sizes, soil fill depths, and guardrail post positioning with respect to both the roadway edge and culvert headwall. Next, a literature review was performed on the previously crash-tested guardrail systems attached to concrete box culverts as well as on existing long-span guardrail systems. Subsequently, seven bogie tests were performed on steel posts attached

to the concrete tarmac in order to determine the dynamic behaviors of various post/base plate/bolt combinations. Following this phase, computer simulation modeling was conducted in order to determine the optimum design for the W-beam guardrail system, including the configuration of the post-to-culvert attachment and post spacing. Two design alternatives were selected for evaluation based on the position of the post with respect to the culvert headwall. Next, the two guardrail systems were constructed at the Midwest Roadside Safety Facility's (MwRSF's) outdoor test site. Two full-scale vehicle crash tests, one on each design alternative, were then performed using $\frac{3}{4}$ -ton pickup trucks, weighing approximately 2,000 kg, at target impact speeds and angles of 100.0 km/hr and 25 degrees, respectively. Finally, the test results were analyzed, evaluated, and documented. Conclusions and recommendations were then made that pertain to the safety performance of the post-to-culvert W-beam guardrail systems.

2 LITERATURE REVIEW

For major drainage structures, such as concrete box culverts, an appropriate traffic barrier is often the most effective way to prevent errant vehicles from running off the edge of the culvert (8). Normally, these traffic barriers are full-strength, rigid bridge rails. However, the use of a rigid bridge rail can potentially create a transition problem between the rigid bridge rail and the flexible roadside guardrail commonly used upstream of the bridge rail. Therefore, roadside guardrails are often continued over low-fill culverts to reduce construction costs.

Problems arise when the guardrails must continue across the culverts because of the shallowness of the soil fill. In such cases, full embedment of the guardrail posts is not possible. Crash testing has previously demonstrated that posts with shallow embedment depths can easily be pulled out of the ground, thus resulting in vehicle snagging or vaulting and causing potentially disastrous results (4). Therefore, the guardrail posts need sufficient embedment to: (1) develop the necessary friction to prevent the posts from pulling out of the ground; (2) develop sufficient lateral soil forces to develop the bending strength of the posts; and (3) provide energy dissipation through post rotation in soil.

Previous designs for wood-post guardrail systems that eliminate the use of the steel posts in the segment over the culvert include unsupported guardrail segments which span across the culverts. Unsupported spans of 3.81 and 5.72 m have been successfully crash tested according to the NCHRP Report No. 230 criteria using “passenger-size” sedans (9-10). These successful designs utilized nested W-beam guardrail. These designs are simpler and less expensive alternatives to the designs which require attachment of the base of the posts to the top of the culvert. These designs have been recommended for use with both wood-post and steel-post guardrail systems due to the compatible

strengths of wood and steel posts (9).

Recently, the MwRSF completed the development effort for a long-span guardrail system (1-3). For this study, a 7.62-m long guardrail span was designed and successfully crash tested according to the NCHRP Report No. 350 criteria using a $\frac{3}{4}$ -ton pickup truck. This design was constructed with a 7.62-m unsupported length of nested W-beam, three CRT timber posts on either side of the unsupported length, and 11.43 m of nested W-beam on both sides of the unsupported length. For this acceptable system, it is recommended that the back face of the guardrail be positioned a minimum of 1.5 m away from the front face of the headwall in order to reduce the potential for the vehicle's wheel or fractured CRT posts to contact the headwall and cause vehicular instabilities.

Another design that alleviates the diminished performance of the guardrail with shallow embedded posts has been developed and successfully crash tested by TTI. This design involved welding base plates to the short steel posts and bolting them to the top surface of the concrete culvert (4). A 457-mm layer of cohesion-less soil was placed over the concrete box culvert and around the attached guardrail posts. However, this design required that the front face of the W-beam be placed 914 mm from the headwall of the culvert in order to provide space for the guardrail and posts to deflect during impact. In some instances, this design required that the culvert be extended outward away from the roadway. This alternative increases the cost of the structure, especially in rehabilitation projects where no other culvert work is needed (4).

In 1992, an alternative design was developed for the Kansas Department of Transportation (KsDOT) that provided a stiffer barrier and reduced the amount of deflection over the culvert (6). The successfully crash tested design according to NCHRP Report No. 230 criteria consisted of a

nested W-beam with half-post spacing. In addition, the steel posts were bolted to the top of the concrete culvert and installed adjacent to the concrete headwall with a 229-mm layer of soil was placed over the concrete box culvert and around the attached steel posts. For an impact with a passenger-size sedan, lateral dynamic guardrail deflections were reduced from 820 mm to 473 mm for the TTI design compared with the KsDOT design. These rigid, steel posts were severely deformed and often pulled loose when impacted by vehicles, significantly damaging the culvert and incurring expensive repairs.

3 TEST REQUIREMENTS AND EVALUATION CRITERIA

3.1 Test Requirements

Longitudinal barriers, such as guardrail systems attached to concrete box culverts, must satisfy the requirements provided in NCHRP Report No. 350 to be accepted for use on new construction projects or as a replacement for existing designs not meeting current safety standards. According to TL-3 of NCHRP Report No. 350, the guardrail system must be subjected to two full-scale vehicle crash tests. The two crash tests are as follows:

1. Test Designation 3-10. An 820-kg small car impacting the guardrail system at a nominal speed and angle of 100 km/hr and 20 degrees, respectively.
2. Test Designation 3-11. A 2,000-kg pickup truck impacting at the guardrail system at a nominal speed and angle of 100 km/hr and 25 degrees, respectively.

However, W-beam barriers struck by small cars have been shown to meet safety performance standards, being essentially rigid, with no significant potential for occupant risk problems arising from vehicle pocketing or severe wheel snagging on the guardrail posts (11-13). Therefore, the 820-kg small car crash test was deemed unnecessary for this project. The test conditions for TL-3 longitudinal barriers are summarized in Table 1.

3.2 Evaluation Criteria

Evaluation criteria for full-scale vehicle crash testing are based on three appraisal areas: (1) structural adequacy; (2) occupant risk; and (3) vehicle trajectory after collision. Criteria for structural adequacy are intended to evaluate the ability of the barrier to contain, redirect, or allow controlled vehicle penetration in a predictable manner. Occupant risk evaluates the degree of hazard to occupants in the impacting vehicle. Vehicle trajectory after collision is a measure of the potential for the vehicle's post-impact trajectory to result in subsequent multi-vehicle accidents. This

criterion also indicates the potential safety hazard for the occupants of other vehicles or the occupants of the impacting vehicle when subjected to secondary collisions with other fixed objects. These three evaluation criteria are defined in Table 2. The full-scale vehicle crash tests were conducted and reported in accordance with the procedures provided in NCHRP Report No. 350.

Table 1. NCHRP Report No. 350 Test Level 3 Crash Test Conditions

Test Article	Test Designation	Test Vehicle	Impact Conditions		Evaluation Criteria ¹
			Speed (km/hr)	Angle (degrees)	
Longitudinal Barrier	3-10	820C	100	20	A,D,F,H,I,K,M
	3-11	2000P	100	25	A,D,F,K,L,M

¹ Evaluation criteria explained in Table 2.

Table 2. NCHRP Report No. 350 Evaluation Criteria for Crash Tests (7)

Structural Adequacy	A. Test article should contain and redirect the vehicle; the vehicle should not penetrate, underride, or override the installation although controlled lateral deflection of the test article is acceptable.
Occupant Risk	D. Detached elements, fragments or other debris from the test article should not penetrate or show potential for penetrating the occupant compartment, or present an undue hazard to other traffic, pedestrians, or personnel in a work zone. Deformations of, or intrusions into, the occupant compartment that could cause serious injuries should not be permitted.
	F. The vehicle should remain upright during and after collision although moderate roll, pitching, and yawing are acceptable.
	H. Longitudinal and lateral occupant impact velocities should fall below the preferred value of 9 m/s, or at least below the maximum allowable value of 12 m/s.
	I. Longitudinal and lateral occupant ridedown accelerations should fall below the preferred value of 15 g's, or at least below the maximum allowable value of 20 g's.
Vehicle Trajectory	K. After collision it is preferable that the vehicle's trajectory not intrude into adjacent traffic lanes.
	L. The occupant impact velocity in the longitudinal direction should not exceed 12 m/sec, and the occupant ridedown acceleration in the longitudinal direction should not exceed 20 G's.
	M. The exit angle from the test article preferably should be less than 60 percent of test impact angle measured at time of vehicle loss of contact with test device.

4 TEST CONDITIONS

4.1 Test Facility

The testing facility is located at the Lincoln Air-Park on the northwest (NW) side of the Lincoln Municipal Airport and is approximately 8.0 km NW of the University of Nebraska-Lincoln.

4.2 Vehicle Tow and Guidance System

A reverse cable tow system with a 1:2 mechanical advantage was used to propel the test vehicle. The distance traveled and the speed of the tow vehicle were one-half that of the test vehicle. The test vehicle was released from the tow cable before impact with the guardrail system. A digital speedometer was located on the tow vehicle to increase the accuracy of the test vehicle impact speed.

A vehicle guidance system developed by Hinch ([14](#)) was used to steer the test vehicle. A guide-flag, attached to the front-right wheel and the guide cable, was sheared off before impact with the guardrail system. The 9.5-mm diameter guide cable was tensioned to approximately 13.3 kN, and supported laterally and vertically every 30.48 m by hinged stanchions. The hinged stanchions stood upright while holding up the guide cable, but as the vehicle was towed down the line, the guide-flag struck and knocked each stanchion to the ground. For tests KC-1 and KC-2, the vehicle guidance systems were approximately 267-m and 297-m long, respectively.

4.3 Test Vehicles

For test KC-1, a 1994 GMC 2500 $\frac{3}{4}$ -ton pickup truck was used as the test vehicle. The test inertial and gross static weights were 1,993 kg. The test vehicle is shown in Figure 1, and vehicle dimensions are shown in Figure 2.

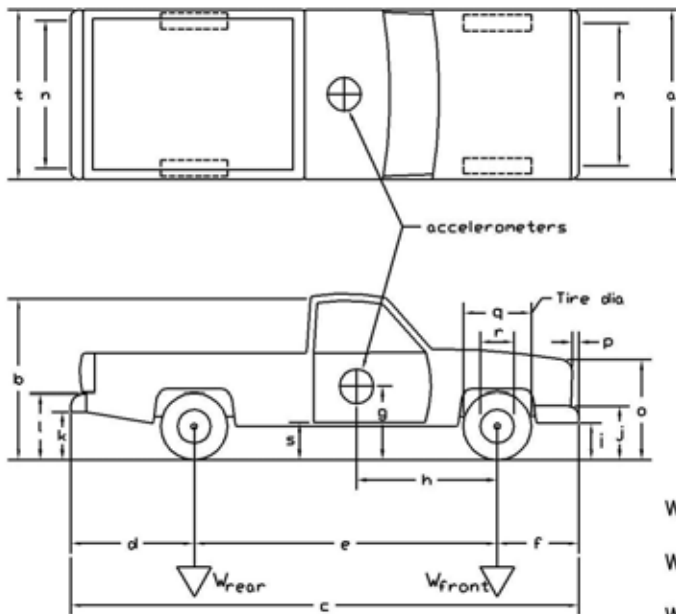
For test KC-2, a 1994 Chevrolet 2500 $\frac{3}{4}$ -ton pickup truck was used as the test vehicle. The



Figure 1. Test Vehicle, Test KC-1

Date: 7/31/01 Test Number: KC-1 Model: 2500
 Make: GMC Vehicle I.D.#: 1GTFC4HORE553308
 Tire Size: 225/75 R16 Year: 1994 Odometer: 147583

*(All Measurements Refer to Impacting Side)



Vehicle Geometry - mm

a 1873 b 1753
 c 5575 d 1289
 e 3327 f 959
 g 667 h 1495
 i 381 j 603
 k 495 l 705
 m 1584 n 1613
 o 972 p 83
 q 724 r 445
 s 400 t 1873

Wheel Center Height Front 352
 Wheel Center Height Rear 368
 Wheel Well Clearance (FR) 886
 Wheel Well Clearance (RR) 838

Weights - kg	Curb	Test Inertial	Gross Static
W_{front}	<u>998</u>	<u>1097</u>	<u>1097</u>
W_{rear}	<u>752</u>	<u>896</u>	<u>896</u>
W_{total}	<u>1750</u>	<u>1993</u>	<u>1993</u>

Engine Type 8 CYL. GAS
 Engine Size 5.0 L 305 CID
 Transmission Type:
☒ Automatic or Manual
 FWD or ☒ RWD or 4WD

Note any damage prior to test: NONE

Figure 2. Vehicle Dimensions, Test KC-1

test inertial and gross static weights were 1,994 kg. The test vehicle is shown in Figure 3, and vehicle dimensions are shown in Figure 4.

The longitudinal component of the center of gravity was determined using the measured axle weights. The location of the final centers of gravity are shown in Figures 1 through 4.

Square black and white-checked targets were placed on the vehicle to aid in the analysis of the high-speed film and E/cam video, as shown in Figures 5 and 6. Round, checkered targets were placed on the center of gravity on the driver's side door, the passenger's side door, and on the roof of the vehicle. The remaining targets were located for reference so that they could be viewed from the high-speed cameras for film analysis.

The front wheels of the test vehicle were aligned for camber, caster, and toe-in values of zero so that the vehicle would track properly along the guide cable. Two 5B flash bulbs were mounted on both the hood and roof of the vehicle to pinpoint the time of impact with the bridge rail on the high-speed film and E/cam video. The flash bulbs were fired by a pressure tape switch mounted on the front face of the bumper. A remote-controlled brake system was installed in the test vehicle so the vehicle could be brought safely to a stop after the test.

4.4 Data Acquisition Systems

4.4.1 Accelerometers

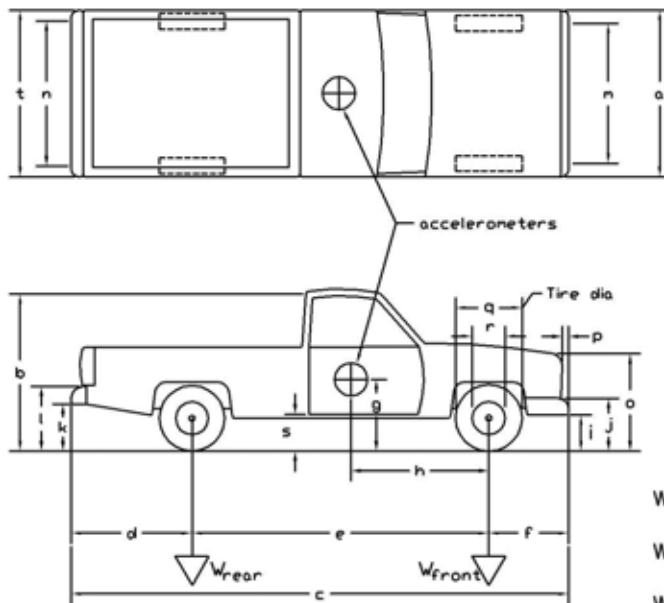
One triaxial piezoresistive accelerometer system with a range of ± 200 G's was used to measure the acceleration in the longitudinal, lateral, and vertical directions at a sample rate of 10,000 Hz. The environmental shock and vibration sensor/recorder system, Model EDR-4M6, was developed by Instrumented Sensor Technology (IST) of Okemos, Michigan and includes three differential channels as well as three single-ended channels. The EDR-4 was configured with 6 Mb



Figure 3. Test Vehicle, Test KC-2

Date: 9/27/01 Test Number: KC-2 Model: 2500
 Make: Chevrolet Vehicle I.D.#: 1GCFC24K9RE104950
 Tire Size: LT 245/75 R16 Year: 1994 Odometer: 216401

*(All Measurements Refer to Impacting Side)



Vehicle Geometry - mm

a 1886 b 1778
 c 5537 d 1327
 e 3327 f 883
 g 667 h 1436
 i 429 j 616
 k 546 l 743
 m 1584 n 1619
 o 975 p 83
 q 765 r 448
 s 445 t 1873

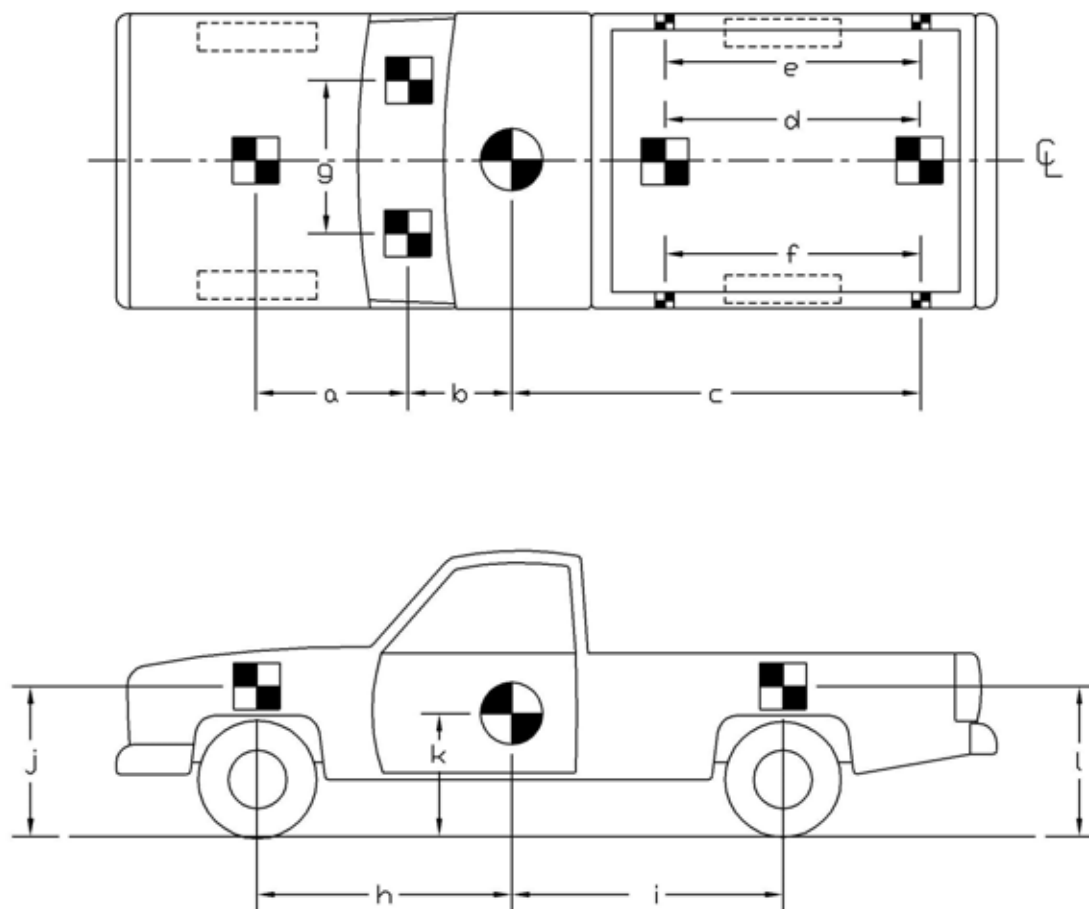
Wheel Center Height Front 368
 Wheel Center Height Rear 371
 Wheel Well Clearance (FR) 854
 Wheel Well Clearance (RR) 914

Weights - kg	Curb	Test Inertial	Gross Static
W_{front}	<u>1044</u>	<u>1134</u>	<u>1134</u>
W_{rear}	<u>796</u>	<u>860</u>	<u>860</u>
W_{total}	<u>1840</u>	<u>1994</u>	<u>1994</u>

Engine Type 8 CYL. GAS
 Engine Size 5.7 L 350 CID
 Transmission Type:
☒ Automatic or Manual
 FWD or ☒ RWD or 4WD

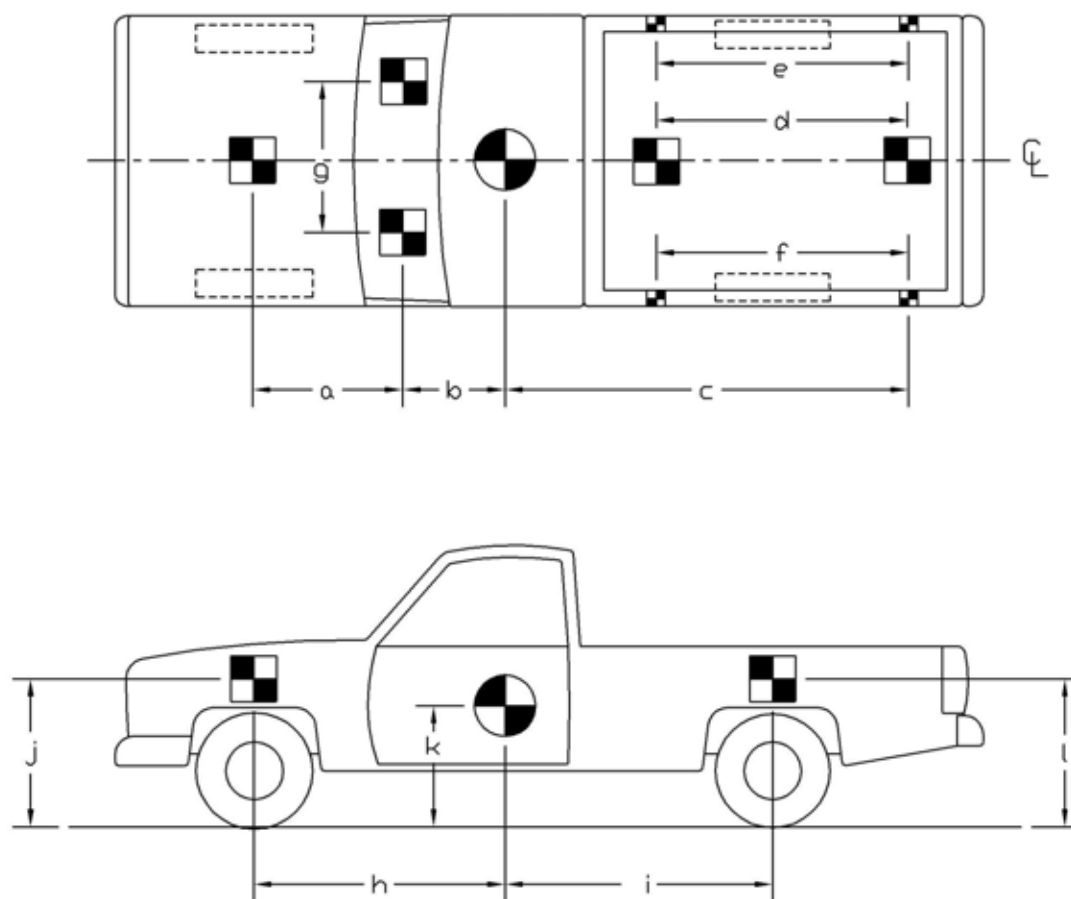
Note any damage prior to test: Rebuilt Driver's Side

Figure 4. Vehicle Dimensions, Test KC-2



TEST #: <u>KC-1</u>			
TARGET GEOMETRY (mm)			
a <u>927</u>	d <u>2146</u>	g <u>1264</u>	j <u>943</u>
b <u>762</u>	e <u>2226</u>	h <u>1495</u>	k <u>667</u>
c <u>2750</u>	f <u>2226</u>	i <u>1832</u>	l <u>991</u>

Figure 5. Vehicle Target Locations, Test KC-1



TEST #: <u>KC-2</u>			
TARGET GEOMETRY (mm)			
a <u>832</u>	d <u>1619</u>	g <u>1000</u>	j <u>956</u>
b <u>762</u>	e <u>2153</u>	h <u>1435</u>	k <u>667</u>
c <u>2603</u>	f <u>2153</u>	i <u>1892</u>	l <u>1016</u>

Figure 6. Vehicle Target Locations, Test KC-2

of RAM memory and a 1,500 Hz lowpass filter. Computer software, “DynaMax 1 (DM-1)” and “DADiSP”, was used to analyze and plot the accelerometer data.

A backup triaxial piezoresistive accelerometer system with a range of ± 200 G’s was also used to measure the acceleration in the longitudinal, lateral, and vertical directions at a sample rate of 3,200 Hz. The environmental shock and vibration sensor/recorder system, Model EDR-3, was developed by Instrumental Sensor Technology (IST) of Okemos, Michigan. The EDR-3 was configured with 256 Kb of RAM memory and a 1,120 Hz lowpass filter. Computer software, “DynaMax 1 (DM-1)” and “DADiSP”, was used to analyze and plot the accelerometer data.

4.4.2 Rate Transducers

A Humphrey 3-axis rate transducer with a range of 360 deg/sec in each of the three directions (pitch, roll, and yaw) was used to measure the rates of motion of the test vehicle. The rate transducer was rigidly attached to the vehicle near the center of gravity of the test vehicle. Rate transducer signals, excited by a 28-volt DC power source, were received through the three single-ended channels located externally on the EDR-4M6 and stored in the internal memory. The raw data measurements were then downloaded for analysis and plotted. Computer software, “DynaMax 1 (DM-1)” and “DADiSP”, was used to analyze and plot the rate transducer data.

4.4.3 High-Speed Photography

For test KC-1, two high-speed 16-mm Red Lake Locam cameras, with operating speeds of approximately 500 frames/sec, were used to film the crash test. Five high-speed Red Lake E/cam video cameras, with operating speeds of 500 frames/sec, were also used to film the crash test. Three Canon digital video cameras, with a standard operating speed of 29.97 frames/sec, were also used to film the crash test. A Locam, with a wide-angle 12.5-mm lens, and two E/cam high-speed video

cameras were placed above the test installation to provide a field of view perpendicular to the ground. A Locam, a Canon digital video camera, a Kodak digital camera, and a Nikon F1 35-mm still camera were placed downstream from the impact point and had a field of view parallel to the barrier. A high-speed E/cam video camera and a Canon digital video camera were placed downstream from the impact point and behind the barrier. Two high-speed E/cam video cameras and a Canon digital video camera were placed upstream from the impact point and behind the barrier. A Canon digital video camera, with a panning view, and a Nikon 995 digital camera were placed on the traffic side of the barrier and had a field of view perpendicular to the barrier. A schematic of all fourteen camera locations for test KC-1 is shown in Figure 7.

For test KC-2, two high-speed 16-mm Red Lake Locam cameras, with operating speeds of approximately 500 frames/sec, were used to film the crash test. Five high-speed Red Lake E/cam video cameras, with operating speeds of 500 frames/sec, were also used to film the crash test. Three Canon digital video cameras, with a standard operating speed of 29.97 frames/sec, were also used to film the crash test. A Locam, with a wide-angle 12.5-mm lens, and three high-speed E/cam video cameras were placed above the test installation to provide a field of view perpendicular to the ground. A Locam was placed downstream from the impact point and had a field of view parallel to the barrier. A high-speed E/cam video camera and a Canon digital video camera were placed upstream from the impact point and behind the barrier. A high-speed E/cam video camera and a Canon digital video camera were placed downstream from the impact point and behind the barrier. A Canon digital video camera, with a panning view, and a Nikon 995 digital camera were placed on the traffic side of the barrier and had a field of view perpendicular to the barrier. A schematic of all eleven camera locations for test KC-2 is shown in Figure 8. The Locam films and E/cam

videos were analyzed using the Vanguard Motion Analyzer and the Redlake Motion Scope software, respectively. Actual camera speed and camera divergence factors were considered in the analysis of the high-speed film.

4.4.4 Pressure Tape Switches

For tests KC-1 and KC-2, five pressure-activated tape switches, spaced at 2-m intervals, were used to determine the speed of the vehicle before impact. Each tape switch fired a strobe light which sent an electronic timing signal to the data acquisition system as the right-front tire of the test vehicle passed over it. Test vehicle speed was determined from electronic timing mark data recorded using the "Test Point" software. Strobe lights and high-speed film analysis are used only as a backup in the event that vehicle speed cannot be determined from the electronic data.

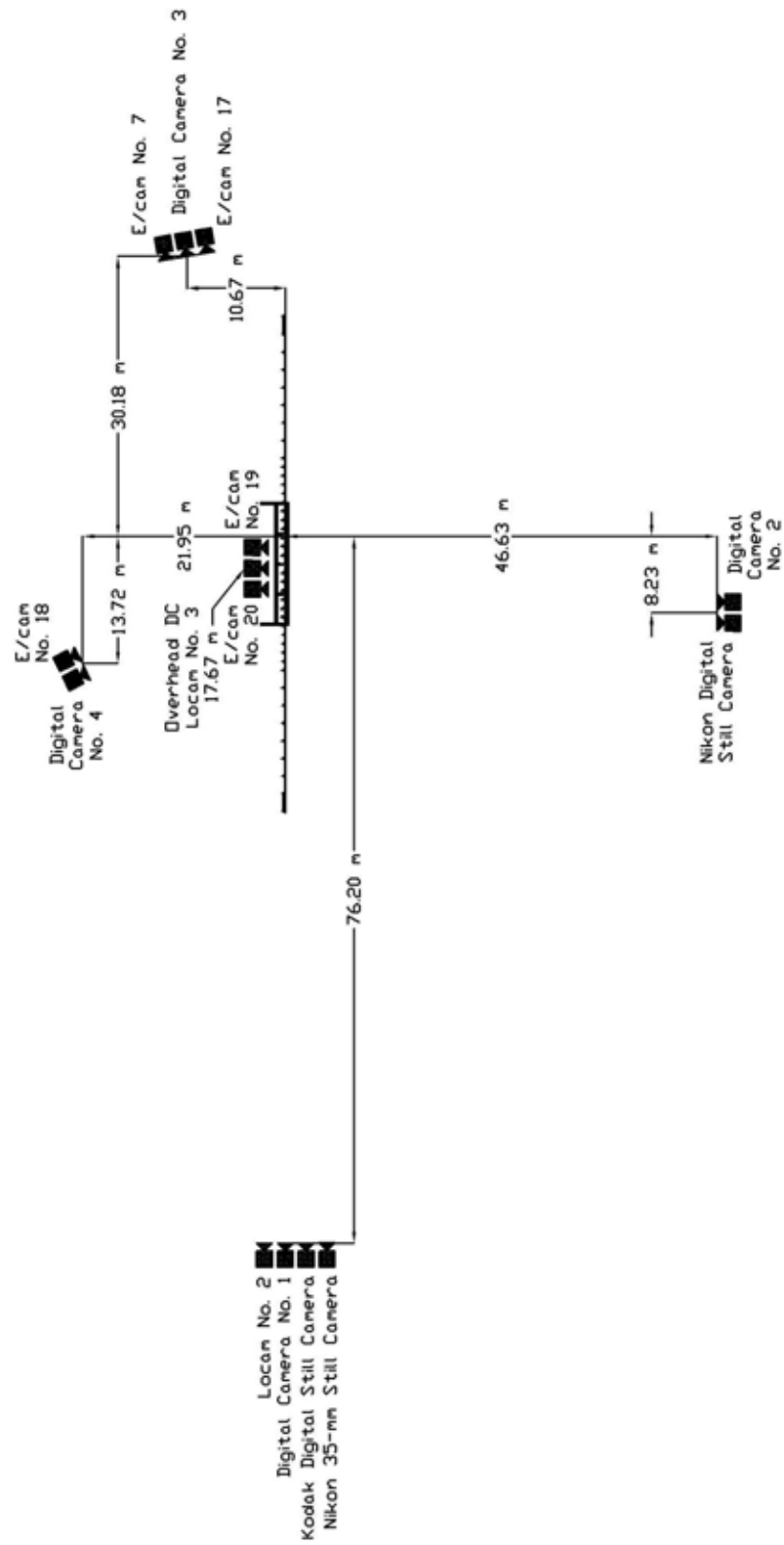


Figure 7. Location of High-Speed Cameras, Test KC-1

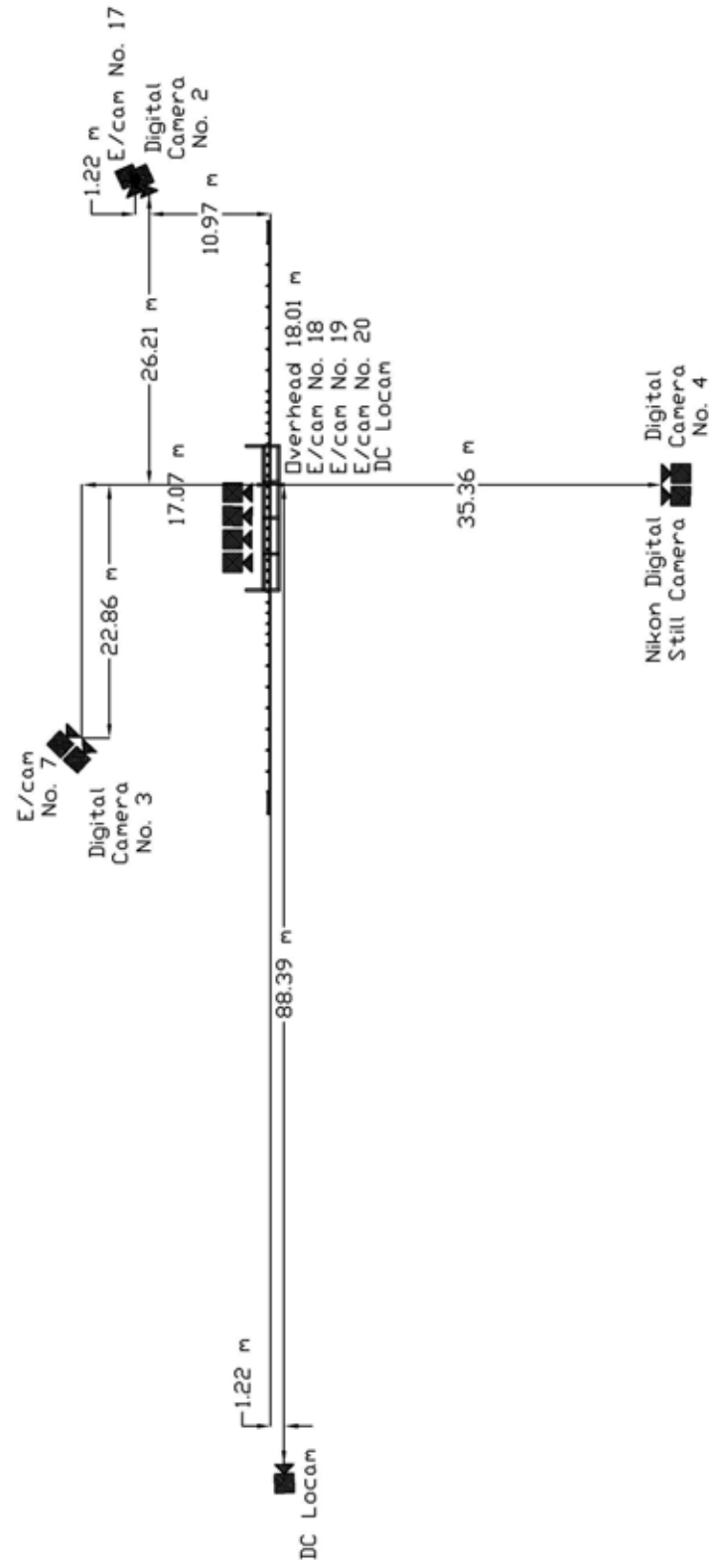


Figure 8. Location of High-Speed Cameras, Test KC-2

5 GENERAL DESIGN CONSIDERATIONS

5.1 Culvert Geometry

Early in this research study, a design review of the Pooled Fund States' standard plans, special plans, and specifications was conducted in order to determine the standard practice for concrete box culverts. Based upon this review, it was determined that concrete box culverts are generally configured with one to three cells, with four cells being an approximate upper limit. In addition, clear span distances and clear heights for the cells ranged between 0.61 to 4.57 m and 0.46 to 3.66 m, respectively. Concrete thicknesses for the top slab, bottom slab, and vertical walls as well as the steel reinforcement varied depending on the clear span, clear height, and depth of soil fill placed on the top of the culvert system. It is noted that standardized design sheets and tables have been developed by most State Departments of Transportation (DOT's) as well as those provided in AASHTO M 273-94 (15).

Following this review, MwRSF researchers determined that the simulated concrete box culvert would be configured with four cells, each with a clear span of 3.05 m. This culvert configuration was selected in order to provide adequate length for attachment of the barrier to the culvert surface and to insure that the barrier deformations would occur only along the length of the culvert system. With the selection of a longer culvert length versus a shorter length, researchers believed that a more accurate indication of the new barrier's safety performance would be achieved since the lateral stiffness of the strong-post W-beam guardrail system adjacent to the culvert system would not effect dynamic barrier deflections.

During discussions with representatives from the State DOT's, concerns were raised with regard to the concrete damage observed to occur when the steel posts and attached base plates were

deformed, twisted, and/or pulled away from the slab surfaces. Since this concrete damage often results in the need for extensive and costly repairs, it was determined that the barrier and culvert slab designs should attempt to reduce and/or prevent significant concrete damage from occurring in the culvert structure (i.e., top slab).

From the literature review, it was also observed that the culvert's top slab thicknesses generally varied between 152 and 305 mm. As a result, a 178-mm thick concrete top slab was selected for the actual culvert design used in the crash testing program. Finally, both the longitudinal and transverse steel reinforcement located in the top slab were found to vary significantly. For the simulated test culvert, all steel reinforcement utilized no. 4 bars spaced on approximately 305-mm centers and would be placed in two rows throughout the 178-mm thick slab. This combination of slab thickness and steel reinforcement were believed to provide a non-conservative slab design for resisting dead and live loads but still provide sufficient capacity in order to minimize concrete damage. Therefore, if satisfactory barrier performance were observed in the crash testing program, then comparable barrier performance would be expected for top slab designs with capacities equal to or greater than that used in the crash tests.

5.2 Depth of Soil Fill

Similarly, a review of the Pooled Fund member states' design details was conducted in order to determine the range of depths of soil fill typically placed over concrete box culverts and near the roadside guardrail. In general, the depths of soil fill were found to range between 0 and 1,118 mm. For a deeper soil fill depth, it was believed that the guardrail system's safety performance would more closely resemble that observed for standard strong-post W-beam guardrail systems. Therefore, MwRSF researchers determined that the most critical soil depth would occur as the depth reached

zero thickness. Since zero or minimal thickness of soil fill is generally not an option for most culvert designs, a 229-mm layer of soil fill was selected for the research study and was believed to still provide a critical safety performance evaluation on the new barrier system.

5.3 Guardrail Post Attachments and Locations

Currently, the Pooled Fund member states utilize various methods for attaching both steel or wood guardrail posts to the surface of concrete box culverts. For wood post systems, options existed for inserting either round or rectangular posts into similarly shaped tubes that were welded to base plates and then bolted to the concrete surface. Another wood post variation consisted of bolting a steel angle to both the front and the back sides of the posts and then attaching the other leg of each angle to the concrete surface. For the more common steel post systems, each W152x13.4 post is typically fabricated with a welded steel plate on its base which allows for a rigid attachment to the concrete surface.

In addition, the actual positioning of the guardrail posts with respect to the front face of the culvert's headwall was found to be even more varied. In some instances, the back side of the posts were positioned 25 mm away from the front face of the headwall, while in other instances, a minimum of 527 mm was specified. However, in some case, no specific distance was provided as the dimensioning was identified with a length denoted by "varies".

For this research study, the steel post option was selected for the design and with two different post locations. Since post location was believed to be a key parameter affecting the barrier's safety performance, crash testing was deemed necessary for both post placement alternatives. For the first and second options, the back side of the steel posts would be positioned 457 mm and 25 mm, respectively, away from the front face of the culvert's headwall.

6 TEST SITE PREPARATION

6.1 Culvert Construction

A simulated full-size, four-cell concrete box culvert system was constructed at MwRSF's outdoor test site for use in the development of the new W-beam guardrail systems. The four-cell system was selected to ensure that the research results were representative of actual box culvert site conditions. In the following sections, site details are provided that pertain to the construction of the test pit and concrete box culvert. Design details for each portion are shown in Figures 9 through 17. Photographs of the culvert construction are shown in Figures 18 through 21.

6.1.1 Test Pit

A test pit, measuring 1.27-m wide by 13.21-m long, was constructed in an existing soil pit. The pit was excavated to a depth of approximately 1.4 m in order to provide sufficient clearance for constructing the concrete box culvert.

6.1.2 Culvert Substructure

After the soil was excavated from the test pit, five reinforced concrete vertical support walls and a soil retaining wall were constructed on the bottom of the test pit. Design details are shown in Figures 9 through 12. Photographs of the concrete support construction as well as the completed supports and retaining wall are shown in Figure 18.

The inner three concrete vertical supports had a center-to-center spacing of 3.25 m. The outer two spacings were also spaced 3.25-m on center. The concrete vertical supports were constructed perpendicular to the roadway, as shown in Figures 9 and 18. The two exterior concrete vertical supports measured 203-mm wide by 3.05-m long by 1.37-m high. The three interior concrete vertical supports measured 203-mm wide by 1.52-m long by 1.37-m high. The soil

retaining wall measured 203-mm wide by 13.21-m long by 1.37-m high. The concrete used for the concrete vertical supports consisted of a Nebraska 47-BD Mix with a minimum compressive strength of 31.03 MPa, while the concrete for the soil retaining wall consisted of a Nebraska LSG-3500 Mix with a minimum compressive strength of 24.13 MPa. The actual concrete compressive strength of the vertical supports on test day, as determined from concrete cylinder testing, was found to be approximately 55.42 MPa. A minimum concrete cover of 38 mm was used for all of the rebar placed within the concrete vertical supports and soil retaining wall. All of the steel reinforcement in the vertical supports and soil retaining wall was Grade 60 epoxy-coated rebar.

The steel reinforcement for the vertical supports utilized No. 4 bars for the transverse, vertical, and bent vertical bars, as shown in Figures 9 through 11. For both the outside and inside vertical supports, the transverse bars were 2,972-mm and 1,448-mm long, respectively, and spaced 432 mm on center with the bottom one placed at ground level, as shown in Figures 9 through 11 and 17. The vertical dowel bars in the outside vertical supports were 1,295-mm long and spaced 508 mm on center, as shown in Figures 10 and 17. For the two outside vertical supports, the long and short bent vertical bars were 1,753-mm and 1,689-mm long, respectively, and spaced 457 mm on center, as shown in Figures 9, 10, and 17. For the inside vertical supports, the bent vertical bars were 1,753-mm long and spaced 457 mm on center, as shown in Figures 9, 11, and 17.

The steel reinforcement for the soil retaining wall also utilized No. 4 bars for the longitudinal and vertical bars, as shown in Figures 9, 12, and 17. Each of the six longitudinal rebar in the soil retaining wall was 13.13-m long. The length of the longitudinal bar can be varied as long as the minimum lap length of 305 mm is maintained. The vertical dowel bars were 1,295-mm long and spaced 813 mm on center, as shown in Figures 9, 12, and 17.

6.1.3 Culvert Top Slab and Curb

Following the completion of the culvert substructure, the culvert's top slab and curb were constructed. Design details are shown in Figures 13 through 16. Construction photographs of the top slab and curb are shown in Figures 18 through 21.

The horizontal deck measured 1,524-mm wide by 178-mm thick by 13.21-m long. The culvert curb, constructed above the top slab, measured 254-mm wide by 254-mm thick by 13.21-m long and was located at the back side of the deck. The concrete used for the culvert's top slab and curb consisted of a Nebraska 47-BD Mix with a minimum compressive strength of 31.03 MPa. The actual concrete compressive strength for the culvert's top slab and the curb on test day, as determined from concrete cylinder testing, were found to be approximately 48.21 MPa and 41.64 MPa, respectively. A minimum concrete cover of 38 mm was used for all of the rebar placed within the top slab and curb. All of the steel reinforcement in the horizontal deck and curb was Grade 60 epoxy-coated rebar.

The steel reinforcement for the top slab utilized No. 4 bars for the longitudinal and transverse bars, as shown in Figures 13 and 17. Each of the twelve longitudinal rebar in the top slab was 13.13-m long. The length of the longitudinal bar can be varied as long as the minimum lap length of 305 mm is maintained. The transverse bars in the top slab were 1,448-mm long, and their spacings varied longitudinally, as shown in Figure 13 through 16. At the outside vertical supports, the transverse bars were spaced 298 mm on center. The transverse bar spacing on either side of the inside vertical supports was 254 mm on center. Between the supports, the spacing of the transverse bars was 305 mm on center. The vertical spacing between the transverse bars was 89 mm on center.

The steel reinforcement for the curb utilized No. 4 bars for the longitudinal and curb loop

bars, as shown in Figures 13 through 14 and 17. Each of the four longitudinal rebar in the curb was 13.13-m long. The length of the longitudinal bar can be varied as long as the minimum lap length of 305 mm is maintained. The curb loop bars were 1334-mm long, and their spacings varied longitudinally, as shown in Figures 13 and 15 through 16. At the outside vertical supports, the curb loop bars were spaced 298 mm on center. The curb loop bar spacing on either side of the inside vertical supports was 254 mm on center. Between the supports, the spacing of the curb loop bars was 305 mm on center.

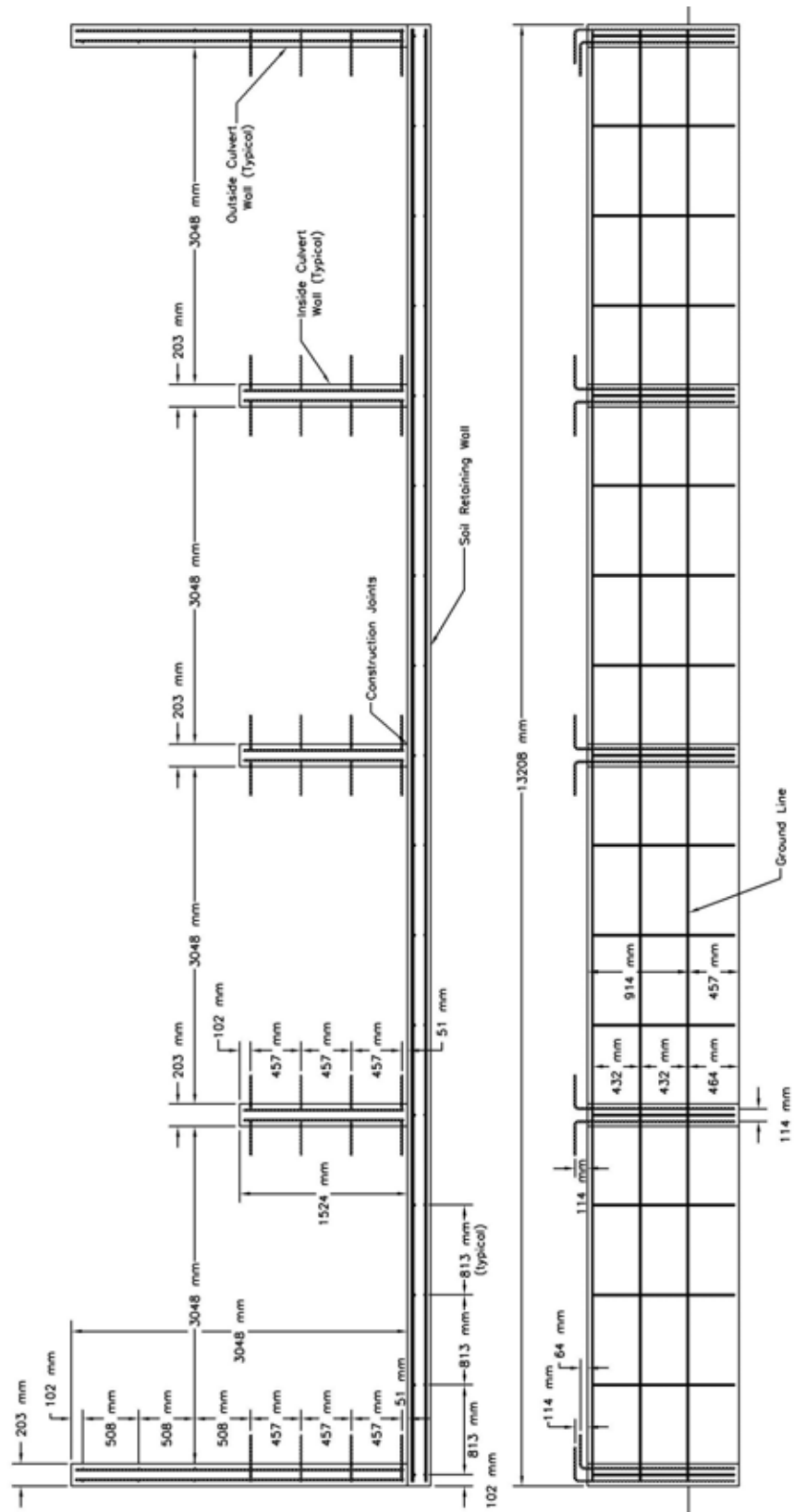


Figure 9. Concrete Culvert Substructure Details

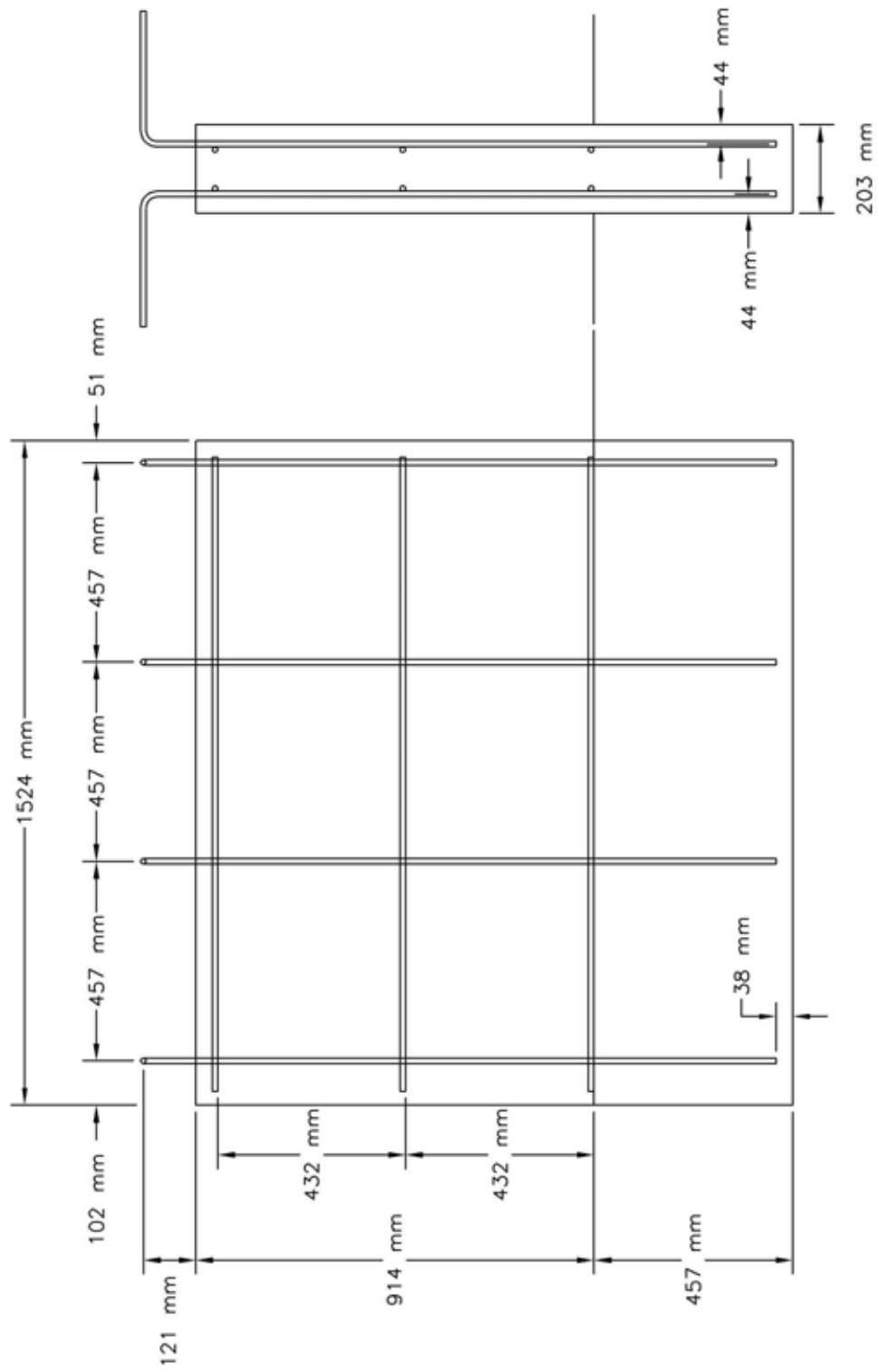


Figure 11. Concrete Culvert Substructure Details - Inside Culvert Wall

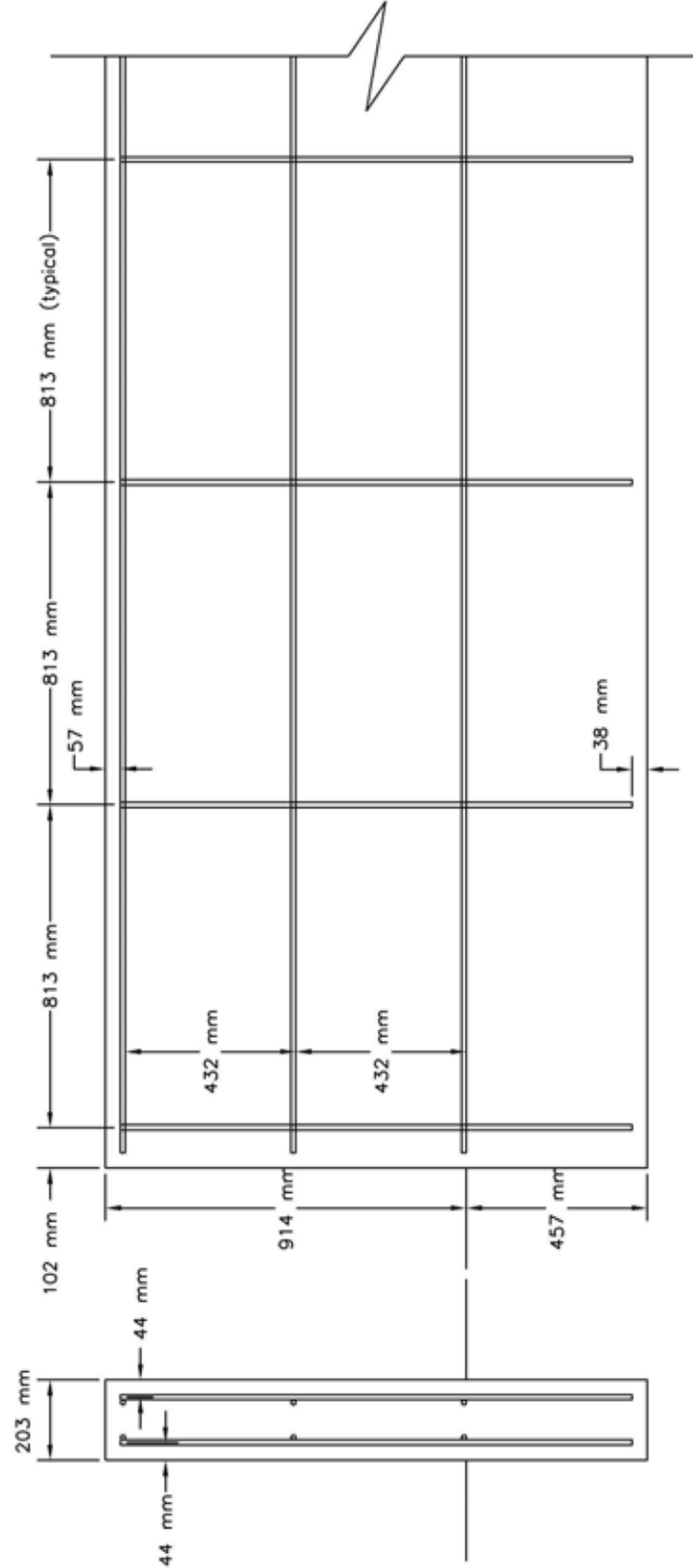


Figure 12. Concrete Culvert Substructure Details - Soil Retaining Wall For Test Purposes Only

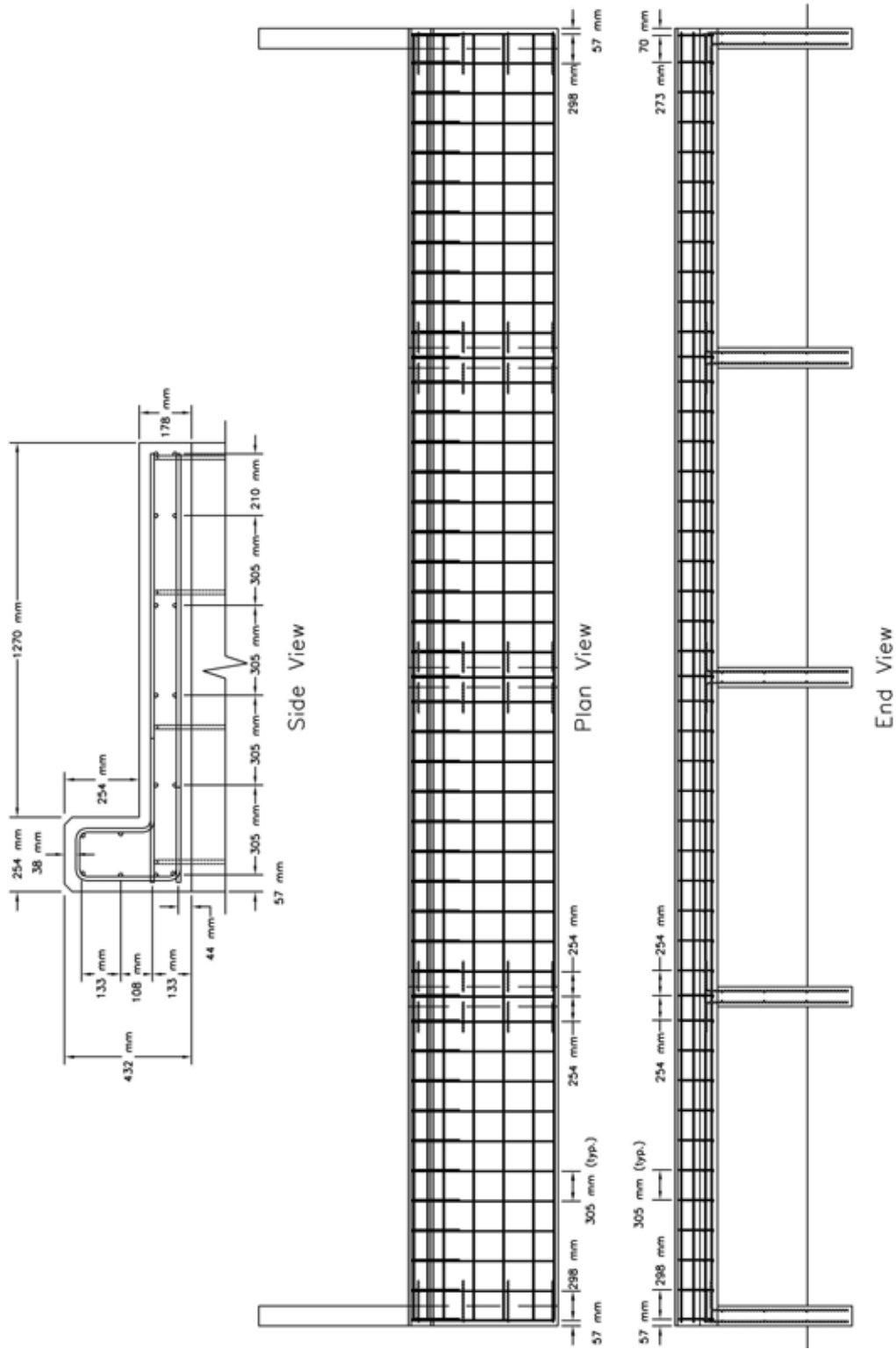


Figure 13. Concrete Culvert Top Slab and Curb Details – Plan, End, and Side Views

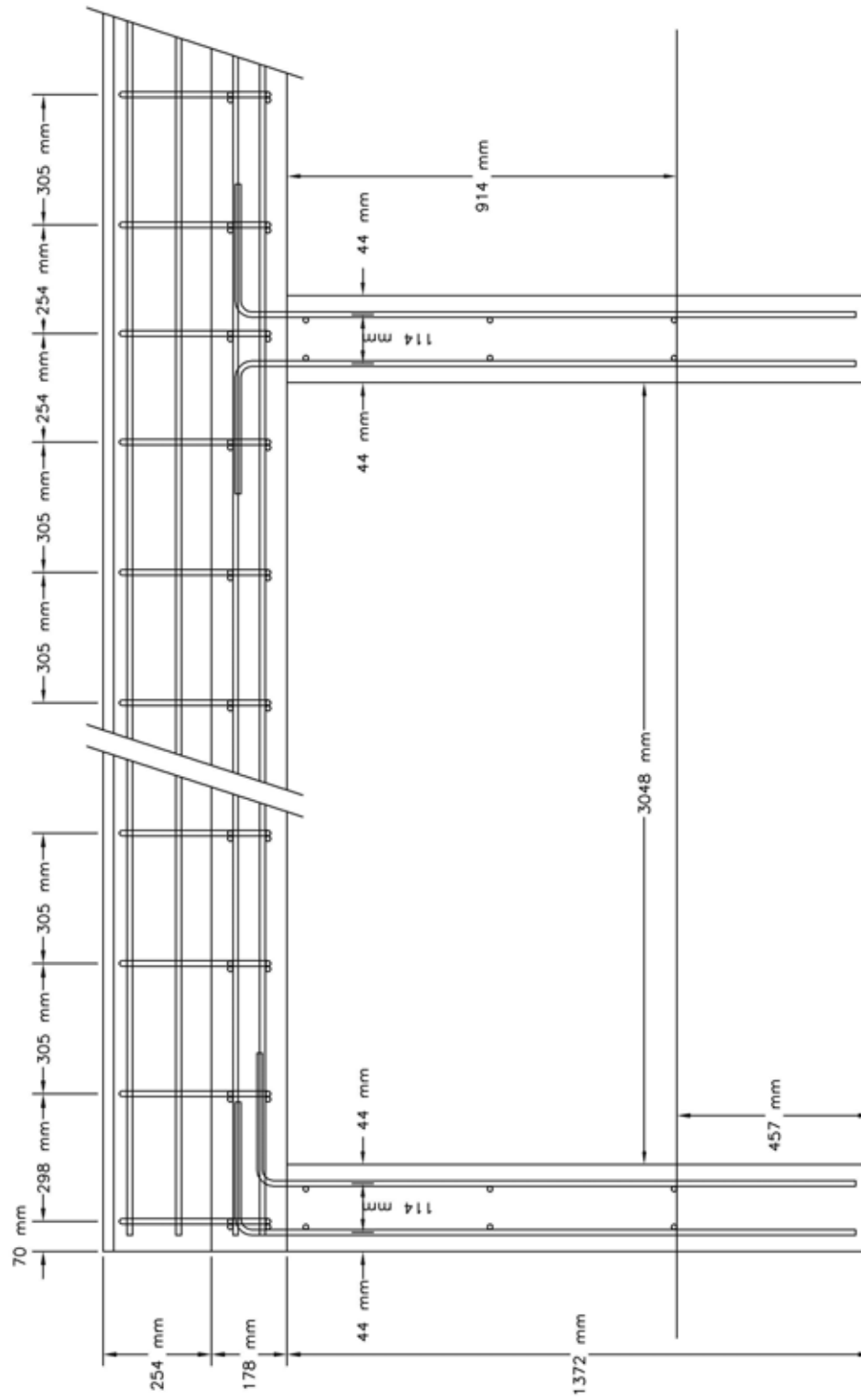


Figure 15. Concrete Culvert Top Slab and Curb Details - End View

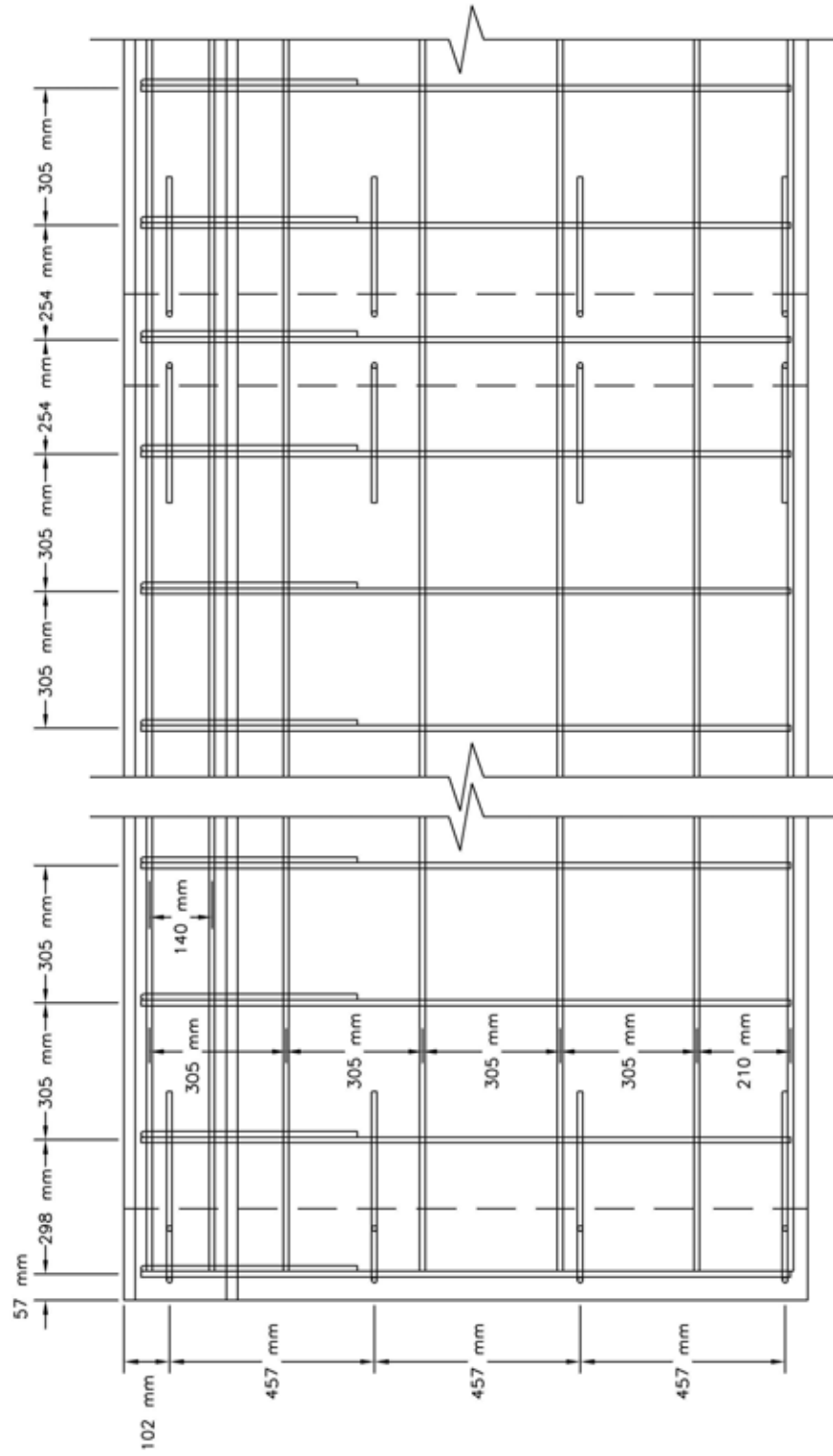


Figure 16. Concrete Culvert Top Slab and Curb Details - Plan View

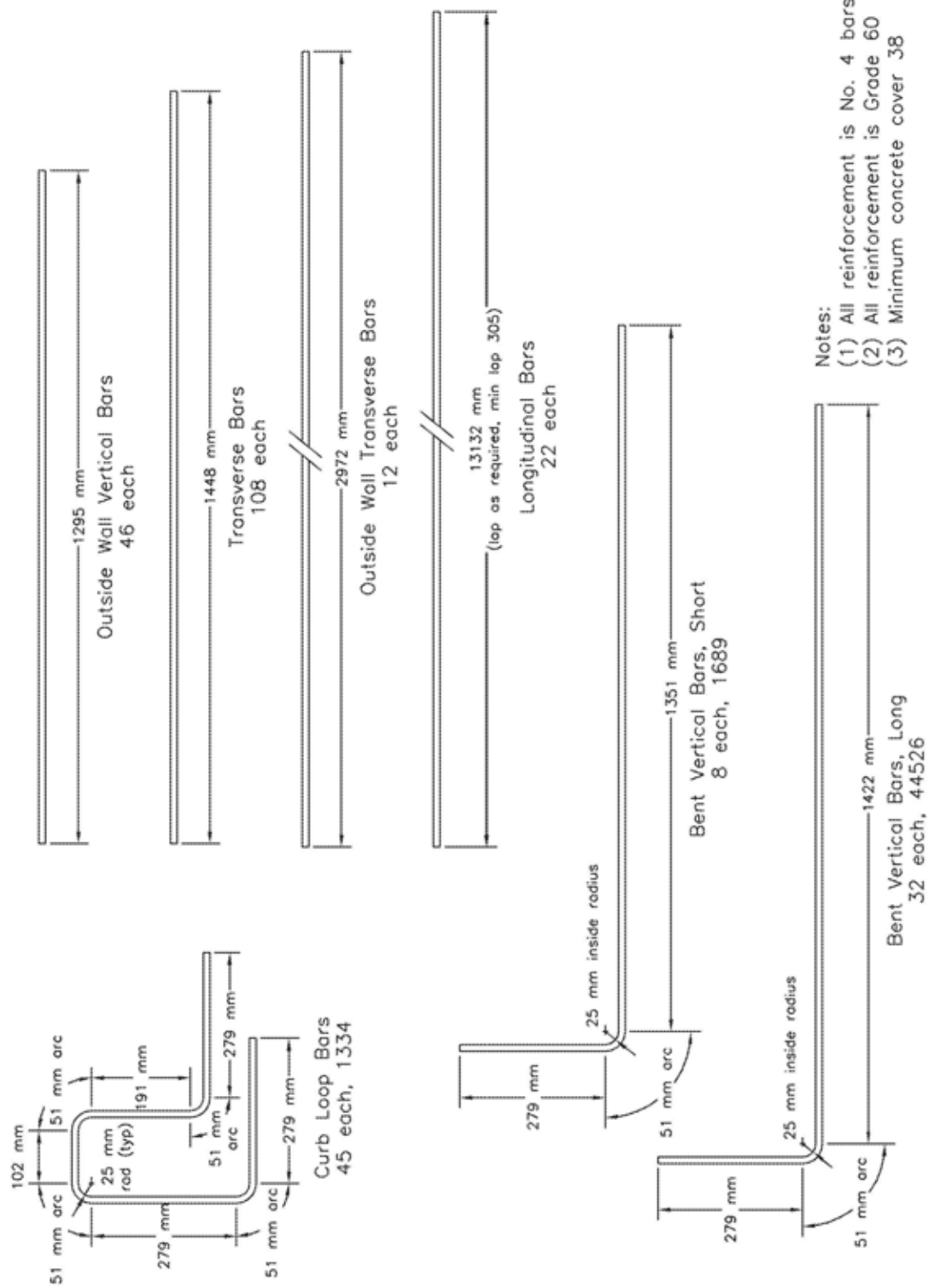


Figure 17. Concrete Culvert Steel Reinforcement Details



Figure 18. Concrete Culvert Walls and Top Slab Formwork



Figure 19. Concrete Culvert Top Slab Formwork (continued)



Figure 20. Concrete Culvert Curb Construction



Figure 21. Concrete Culvert Substructures, Top Slab, and Curb

7 DEVELOPMENT OF POST-TO-CULVERT SLAB ATTACHMENT

7.1 Design Considerations

The majority of strong-post W-beam guardrail systems attached to low-fill concrete culverts use ASTM A36 W152x13.4 steel posts fitted with welded steel base plates, each rigidly anchored through the culvert's top slab with four 19.0-mm diameter ASTM A307 bolts (4, 6). The ASTM A36 steel base plates have generally measured 152-mm wide by 254-mm long by 15.9-mm thick. The centerline distance between the traffic- and back-side bolt rows typically have measured 127 mm. About the post's weak axis, the centerline distance between the upstream- and downstream-side bolt rows have measured 89 mm.

As discussed in Section 5, the culvert's top slab can become damaged as the steel posts and base plates deform, twist, and/or pull away from the concrete surface during an impact event. Based on prior research and review, a 178-mm thick top slab with two rows of no. 4 bars spaced 305-mm on center was to be utilized for this design effort. However, the existing base plate configuration placed the four vertical bolts in close proximity to one another, especially about the post's weak axis. This bolt spacing, in combination with a 15.9-mm thick base plate, increased the potential for a higher, more concentrated loading to be applied to the culvert's top slab located directly below the base plate. Therefore, MwRSF researchers deemed it necessary to consider alternative base plate thicknesses and bolt group spacings in order to prevent concrete damage from occurring to the culvert's top slab.

An experimental investigation was conducted in order to determine the dynamic impact behavior of steel posts attached to a rigid concrete foundation and with various base plate geometries

and bolt sizes. Three base plates sizes and thicknesses and two bolt group configurations and bolt sizes were considered. Details of this investigation are provided in Section 8.

8 DYNAMIC POST TESTING

8.1 Test Matrix

Dynamic bogie testing was used to obtain the force-deflection behavior of various post-to-culvert attachment configurations. The W152 x 13.4 steel posts with attached base plates were anchored to the concrete tarmac using epoxied USS Grade 2 threaded rods of various sizes. The steel posts were impacted at the target speed of 16.1 km/hr using a 2,217-kg and 2,199-kg rigid frame bogie vehicle for the first test and last six tests, respectively. All seven of the steel posts were impacted perpendicular to the front face of the posts (i.e., about the post's strong axis of bending) with the center of the bumper located 779 mm above the ground line. The bogie test matrix is shown in Table 3.

Table 3. Steel Post Bogie Impact Test Matrix

Test No.	Plate Size (mm x mm)	Plate Thickness (mm)	USS Grade 2 Threaded Rod Diameter (mm)	Bolt Spacing (mm)		Target Speed (km/hr)
				Weak Axis	Strong Axis	
KCB-1b	152 x 254	6.4	19.05	89	127	16.1
KCB-2	152 x 254	15.9	19.05	127	178	16.1
KCB-3	203 x 305	6.4	19.05	127	178	16.1
KCB-4	203 x 305	15.9	19.05	127	178	16.1
KCB-5	216 x 305	6.4	25.4	127	178	16.1
KCB-6	216 x 305	9.5	25.4	127	178	16.1
KCB-7	216 x 305	12.7	25.4	127	178	16.1

8.2 Test Conditions

8.2.1 Bogie Vehicle

A rigid frame bogie vehicle was used to conduct the component testing. Design details of the bogie vehicle are shown in Figure 22. Complete design and fabrication details are shown in Appendix A. Photographs of the bogie vehicle are shown in Figure 23. The main frame of the bogie vehicle consists of two 3,875-mm long by 203-mm x 152-mm x 6-mm steel tubes on the sides and a pair of 1,829-mm long by 457-mm x 152-mm x 13-mm steel tubes on the front and back. The front and back tubes of the bogie are filled with concrete and drilled with a series of holes for mounting various impact heads and other frame attachments. In addition to these main tubes, the frame is reinforced by six 203-mm x 152-mm x 6-mm steel tubes, six C254 x 29.8 channel sections, and 254-mm x 51-mm x 6-mm steel tubes. The bogie vehicle rolls on four standard-size pickup truck wheels that are mounted on independent axles and outfitted with remote-controlled brakes.

For the dynamic component tests described here, the bogie was modified by adding a wooden front bumper configured out of five vertical posts and two horizontal 152 mm x 203 mm wood posts, as shown in Figure 23. The total weight of the bogie vehicle and its attachments were 2,217-kg and 2,199 kg for the first test and for the last six tests, respectively.

8.2.2 Bogie Tow and Guidance System

A reverse cable tow system with a 1:1 mechanical advantage was used to propel the bogie vehicle. The distance traveled and the speed of the tow vehicle were equal to that of the bogie vehicle. The bogie guide track was 30.5-m long. The guide track was constructed with 57-mm diameter by 2.96-m long steel pipes with a wall thickness of 4.76 mm. The pipes were supported every 3,048 mm by steel stanchions. The bogie vehicle was released from the tow cable and the



Figure 23. Large Bogie Vehicle

bogie guide track before impact with the guardrail post, thus allowing the bogie vehicle to become a free projectile as it came off the bogie guide track.

8.2.3 Post Installation Procedure

The posts were installed by attaching them to the concrete tarmac. Four holes for the bolt anchors were drilled in the concrete apron. The USS Grade 2 threaded rod anchors were then installed in the holes using Power-Fast Epoxy Injection Gel which is a two-component (Sikadur Injection Gel Base Resin and Hardener), structural epoxy adhesive gel.. After the epoxy had properly cured, the posts and attached base plates were anchored to the concrete using ASTM A307 bolts of various sizes. Each post installation, along with its corresponding damage, is shown in Figures 24 through 30.

8.2.4 Data Acquisition Systems

8.2.4.1 Accelerometer

For the bogie tests KCB-1b through KCB-4, a triaxial piezoresistive accelerometer system with a range of ± 200 G's was used to measure the acceleration in the longitudinal, lateral, and vertical directions at a sample rate of 3,200 Hz. The environmental shock and vibrations sensor/recorder system, Model EDR-3, was developed by Instrumented Sensor Technology (IST) of Okemos, Michigan. The EDR-3 was configured with 256 Kb of RAM memory and a 1,120 Hz lowpass filter. Computer software, "DynaMax 1 (DM-1)" and "DADiSP" were used to digitize, analyze, and plot the accelerometer data.

For the bogie tests KCB-5 through KCB-7, a triaxial piezoresistive accelerometer system with a range of ± 200 G's was used to measure the acceleration in the longitudinal, lateral, and vertical directions at a sample rate of 10,000 Hz. The environmental shock and vibration

sensor/recorder system, Model EDR-4M6, was developed by Instrumented Sensor Technology (IST) of Okemos, Michigan and includes three differential channels as well as three single-ended channels. The EDR-4 was configured with 6 Mb of RAM memory and a 1,500 Hz lowpass filter. Computer software, “DynaMax 1 (DM-1)” and “DADiSP”, was used to analyze and plot the accelerometer data.

8.2.4.2 High-Speed Photography

For bogie test KCB-1b, a high-speed Red Lake E/cam video camera, with an operating speed of 500 frames/sec, was placed on the left side of the post and had a close-up field of view perpendicular to the lower portion of the post. A Canon digital video camera was also placed on the left side of the post and had a field of view perpendicular to the post and impact.

For bogie tests KCB-2 through KCB-7, a high-speed Red Lake E/cam video camera, with an operating speed of 500 frames/sec, was placed on the left side of the post and had a close-up field of view perpendicular to the lower portion of the post. A Canon digital video camera was placed on the right side of the post and had a field of view perpendicular to the post and impact.

8.2.4.3 Pressure Tape Switches

For bogie test KCB-1b, one set of three pressure-activated tape switches, spaced at 1-m intervals, was used to determine the speed of the bogie before impact. Each tape switch fired a strobe light as the right-front tire of the test vehicle passed over it. Test bogie speeds were determined from high-speed E/cam video analysis. This was accomplished by utilizing the Redlake Motion Scope software to determine the firing time of each strobe light in the high-speed E/cam video.

For bogie tests KCB-2 through KCB-7, a digital speedometer in the tow vehicle was used

to determine the speed of the bogie before impact.

8.3 Test Results

Seven bogie tests were performed and are summarized in Table 4. For bogie tests KCB-1b through KCB-6, failure occurred in either the weld between the post and base plate or in the threaded rods used to anchor the plate to the concrete. For bogie test KCB-7, the post and plate yielded without any bolt damage or weld failure. Because this failure mechanism is more readily reproducible than weld failure, the post-to-culvert attachment configuration used in bogie test KCB-7 was recommended for further evaluation using computer simulation modeling. Post and plate damage for each bogie test are shown in Figures 24 through 30. Force-deflection plots for each post test are shown graphically in Appendix B.

Table 4. Steel Post Bogie Test Results

Test No.	Speed (km/hr)	Peak Load (kN)	Deflection at Peak Load (mm)	Results
KCB-1b	16.4	49.7	86.6	Plate failure, fractured away with post
KCB-2	16.1	91.6	36.1	Weld failure
KCB-3	16.1	49.3	116.6	Bolts failed in tension, plate deformed
KCB-4	16.1	82.0	117.6	Weld failure
KCB-5	16.1	38.5	162.3	Plate buckled and weld failure
KCB-6	16.1	60.5	327.2	Plate buckled and weld failure
KCB-7	17.7	65.3	61.2	Post and plate yielded, no bolt damage or weld failure



Figure 24. Post and Plate Damage, Bogie Test KCB-1b



Figure 25. Post and Plate Damage, Bogie Test KCB-2



Figure 26. Post and Plate Damage, Bogie Test KCB-3



Figure 27. Post and Plate Damage, Bogie Test KCB-4



Figure 28. Post and Plate Damage, Bogie Test KCB-5



Figure 29. Post and Plate Damage, Bogie Test KCB-6



Figure 30. Post and Plate Damage, Bogie Test KCB-7

9 COMPUTER SIMULATION

9.1 Background

BARRIER VII computer simulation modeling (16) was used in the development of a strong-post, W-beam guardrail system for use over low-fill concrete culverts. More specifically, simulation runs were conducted in order to analyze and predict the dynamic performance of various guardrail system alternatives prior to full-scale vehicle crash testing. These simulations were performed modeling a 2,000-kg pickup truck impacting at a speed of 100.0 km/hr and at an angle of 25 degrees.

Typically, computer simulation modeling is also used to determine the critical impact point (CIP) for longitudinal barrier systems. In past studies, the CIP has been based upon the impact condition which maximized: (1) wheel-assembly snagging on guardrail posts, (2) vehicle pocketing into the guardrail system, (3) predicted strains in the W-beam rail, or (4) combinations thereof. In addition to BARRIER VII simulation modeling, the CIP can be determined using the graphical procedures outlined in NCHRP Report No. 350.

The maximum longitudinal strain in the W-beam rail is the best indicator of rail rupture. Although the AASHTO M180 steel used in W-beam guardrails is a relatively ductile material and can sustain significant plastic strain without failure, full-scale crash tests have indicated that guardrails tend to fail at relatively low plastic strains due to the cross section of a W-beam rail element being reduced by approximately 15 percent at the rail splice. This cross sectional reduction tends to localize strain in the splice region and leads to rail rupture near the point that the full cross section begins to yield. Full cross-sectional yield was selected as another key parameter used in the design of the barrier system. This yield condition would correspond to a limiting strain of approximately 0.0017.

9.2 Design Alternatives

Historically, the maximum dynamic deflection for strong-post, W-beam guardrail systems have ranged between 889 and 1,016 mm when impacted according to the TL-3 test conditions (test designation no. 3-11) of NCHRP Report No. 350. For the new guardrail system, MwRSF researchers deemed it prudent to maintain a maximum dynamic barrier deflection equal to or less than those observed for W-beam guardrails installed in standard roadside applications and on level terrain. This design limitation was believed to be necessary in order to reduce the potential for severe wheel snag on the exposed posts and to decrease the potential for vehicle climbing and vaulting over the flattened, displaced, and rotated W-beam rail. In culvert applications where the post is rigidly anchored only 229 mm below the soil surface, it was reasoned that a post's exposure on the traffic- and upstream-side faces would be intensified in situations where greater barrier deflections had occurred. In addition, an exposed post, in combination with increased barrier displacement, would provide a more gradual inclined surface for vaulting vehicles over the guardrail system. Therefore, it was believed that reduced dynamic rail and post deflections would actually increase the safety performance of the new barrier system.

As a result, computer simulation modeling was performed on two guardrail system alternatives which were configured for use on a low-fill culvert applications. The design alternatives included:

1. a single 12-gauge, W-beam guardrail system with W152x13.4 steel posts spaced 1,905 mm on center (standard post spacing) and with 229 mm of soil embedment; and
2. a single 12-gauge, W-beam guardrail system with W152x13.4 steel posts spaced 952.5 mm on center (half-post spacing) and with 229 mm of soil embedment.

Furthermore, the finite element models for each of these two design options are provided in Appendix C. A typical computer simulation input data file is shown in Appendix D.

9.3 Barrier VII Results

The computer simulation results for the two design alternatives are shown in Table 5. For the first design alternative using standard post spacing and for various impact locations (i.e., run nos. 1B through 9B), the computer simulations predicted maximum dynamic deflections between 662 to 701 mm would occur at the center height of the rail. It is noted that these rail deflections are less than those observed for standard, strong-post W-beam guardrail systems. However, researchers believed that further reducing rail deflections would significantly decrease the potential for the vehicle to climb and vault over the barrier system as well as to prevent vehicle snag on exposed posts located on the traffic-side face of the barrier system. In addition, the simulations predicted maximum longitudinal rail strain between 0.00120 and 0.00137 which were all less than the limiting strain of 0.0017.

For the second design alternative using half-post spacing and for various impact locations (i.e., run nos. 1 through 9), the computer simulations predicted maximum dynamic deflections between 418 and 427 mm would occur at the center height of the rail. For the half-post spacing option, maximum dynamic deflections were reduced significantly from those observed for standard, strong-post W-beam guardrail systems. With these reduced barrier deflections, researchers now believed that vehicle climbing and vaulting over the barrier system would likely be mitigated. Finally, the simulations predicted maximum longitudinal rail strain between 0.00131 and 0.00143 which once again were all less than the limiting strain of 0.0017.

Following this analysis, the second design alternative utilizing steel posts spaced 952.5 mm

on center was chosen as the guardrail system to be evaluated by full-scale vehicle crash testing. As previously discussed, BARRIER VII computer simulation modeling or the NCHRP Report No. 350 procedures can be used to determine the impact location. As a result, the CIP procedures outlined in NCHRP Report No. 350 were used for this study. Using a plastic moment of barrier rail, M_p , equal to 10.9 kN-m, a post dynamic yield force per unit length of barrier, F_p , equal to 51.4 kN/m, and the graph provided in Figure 3.10 of NCHRP Report No. 350, the CIP was found to be approximately 3 m upstream from the centerline of the guardrail system at post no. 21.

Table 5. Computer Simulation Results

Run No.	Impact Node	Impact Conditions		Maximum Dynamic Rail Deflection ¹ (mm)	Maximum Rail Tension ² (kN)	Maximum Rail Strain ² (mm/mm)	Post Spacing (mm)	Exit Conditions		
		Speed (km/hr)	Angle (deg.)					Time (sec)	Resultant Velocity (km/hr)	Velocity Trajectory (deg.)
1B	78	100.0	25.0	686 @ Node 94	270.5 @ Element 82	0.00126 @ Node 85	1,905	0.4350	62.65	10.1
2B	79	100.0	25.0	698 @ Node 94	267.8 @ Element 82	0.00120 @ Node 85	1,905	0.3615	62.65	9.9
3B	80	100.0	25.0	701 @ Node 95	279.3 @ Element 89	0.00120 @ Node 85	1,905	0.4900	62.51	10.1
4B	81	100.0	25.0	666 @ Node 95	295.8 @ Element 87	0.00128 @ Node 90	1,905	0.5000	62.91	11.4
5B	82	100.0	25.0	662 @ Node 97	293.1 @ Element 89	0.00126 @ Node 92	1,905	0.5120	62.41	12.5
6B	83	100.0	25.0	678 @ Node 98	297.6 @ Element 89	0.00132 @ Node 95	1,905	0.5015	61.62	12.5
7B	84	100.0	25.0	685 @ Node 99	280.7 @ Element 87	0.00137 @ Node 95	1,905	0.5155	61.51	12.1
8B	85	100.0	25.0	688 @ Node 100	281.1 @ Element 89	0.00136 @ Node 95	1,905	0.5015	61.83	11.4
9B	87	100.0	25.0	690 @ Node 102	285.1 @ Element 90	0.00137 @ Node 95	1,905	0.4085	62.57	10.3
1	78	100.0	25.0	425 @ Node 90	318.5 @ Element 82	0.00135 @ Node 84	952.5	0.3890	64.44	11.1
2	79	100.0	25.0	426 @ Node 91	323.8 @ Element 82	0.00131 @ Node 85	952.5	0.3970	64.07	12.2
3	80	100.0	25.0	427 @ Node 91	322.1 @ Element 87	0.00136 @ Node 90	952.5	0.4045	63.99	12.7
4	81	100.0	25.0	418 @ Node 91	315.4 @ Element 87	0.00140 @ Node 90	952.5	0.3895	64.70	11.1
5	82	100.0	25.0	422 @ Node 94	317.6 @ Element 87	0.00143 @ Node 90	952.5	0.3975	64.84	10.6
6	83	100.0	25.0	422 @ Node 95	319.8 @ Element 90	0.00140 @ Node 90	952.5	0.4035	64.45	11.8
7	84	100.0	25.0	424 @ Node 95	317.2 @ Element 90	0.00138 @ Node 92	952.5	0.4030	64.45	11.9
8	85	100.0	25.0	427 @ Node 95	318.9 @ Element 87	0.00137 @ Node 93	952.5	0.3895	64.50	11.2
9	87	100.0	25.0	421 @ Node 98	306.5 @ Element 90	0.00142 @ Node 95	952.5	0.3945	64.82	10.8

¹ - Lateral distance measured at the center height of the rail.

² - A single, 2.67-mm thick W-beam rail was used in the analysis.

10 W-BEAM GUARDRAIL SYSTEM DESIGN DETAILS (OPTION NO. 1)

The test installation consisted of 53.34 m of standard 2.66-mm thick W-beam guardrail supported by steel posts, as shown in Figures 31 through 33. Anchorage systems similar to those used on tangent guardrail terminals were utilized on both the upstream and downstream ends of the guardrail system. Photographs of the test installation are shown in Figure 34 through 39.

The entire system was constructed with forty-one guardrail posts. Post nos. 3 through 14 and 28 through 39 were galvanized ASTM A36 steel W152x13.4 sections measuring 1,829-mm long. Post nos. 15 through 27 were also ASTM A36 steel W152x13.4 sections but measured 946-mm long. Post nos. 1, 2, 40, and 41 were timber posts measuring 140-mm wide x 190-mm deep x 1,080-mm long and were placed in steel foundation tubes. The timber posts and foundation tubes were part of anchor systems designed to replicate the capacity of a tangent guardrail terminal.

Post nos. 1 through 9 and 33 through 41 were spaced 1,905-mm on center. Post nos. 9 and 33 were spaced 952.5-mm on center, as shown in Figure 31. For post nos. 3 through 14 and 28 through 39, the soil embedment depth was 1,100 mm. For post nos. 15 through 27, the soil embedment depth was 229 mm. The posts were placed in a compacted course, crushed limestone material that met Grading B of AASHTO M147-65 (1990) as found in NCHRP Report No. 350. In addition, 152-mm wide x 203-mm deep x 356-mm long, routed wood spacer blockouts were used to block the rail away from post nos. 3 through 39, as shown in Figures 35 through 37.

Post nos. 15 through 27 were anchored to the top of the concrete culvert using welded steel plates. The backside of these posts were placed 457 mm from the front of the culvert's headwall, as shown in Figures 31 through 36. A 12.7-mm thick x 216-mm wide x 305-mm long ASTM A36 steel plate was welded to the bottom of each of these steel posts. Four 25-mm diameter by 241-mm

long, ASTM A307 hex head bolts were placed through each top base plate and the concrete deck and were held in place with steel washer plates below the top slab, as shown in Figure 38. The ASTM A36 steel washer plates measured 6.4-mm thick x 216-mm wide x 280-mm long. In addition, post no. 21 was anchored using epoxied threaded rods due to the presence of the culvert's inner wall support.

Three standard 2.66-mm thick W-beam rails, each measuring 7,620-mm long, were placed between post nos. 1 and 17, as shown in Figure 31. Subsequently, two standard 2.66-mm thick W-beam rails, each measuring 3,810-mm long, were placed between post nos. 17 and 25, as shown in Figure 31. Three standard 2.66-mm thick W-beam rails, each measuring 7,620-mm long, were placed between post nos. 25 and 41, as shown in Figure 31. The top mounting height of the W-beam rail was 706 mm. All lap-splice connections between the rail sections were configured to reduce vehicle snagging at the splice during the crash test.

A concrete culvert as previously described in Section 6.1 was constructed at the center of the system, as shown in Figures 31 through 36. The maximum dimensions of the culvert's top slab were 1,270-mm wide and 178-mm thick with a 254-mm wide x 254-mm deep headwall positioned flush with the backside of the top slab, as described previously. The length of the culvert was 13.21 m, spanning from 889-mm upstream from the center of post no. 15 to 889-mm downstream from the center of post no. 27.

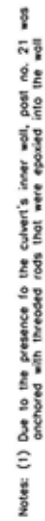


Figure 31. W-Beam Guardrail Attached to a Low-Fill Culvert (Option No. 1)

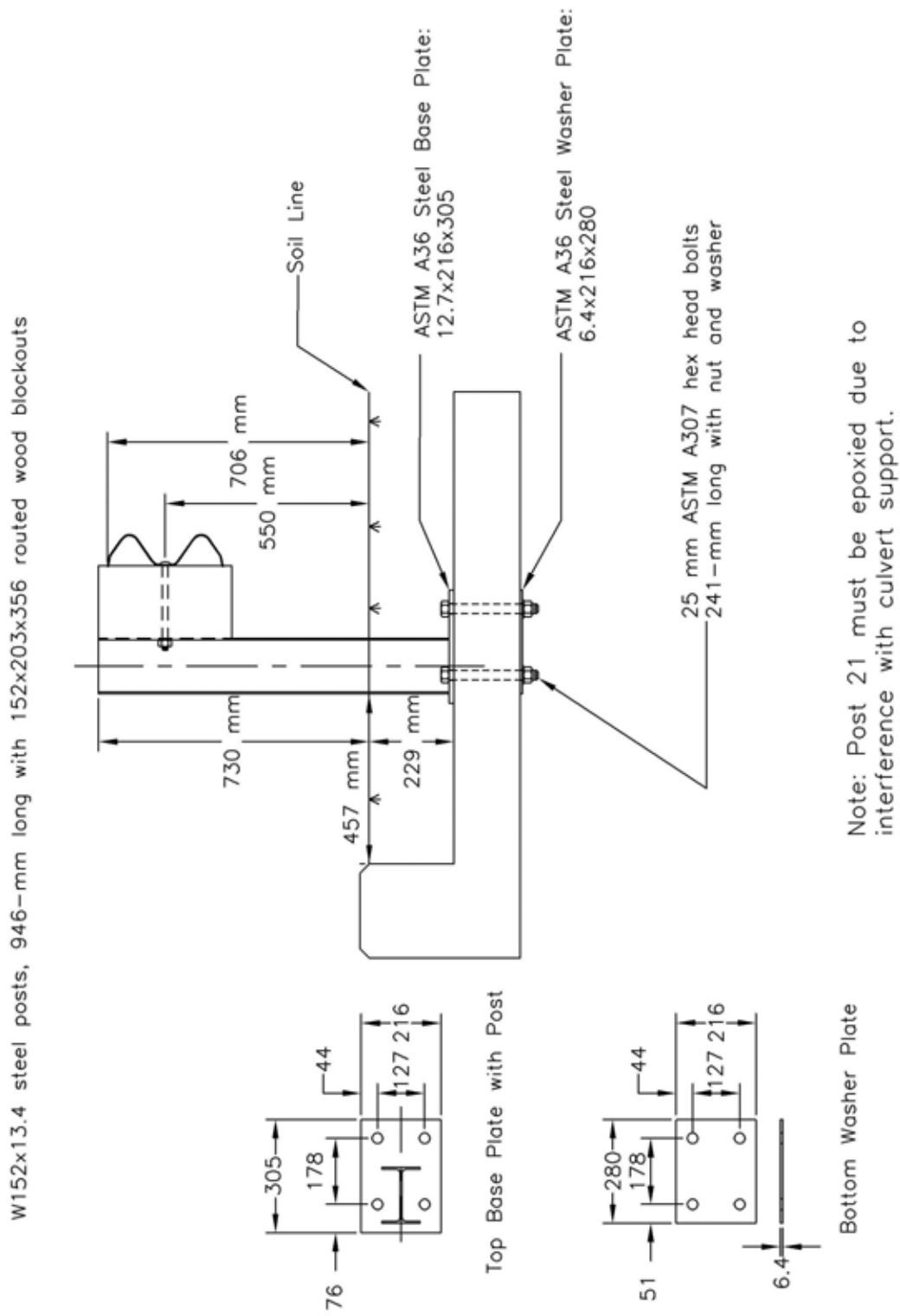


Figure 32. W-Beam Guardrail Attached to a Low-Fill Culvert Post Nos. 15 through 27 (Option No. 1)

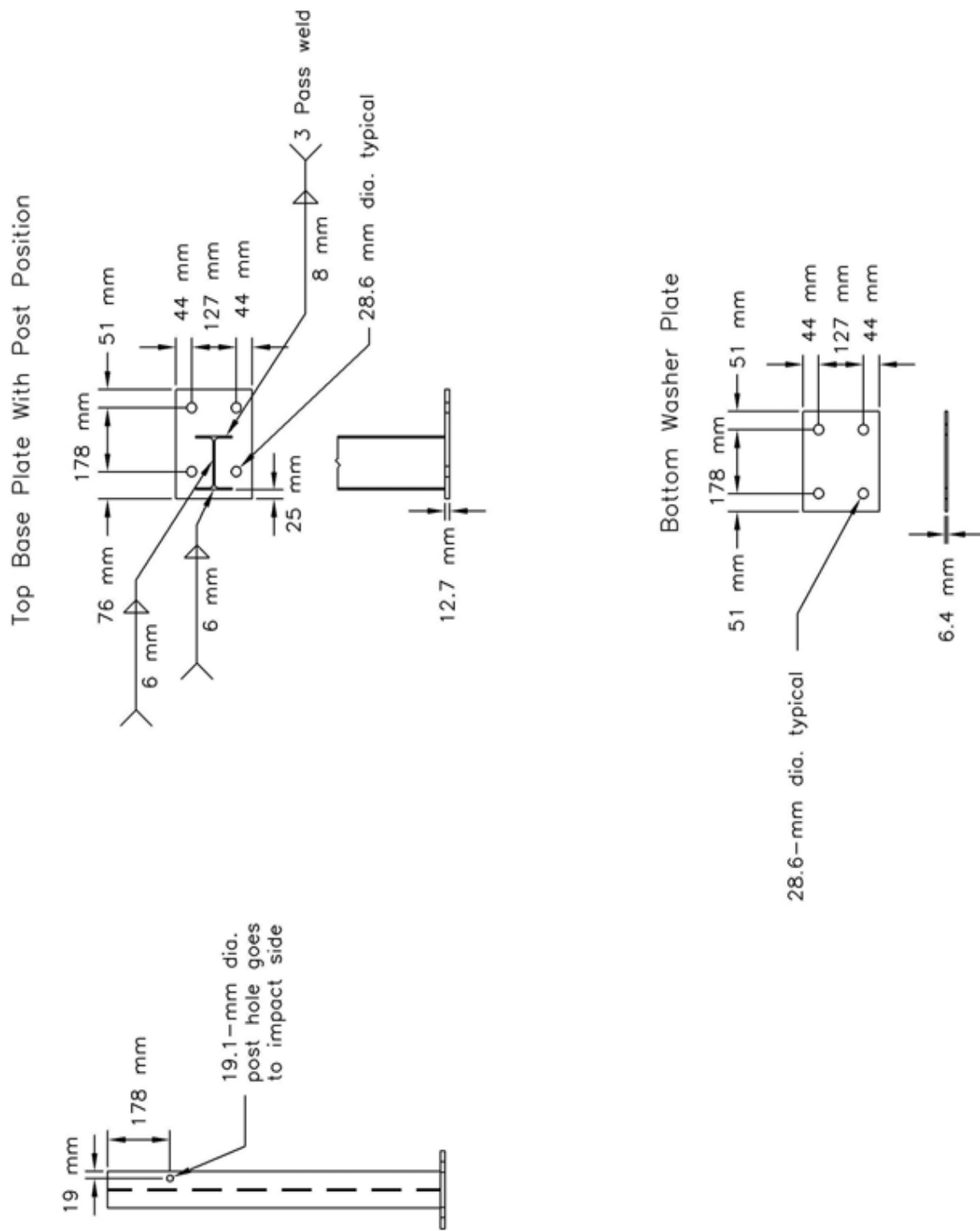


Figure 33. W-Beam Guardrail Attached to a Low-Fill Culvert (Option No. 1)



Figure 34. W-Beam Guardrail Attached to a Low-Fill Culvert (Option No. 1)



Figure 35. W-Beam Guardrail Attached to a Low-Fill Culvert (Option No. 1)



Figure 36. W-Beam Guardrail Attached to a Low-Fill Culvert (Option No. 1)

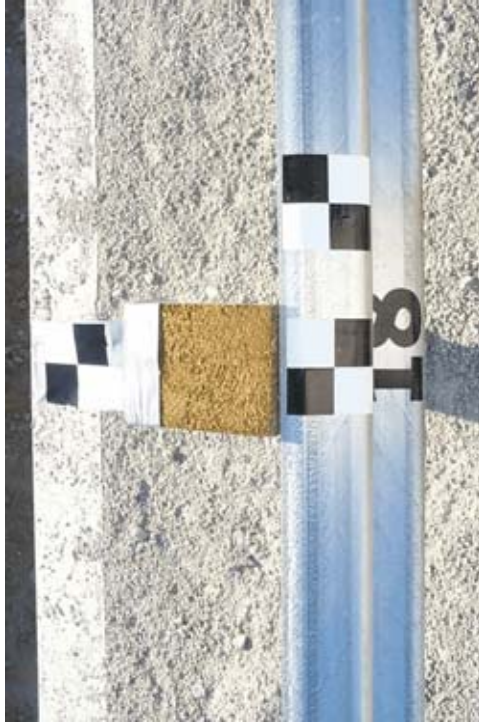
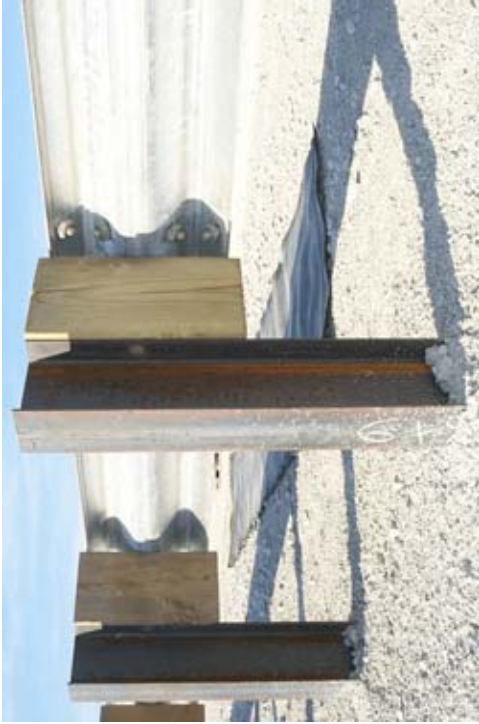


Figure 37. Typical Post for W-Beam Guardrail Attached to a Low-Fill Culvert (Option No. 1)



Figure 38. Steel Post Connection Details on Bottom Side of Culvert's Top Slab



Figure 39. End Anchorage Systems

11 CRASH TEST NO. 1 (OPTION NO. 1)

11.1 Test KC-1

The 1,993-kg pickup truck impacted the W-beam guardrail at a speed of 103.3 km/hr and at an angle of 25.3 degrees. A summary of the test results and the sequential photographs are shown in Figure 40. Additional sequential photographs are shown in Figures 41 and 42. Documentary photographs of the crash test are shown in Figures 43 through 45.

11.2 Test Description

Initial impact was to occur between post nos. 17 and 18 or 810-mm downstream from the center of post no. 17, as shown in Figure 46. Actual vehicle impact occurred 873.5-mm downstream from the center of post no. 17. At 0.046 sec after impact, the right-front corner of the vehicle was at post no. 19. At 0.054 sec, the right-front tire snagged on post no. 19 with the right-front fender deforming inward. At 0.077 sec, the front of the vehicle deflected post no. 20 backward as post no. 19 twisted causing the guardrail to release from post no. 19. At 0.088 sec, post no. 20 had deflected downstream and rotated backward approximately 45 degrees. At 0.091 sec, the right-front tire contacted post no. 20 as the guardrail released from post no. 20. At this same time, post no. 21 was twisting and deflecting backward as post no. 22 began to deflect. At 0.113 sec, the vehicle began to redirect with post no. 20 located under the vehicle. At this same time, post no. 22 twisted as post no. 20 nearly deflected toward the ground. At 0.136 sec, the wooden blockout at post no. 20 disengaged from the system. At 0.141 sec, the right-front corner of the vehicle reached its maximum intrusion of 899 mm over the rail. At 0.152 sec, the front of the vehicle was at post no. 22, and post no. 21 was located under the vehicle. At this same time, post no. 24 twisted. At 0.162 sec, the wooden blockout at post no. 22 had disengaged from the system. At 0.170 sec, the right-rear tire

was at post no. 18. At 0.186 sec, the front of the vehicle was at post no. 23. At 0.206 sec, the rear of the vehicle extended over the rail near post no. 18 as the vehicle began to pitch forward. At this same time, post no. 23 was positioned under the vehicle as post no. 24 was deflected slightly. At 0.216 sec, the right-rear tire contacted post no. 23. At 0.238 sec, the vehicle encountered slight counter-clockwise (CCW) roll toward the rail. The vehicle became parallel to the guardrail at 0.257 sec after impact with a resultant velocity of 68.5 km/hr. At this same time, post nos. 20 through 24 were positioned under the vehicle. At 0.289 sec, the front of the vehicle was at post no. 25. At 0.310 sec, both rear tires were airborne with the rear of the vehicle located over the rail. At 0.336 sec, the front of the vehicle was no longer in contact with the guardrail while the rear of the vehicle was at post no. 20. At 0.383 sec, the truck box reached its maximum intrusion of 784 mm over the rail. At 0.438 sec, the right-rear tire was positioned over the top of the rail. At 0.445 sec, the vehicle showed more CCW roll toward the rail. At 0.485 sec, the right-rear corner of the vehicle was at post no. 23. At this same time, the vehicle continued to roll CCW toward the rail and encountered significant pitching toward its right-front corner. At 0.498 sec, the right-front corner of the vehicle contacted the ground. At 0.544 sec after impact, the left-rear tire was airborne. At 0.578 sec after impact, the vehicle exited the guardrail at a trajectory angle of 19.5 degrees and at a resultant velocity of 62.9 km/hr. At 0.621 sec, the vehicle reached its maximum pitch angle of 11.4 degrees downward. At 0.635 sec, the right-rear corner of the vehicle was near post no. 25. At 0.656 sec, the vehicle began to roll clockwise (CW) away from the rail. At 0.712 sec, the rear of the truck began to descend toward the ground. At 0.875 sec, the vehicle reached its maximum CW roll angle of 4.5 degrees away from the rail. At 1.014 sec, the trajectory of the vehicle showed that the vehicle yawed back toward the system. At 1.613 sec, the vehicle reached its maximum CCW roll

angle of 10.7 degrees. The vehicle's post-impact trajectory is shown in Figures 40 and 47. The vehicle came to rest 24.41-m downstream from impact and 2.13-m laterally away from the traffic-side face of the rail, as shown in Figures 40 and 47.

11.3 Barrier Damage

Damage to the barrier was moderate, as shown in Figures 48 through 62. Barrier damage consisted mostly of deformed W-beam, contact marks on a guardrail section, and deformed guardrail posts.

The guardrail damage consisted of moderate deformation and flattening of the impacted section of the W-beam rail between post nos. 18 and 24. Contact marks were found on the guardrail between post nos. 18 and 25. The guardrail was buckled at 305-mm downstream from the center of post no. 25. The W-beam was pulled off of post nos. 19 through 23. No significant guardrail damage occurred upstream of post no. 17 nor downstream of post no. 26.

Steel post no. 18 rotated backward slightly while steel post no. 19 bent laterally backward and longitudinally downstream. Steel post nos. 20 through 22 were bent longitudinally toward the ground in the downstream direction. Steel post no. 23 was bent longitudinally downstream but not as extensively as post nos. 20 through 22. Steel post no. 24 was slightly twisted and bent longitudinally downstream. Contact marks were found on the front face of post nos. 18 through 24. No significant post damage occurred to post nos. 1 through 17 nor 25 through 41. The upstream anchorage system was slightly moved longitudinally, while the downstream anchorage system remained unmoved. The posts in both the upstream and downstream anchorage systems were not damaged.

The wooden blockout at post no. 20 disengaged from the system and came to rest

approximately 7.6-m downstream from its original position and 15.2-m laterally from the backside of the system. The blockout at post no. 21 split into many pieces and disengaged from the post bolt. The wooden blockout bolt at post no. 22 sheared on the rail side and the blockout disengaged from the system. The blockout bolt at post no. 23 bent and subsequently rotated the blockout toward the upstream side of the post. The blockouts at post nos. 3 through 19 and 24 through 39 remained undamaged.

The permanent set of the guardrail and posts is shown in Figures 48 through 59. The upstream cable anchor end encountered slight permanent set deformations, as shown in Figure 62. The maximum lateral permanent set rail and post deflections were approximately 401 mm at the centerline of post no. 21 and 315 mm at post no. 19, respectively, as determined from high-speed film analysis. The maximum lateral dynamic rail and post deflections were 416 mm at post no. 19, as determined from the high-speed film analysis.

11.4 Vehicle Damage

Exterior vehicle damage was moderate, as shown in Figures 63 through 65. Minimal occupant compartment deformations occurred with only slight deformations of the firewall. Occupant compartment deformations and the corresponding locations are provided in Appendix E. Contact marks were found along the lower portion of the entire right side of the vehicle. The right-front fender was deformed downward and inward toward the engine compartment. The right-front side of the bumper was deformed inward and contacted the upper A-frame control arm. A buckling point was found at the center of the front bumper. The right-front steel rim was deformed, and the tire was torn and deflated. Scuff marks were found on the right-rear tire side wall. The right-side headlight region was crushed inward toward the engine compartment, and the headlight broke. The

grill was only broken and deformed around the right-side headlight. The windshield sustained six minor vertical cracks. The roof, the hood, the left side, and the rear of the vehicle remained undamaged. The left-side, right-side, and rear window glass also remained undamaged.

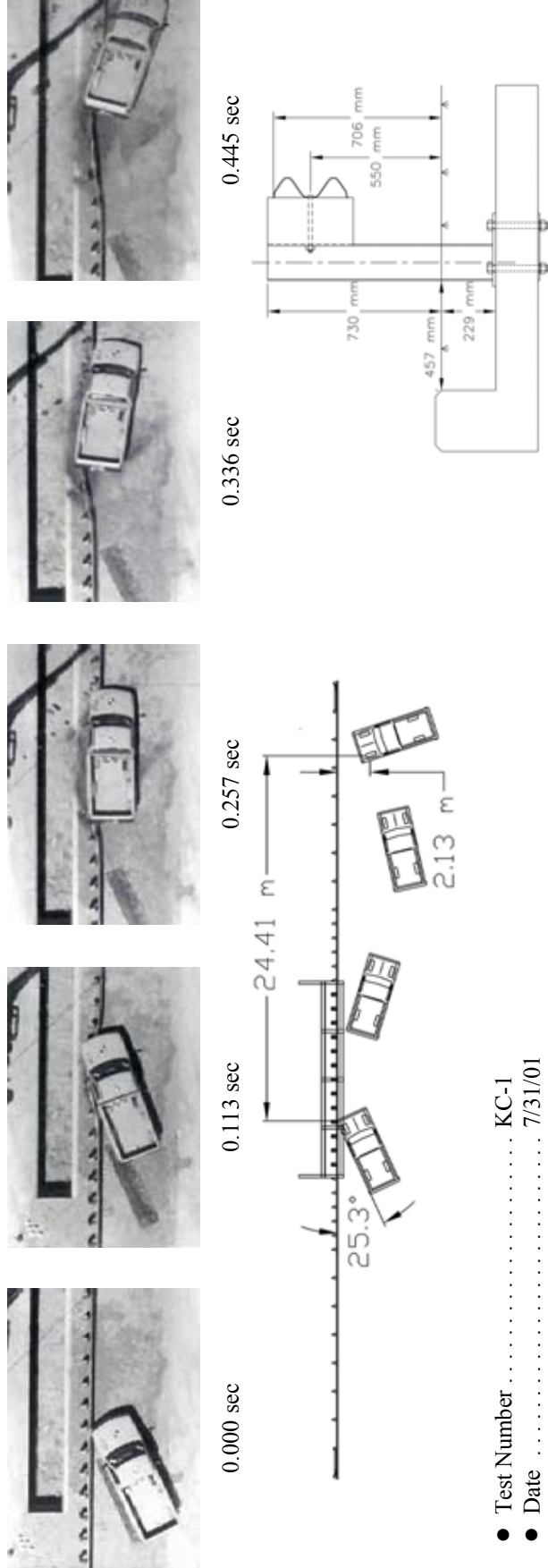
11.5 Occupant Risk Values

The longitudinal and lateral occupant impact velocities were determined to be 6.62 m/sec and 4.99 m/sec, respectively. The maximum 0.010-sec average occupant ridedown decelerations in the longitudinal and lateral directions were 8.28 g's and 10.12 g's, respectively. It is noted that the occupant impact velocities (OIV's) and occupant ridedown decelerations (ORD's) were within the suggested limits provided in NCHRP Report No. 350. The results of the occupant risk, determined from the accelerometer data, are summarized in Figure 40. Results are shown graphically in Appendix F. The results from the rate transducer are shown graphically in Appendix G.

11.6 Discussion

The analysis of the test results for test KC-1 showed that the W-beam guardrail attached to the concrete box culvert adequately contained and redirected the vehicle with controlled lateral displacements of the barrier system. There were no detached elements nor fragments which showed potential for penetrating the occupant compartment nor presented undue hazard to other traffic. Deformations of, or intrusion into, the occupant compartment that could have caused serious injury did not occur. The test vehicle did not penetrate or ride over the W-beam guardrail and remained upright during and after the collision. Vehicle roll, pitch, and yaw angular displacements were noted, but they were deemed acceptable because they did not adversely influence occupant risk safety criteria nor cause rollover. After collision, the vehicle's trajectory revealed minimum

intrusion into adjacent traffic lanes. In addition, the vehicle's exit angle of 19.5 degrees was greater than 60 percent of the impact angle of 25.3 degrees. However, it should be noted that this evaluation criterion is only preferred and not required. Therefore, test KC-1 conducted on the W-beam guardrail attached to the concrete box culvert was determined to be acceptable according to the TL-3 safety performance criteria found in NCHRP Report No. 350.



● Test Number	KC-1	● Vehicle Angle	
● Date	7/31/01	Impact	25.3 deg
● Appurtenance	W-beam guardrail with steel posts attached to culvert's top slab	Exit (trajectory)	19.5 deg
● Total Length	53.34 m	● Vehicle Snagging	Minor on post nos. 19 and 20
● Distance Between Posts and Headwall	457 mm	● Vehicle Pocketing	None
● Steel W-Beam		● Vehicle Stability	Satisfactory
Thickness	2.66 mm	● Occupant Ridedown Deceleration (10 msec avg.)	
Top Mounting Height	706 mm	Longitudinal	8.28 < 20 G's
● Steel Posts		Lateral (not required)	10.12
Post Nos. 3 - 14, 28 - 39	W152x13.4 by 1,829-mm long	● Occupant Impact Velocity	
Post Nos. 15 - 27	W152x13.4 by 946-mm long	Longitudinal	6.62 < 12 m/s
● Wood Posts		Lateral (not required)	4.99
Post Nos. 1 - 2, 40 - 41 (BCT) ...	140 mm x 190 mm by 1,080-mm long	● Vehicle Damage	Moderate
● Wood Spacer Blocks		TAD ¹⁷	1-RFQ-4
Post Nos. 2 - 39	152 mm x 203 mm by 356-m long	SAE ¹⁸	1-RFEE5
● Soil Type	Grading B - AASHTO M 147-65 (1990)	● Vehicle Stopping Distance	24.41 m downstream
● Vehicle Model	1994 GMC 2500 ¾-ton pickup	2.13 m traffic-side face	
Curb	1,750 kg	● Barrier Damage	Moderate
Test Inertial	1,993 kg	● Maximum Deflections	
Gross Static	1,993 kg	Permanent Set	401 mm
● Vehicle Speed		Dynamic	416 mm
Impact	103.3 km/hr	● Working Width	899 mm
Exit (resultant)	62.9 km/hr		

Figure 40. Summary of Test Results and Sequential Photographs, Test KC-1



0.000 sec



0.100 sec



0.200 sec



0.367 sec



0.534 sec



0.701 sec



0.000 sec



0.078 sec



0.116 sec



0.206 sec



0.288 sec



0.412 sec

Figure 41. Additional Sequential Photographs, Test KC-1



0.042 sec



0.000 sec



0.116 sec



0.036 sec



0.246 sec



0.054 sec



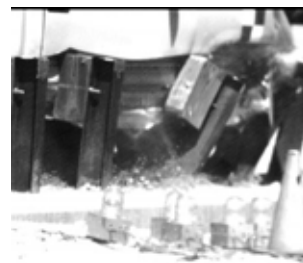
0.354 sec



0.068 sec



0.744 sec



0.090 sec

Figure 42. Additional Sequential Photographs, Test KC-1



Figure 43. Documentary Photographs, Test KC-1



Figure 44. Documentary Photographs, Test KC-1

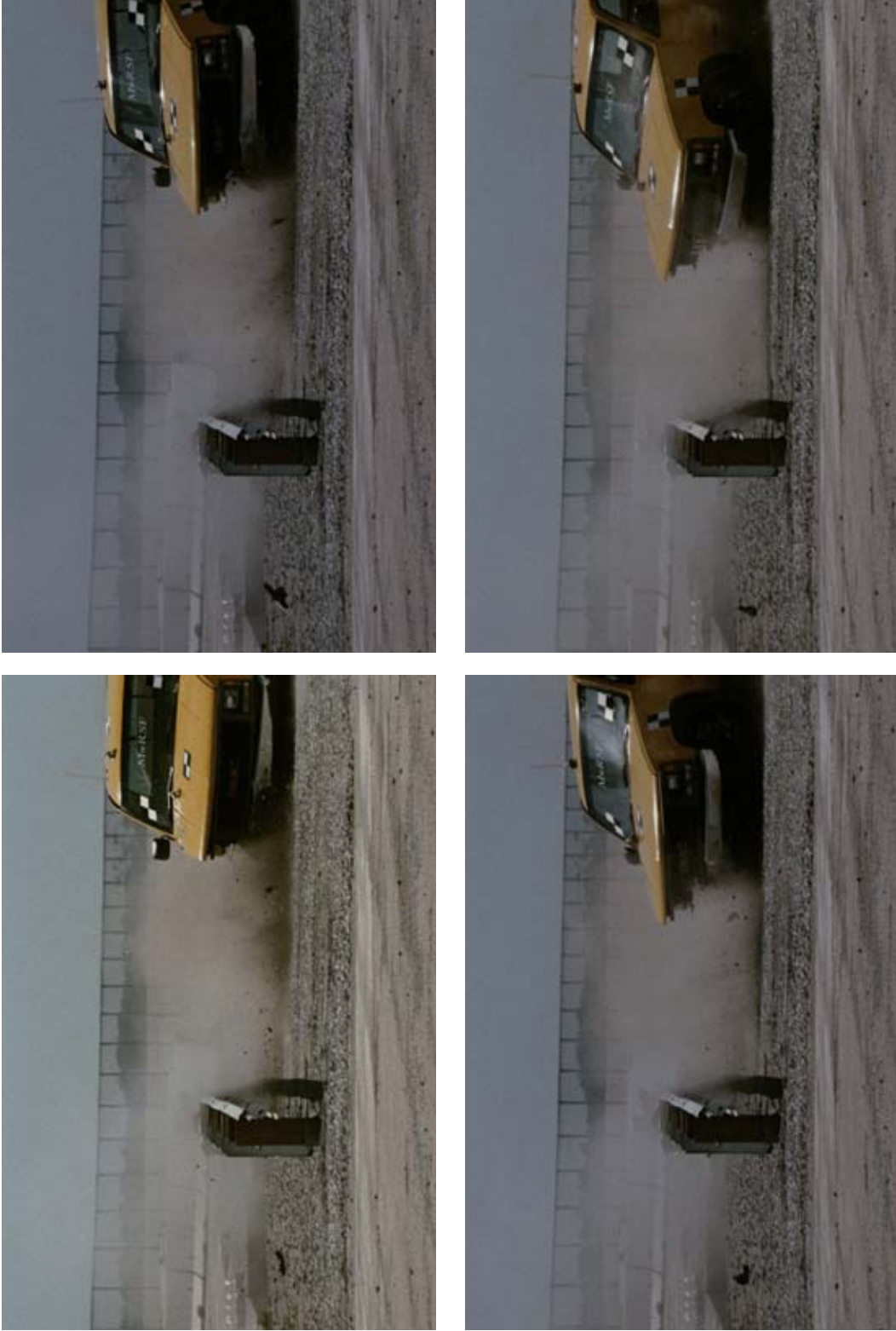


Figure 45. Documentary Photographs, Test KC-1



Figure 46. Impact Location, Test KC-1



Figure 47. Vehicle Final Position and Trajectory Marks, Test KC-1



Figure 48. W-Beam Guardrail System Damage, Test KC-1



Figure 49. W-Beam Guardrail System Damage, Test KC-1



Figure 50. W-Beam Guardrail System Damage, Test KC-1



Figure 51. W-Beam Guardrail System Damage, Test KC-1



Figure 52. Post Nos. 18 and 19 Damage, Test KC-1



Figure 53. Post Nos.18 and 19 Damage, Test KC-1



Figure 54. Post Nos. 20 and 21 Damage, Test KC-1



Figure 55. Post Nos. 20 and 21 Damage, Test KC-1



Figure 56. Post Nos. 22 and 23 Damage, Test KC-1



Figure 57. Post Nos. 22 and 23 Damage, Test KC-1



Figure 58. Post Nos. 24 and 25 Damage, Test KC-1



Figure 59. Post Nos. 24 and 25 Damage, Test KC-1



Figure 60. Culvert's Top Slab Damage, Test KC-1



Figure 61. Culvert's Top Slab Damage, Test KC-1



Figure 62. End Anchorage Permanent Set Deflection, Test KC-1



Figure 63. Vehicle Damage, Test KC-1



Figure 64. Vehicle's Right-Side Damage, Test KC-1



Figure 65. Occupant Compartment Deformations, Test KC-1

12 W-BEAM GUARDRAIL SYSTEM DESIGN DETAILS (OPTION NO. 2)

The alternative installation of a guardrail system for use over a low-fill culvert was identical to the previous system except for the lateral placement of the steel posts with respect to the culvert's headwall. In option no. 1 (test KC-1), the back side of the steel posts were positioned 457 mm away from the front face of the culvert's headwall. For option no. 2, the back side of the steel posts were positioned only 25 mm away from the front face of the culvert's headwall. Additionally, option no. 2 used four individual ASTM A36 steel washer plates measuring 6.4-mm thick x 114-mm wide x 152-mm long, one at each bolt location of post nos. 18 through 20 and 22.

Once again, the test installation consisted of 53.34 m of standard 2.66-mm thick W-beam guardrail supported by steel posts, as shown in Figures 66 through 69. Also, anchorage systems similar to those used on tangent guardrail terminals were utilized on both the upstream and downstream ends of the guardrail system. Photographs of the test installation are shown in Figure 70 through 73.



W152x13.4 steel posts, 946-mm long with 152x203x356 routed wood blockouts
(Post nos. 15 through 17, 21, and 23 through 27)

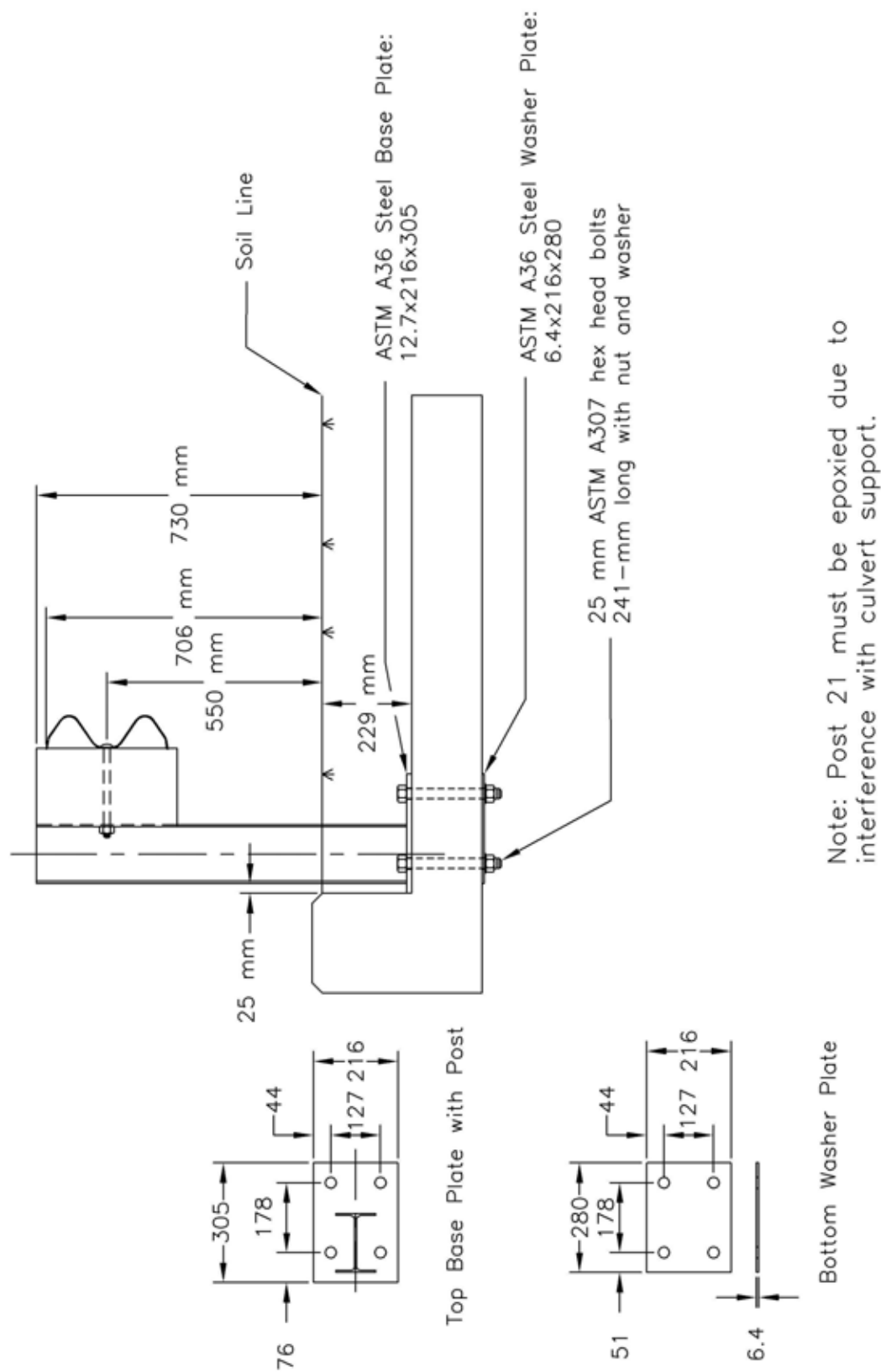


Figure 67. W-Beam Guardrail Attached to a Low-Fill Culvert Post Nos. 15 through 17, 21, and 23 through 27 (Option No. 2)

W152x13.4 steel posts, 946-mm long with 152x203x356 routed wood blockouts
(Post nos. 18 through 20 and 22)

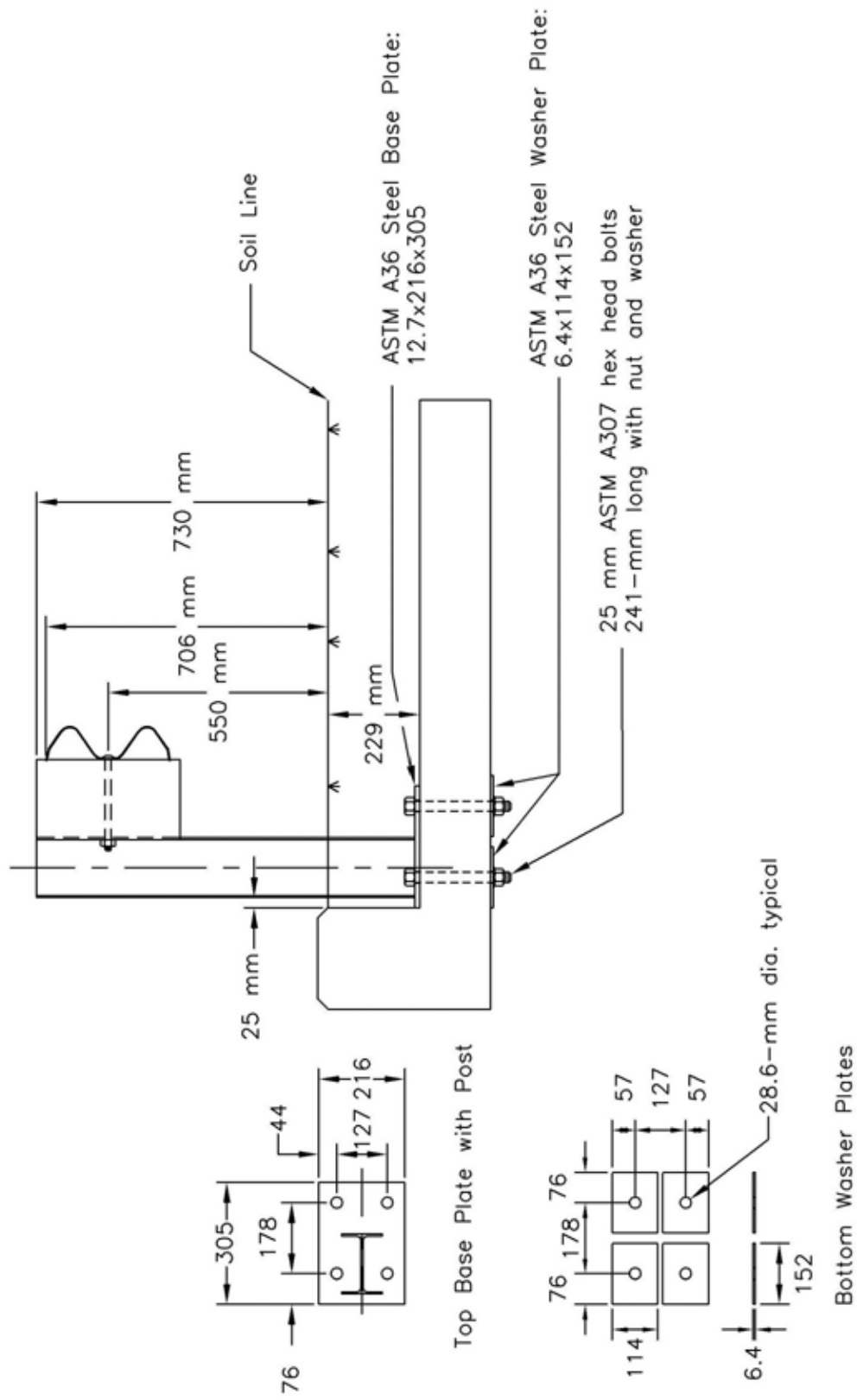
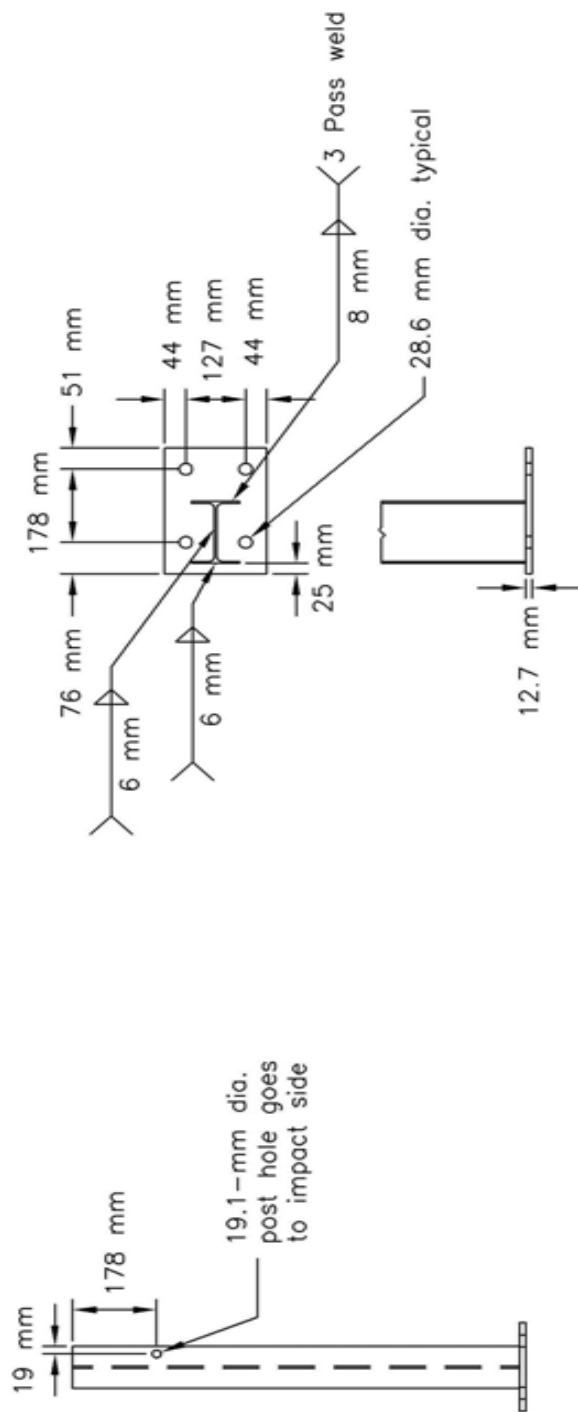
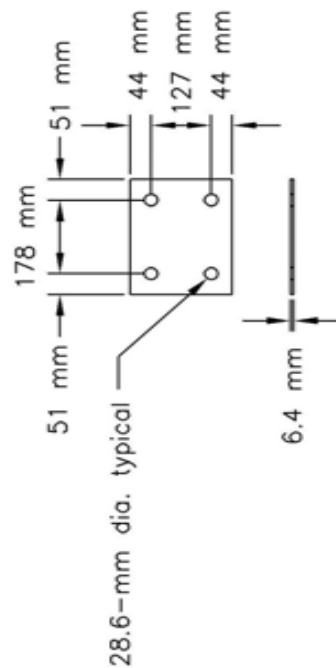


Figure 68. W-Beam Guardrail Attached to a Low-Fill Culvert Post Nos. 18 through 20 and 22 (Option No. 2)

Top Base Plate With Post Position



Bottom Washer Plate (Post nos. 15-17, 23-27)



Bottom Washer Plate (Post nos. 18-20, 22)

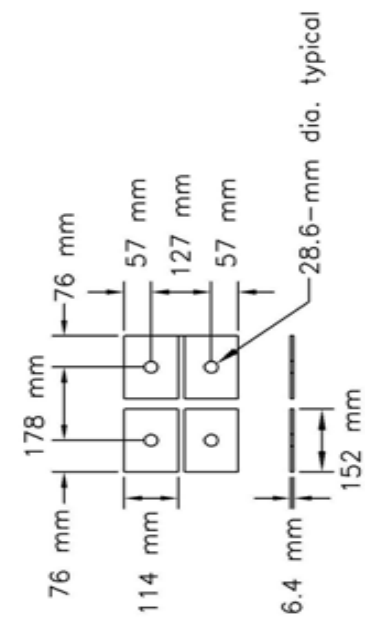


Figure 69. W-Beam Guardrail Attached to a Low-Fill Culvert (Option No. 2)



Figure 70. W-Beam Guardrail Attached to a Low-Fill Culvert (Option No. 2)



Figure 71. Typical Posts for W-Beam Guardrail Attached to a Low-Fill Culvert (Option No.2)



Figure 72. Steel Washer Plate Connection Details on Bottom Side of Culvert's Top Slab



Figure 73. End Anchorage Systems

13 CRASH TEST NO. 2 (OPTION NO. 2)

13.1 Test KC-2

The 1,994-kg pickup truck impacted the W-beam guardrail at a speed of 99.7 km/hr and at an angle of 24.8 degrees. A summary of the test results and the sequential photographs are shown in Figure 74. Additional sequential photographs are shown in Figures 75 through 77. Documentary photographs of the crash test are shown in Figures 78 and 79.

13.2 Test Description

Initial impact was to occur between post nos. 17 and 18 or 810-mm downstream from the center of post no. 17, as shown in Figure 80. Actual vehicle impact occurred 937-mm downstream from the center of post no. 17. At 0.036 sec after impact, the right-front corner of the vehicle was at post no. 19. At 0.074 sec, the right-front corner of the vehicle was at post no. 20 as post no. 19 continued to deflect backwards. At 0.100 sec, the front of the vehicle was at post no. 21 as the rear end of the vehicle began to yaw toward the rail. At this same time, the right-front tire snagged on post no. 20 and caused the post to deflect downstream. Also, at this time, the guardrail released away from post no. 20, and the wooden blockout had rotated about the bolt. At 0.110 sec, the top of the rail buckled between post nos. 22 and 23. At 0.122 sec, the guardrail released away from post no. 21, and the wooden blockout released off of post no. 21. At 0.130 sec, the right-front corner of the vehicle reached its maximum intrusion of 781 mm over the rail. At 0.140 sec, the front of the vehicle was at post no. 22 as the vehicle began to redirect and roll CCW toward the rail. At 0.200 sec, the right-rear corner of the vehicle was located over the rail near post no. 19 as it began to extend over the top of the rail. At 0.222 sec, the vehicle's front-end pitched downward. At 0.240 sec, the right-front corner of the vehicle was at post no. 24. At 0.252 sec, the right-rear tire was

airborne. The vehicle became parallel to the guardrail at 0.260 sec after impact with a resultant velocity of 69.4 km/hr. At 0.272 sec, the right-rear tire appeared to have snagged on post no. 21 as the vehicle began to roll CCW toward the rail. At 0.282 sec, the right-front corner of the vehicle lost contact with the system near post no. 25. At 0.350 sec, the truck box reached its maximum intrusion of 741 mm over the rail. At 0.405 sec, the vehicle reached its maximum yaw angle of 33.4 degrees. At 0.412 sec, the vehicle showed significant CCW roll toward the rail. At this same time, the right-rear corner of the vehicle was at the midspan between post nos. 21 and 22. At 0.495 sec after impact, the vehicle exited the guardrail at a trajectory angle of 11.8 degrees and at a resultant velocity of 68.0 km/hr. At this same time, the front of the vehicle continued to pitch downward as it rolled CCW toward the rail and reached its maximum roll angle of 7.5 degrees toward the rail. At 0.544 sec, the right-front corner of the vehicle contacted the ground. At 0.598 sec, the vehicle began to roll CW away from the rail as the right side of the front bumper remained in contact with the ground. At 0.621 sec, the rear of the truck reached its maximum pitch angle of 7.7 degrees. At 0.651 sec, the vehicle showed significant CW roll away from the rail. At 1.646 sec, the vehicle had rolled onto its left side with the rear portion of the truck airborne. At 3.426 sec, the vehicle had returned to an upright position after rolling completely over. The vehicle's post-impact trajectory is shown in Figures 74 and 81. The vehicle came to rest 24.56-m downstream from impact and 2.77-m laterally away from the traffic-side face of the rail, as shown in Figures 74 and 81.

13.3 Barrier Damage

Damage to the barrier was moderate, as shown in Figures 82 through 89. Barrier damage consisted mostly of deformed W-beam, contact marks on a guardrail section, and deformed guardrail posts.

The guardrail damage consisted of moderate deformation and flattening of the lower portion of the impacted section of the W-beam rail between post nos. 17 and 23. Deformation and flattening of the upper portion of the impacted section of W-beam rail occurred between post nos. 17 and 24. Contact marks were found on the guardrail between post nos. 17 and 24. The bottom of the guardrail at post no. 19 deformed around the bottom of the wood blockout. The top of the guardrail was buckled at 152-mm downstream from the center of post no. 24. The W-beam was pulled off of post nos. 20 through 22. No significant guardrail damage occurred upstream of post no. 17 nor downstream of post no. 25.

Steel post nos. 3 through 17 were twisted slightly. Steel post no. 18 rotated backward near the ground. Steel post nos. 19 through 22 were twisted and bent toward the ground. The traffic-side of steel post no. 19 was deformed 787 mm from the top, and the back side of this post was deformed against the concrete. Significant soil movement was observed around post no. 19. At post no. 19, severe concrete spalling was found on the headwall. Contact marks were found on the front face of post nos. 19 through 21. The wooden blockout at post nos. 20 through 23 remained attached to the posts but were rotated and damaged. No significant post damage or movement occurred to post nos. 23 through 41, and the blockouts at post nos. 3 through 19 and 24 through 39 remained undamaged. The upstream anchorage system was slightly moved longitudinally, while the downstream anchorage system remained unmoved. The posts in both the upstream and downstream anchorage systems were not damaged.

The permanent set of the guardrail and posts is shown in Figures 82 through 88. The upstream cable anchor end encountered slight permanent set deformations, as shown in Figure 89. The maximum lateral permanent set rail and post deflections were approximately 279 mm at the

centerline of post no. 21 and 459 mm at post no. 20, as determined from the high-speed film analysis. The maximum lateral dynamic rail and post deflections were 473 mm at post no. 22, as determined from the high-speed film analysis.

13.4 Vehicle Damage

Exterior vehicle damage was extensive, as shown in Figures 90 through 92. Minimal occupant compartment deformations occurred with only slight deformation of the forward floorpan area. Occupant compartment deformations and the corresponding locations are provided in Appendix H. Light contact marks were found along the lower portion of the entire right side of the vehicle. The front corner of the right-front fender was deformed downward and inward toward the engine compartment. The sheet metal at the joint between the lower-front portion of the right-side door and the right-front fender was sliced open and then crushed inward. The right-front side of the bumper was flattened and deformed inward. A buckling point was found at the center of the front bumper. The right-front steel rim was severely deformed, and the tire was removed from the steel rim. The front, rear, right-side, and left-side window glass as well as the sheet metal on the roof and the left-side fender and door were severely crushed during vehicle rollover. The rear of the vehicle and the right-rear, left-front, and left-rear tires and steel rims remained undamaged.

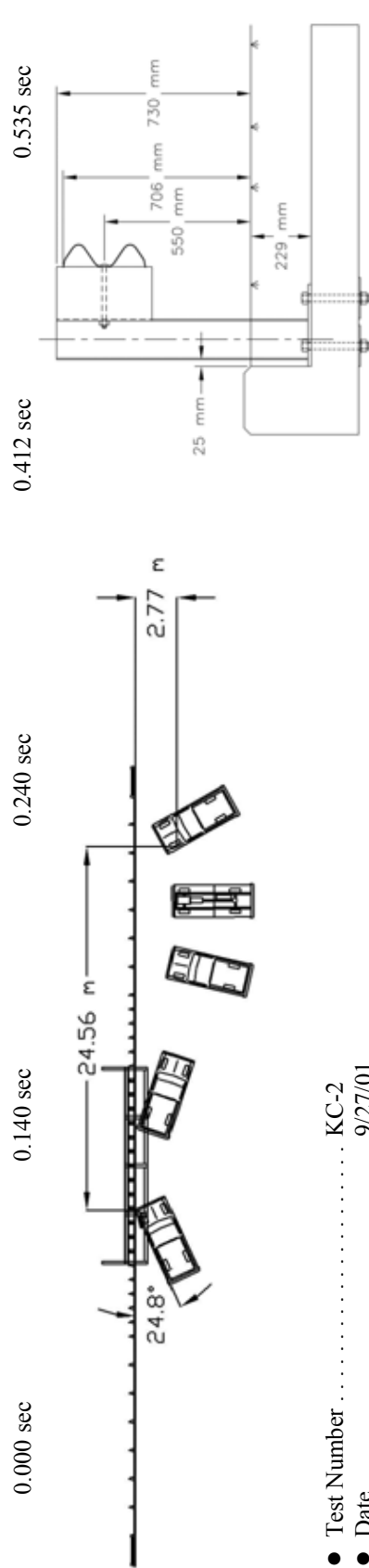
13.5 Occupant Risk Values

The longitudinal and lateral occupant impact velocities were determined to be 5.90 m/sec and 5.10 m/sec, respectively. The maximum 0.010-sec average occupant ridedown decelerations in the longitudinal and lateral directions were 11.59 g's and 10.24 g's, respectively. It is noted that the occupant impact velocities (OIV's) and occupant ridedown decelerations (ORD's) were within the suggested limits provided in NCHRP Report No. 350. The results of the occupant risk,

determined from the accelerometer data, are summarized in Figure 74. Results are shown graphically in Appendix I. The results from the rate transducer are shown graphically in Appendix J.

13.6 Discussion

The analysis of the test results for test KC-2 showed that the W-beam guardrail attached to the concrete box culvert adequately contained the vehicle, but inadequately redirected the vehicle since the vehicle did not remain upright after collision with the W-beam guardrail system. There were no detached elements nor fragments which showed potential for penetrating the occupant compartment nor presented undue hazard to other traffic. Deformations of, or intrusion into, the occupant compartment that could have caused serious injury did not occur. After collision, the vehicle's trajectory revealed minimum intrusion into adjacent traffic lanes, but the roll over of the vehicle was unacceptable. In addition, the vehicle's exit angle was less than 60 percent of the impact angle. Therefore, test KC-2 conducted on the W-beam guardrail attached to the concrete box culvert was determined to be unacceptable according to the TL-3 safety performance criteria found in NCHRP Report No. 350.



● Test Number	KC-2	● Vehicle Angle	Impact	24.8 deg
● Date	9/27/01	Exit (trajectory)	17.3 deg	17.3 deg
● Appurtenance	W-beam guardrail with steel posts attached to culvert's top slab	● Vehicle Snagging	Wheel snag on post no. 20	
● Total Length	53.34 m	● Vehicle Pocketing	None	
● Distance Between Posts and Headwall	25 mm	● Vehicle Stability	Vehicle rollover	
● Steel W-Beam		● Occupant Ridedown Deceleration (10 msec avg.)	Longitudinal	11.59 < 20 G's
Thickness	2.66 mm	Lateral (not required)	10.24	
Top Mounting Height	706 mm	● Occupant Impact Velocity	Longitudinal	5.90 < 12 m/s
● Steel Posts		Lateral (not required)	5.10	
Post Nos. 3 - 14, 28 - 39	W152x13.4 by 1,829-mm long	● Vehicle Damage	Extensive	
Post Nos. 15 - 27	W152x13.4 by 946-mm long	TAD ¹⁷	1-R&T-4	
● Wood Posts		SAE ¹⁸	1-RYAE9	
Post Nos. 1 - 2, 40 - 41 (BCT)	140 mm x 190 mm by 1,080-mm long	● Vehicle Stopping Distance	24.56 m downstream	
● Wood Spacer Blocks		● Barrier Damage	2.77 m traffic-side face	
Post Nos. 2 - 39	152 mm x 203 mm by 356-m long	● Maximum Deflections	Moderate	
● Soil Type	Grading B - AASHTO M 147-65 (1990)	Permanent Set	459 mm	
● Vehicle Model	1994 Chevrolet 2500 ¾-ton pickup	Dynamic	473 mm	
Curb	1,840 kg	● Working Width	781 mm	
Test Inertial	1,994 kg			
Gross Static	1,994 kg			
● Vehicle Speed				
Impact	99.7 km/hr			
Exit (resultant)	68.0 km/hr			

Figure 74. Summary of Test Results and Sequential Photographs, Test KC-2



0.000 sec



0.196 sec



0.040 sec



0.248 sec



0.100 sec



0.284 sec



0.126 sec



0.346 sec



0.160 sec



0.424 sec

Figure 75. Additional Sequential Photographs, Test KC-2



0.000 sec



0.252 sec



0.060 sec



0.272 sec



0.100 sec



0.476 sec



0.148 sec



0.696 sec

Figure 76. Additional Sequential Photographs, Test KC-2



0.000 sec



0.000 sec



0.066 sec



0.233 sec



0.166 sec



0.667 sec



0.267 sec



1.201 sec



0.467 sec



1.835 sec

Figure 77. Additional Sequential Photographs, Test KC-2



Figure 78. Documentary Photographs, Test KC-2



Figure 79. Documentary Photographs, Test KC-2



Figure 80. Impact Location, Test KC-2



Figure 81. Final Vehicle Position and Trajectory Marks, Test KC-2



Figure 82. W-Beam Guardrail System Damage, Test KC-2



Figure 83. W-Beam Guardrail System Damage, Test KC-2

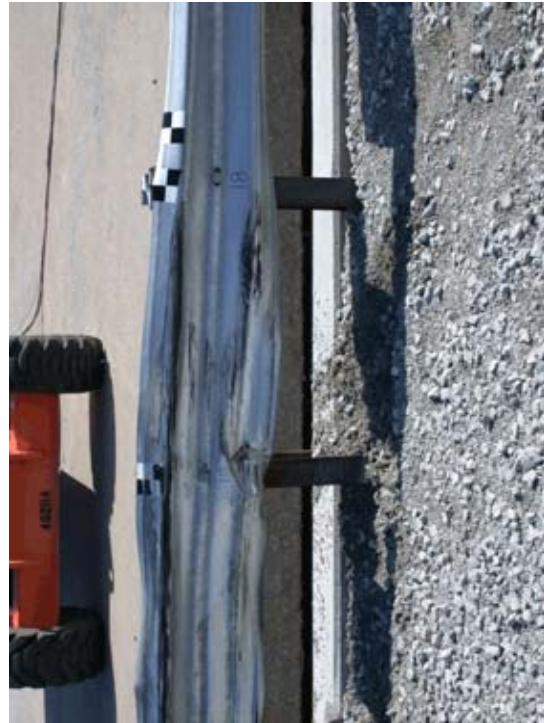


Figure 84. W-Beam Guardrail System Damage, Test KC-2



Figure 85. Post Nos. 18 and 19 Damage, Test KC-2



Figure 86. Post Nos. 20 and 21 Damage, Test KC-2



Figure 87. Post Nos. 22 and 23 Damage, Test KC-2



Figure 88. Post Nos. 24 and 25 Damage, Test KC-2



Figure 89. End Anchorage Permanent Set Deflections, Test KC-2



Figure 90. Vehicle Damage, Test KC-2



Figure 91. Vehicle Right-Front Corner Damage, Test KC-2



Figure 92. Undercarriage Vehicle Damage, Test KC-2

14 SUMMARY AND CONCLUSIONS

Two W-beam guardrail systems for attachment to the top of a low-fill concrete culvert were designed, tested, and evaluated. The full-scale vehicle crash tests were performed according to the TL-3 criteria found in NCHRP Report No. 350.

The first guardrail system (Option No. 1) was configured with W-beam rail supported by steel posts. Thirteen of the steel posts were attached to the concrete culvert's top slab with the back side of the posts placed 457 mm away from the front of the headwall. One full-scale vehicle crash test, KC-1, was performed on this guardrail system with a $\frac{3}{4}$ -ton pickup truck and was determined to be acceptable according to the TL-3 safety performance criteria presented in NCHRP Report No. 350. From an analysis of the crash test results of KC-1, it should be noted that the bulk of the post motion occurred at the ground line of the impact and was found to be 254 mm.

The second guardrail system (Option No. 2) was basically identical to the first system except for the placement of the steel posts attached to the culvert. For this design, the steel posts were spaced 25 mm away from the front of the culvert's headwall. Once again, one full-scale vehicle crash test, KC-2, was performed on this guardrail system with a $\frac{3}{4}$ -ton pickup truck. During vehicle redirection, the pickup truck rolled over, and the test was determined to be unacceptable according to the TL-3 safety performance criteria presented in NCHRP Report No. 350. The vehicle's instability was attributed to the interaction of the vehicle's front tire and suspension with the steel post immediately beyond impact. The headwall of the culvert prevented the post from continuing to rotate backward, and subsequently caused a snag point for the vehicle's tire. A summary of the safety performance evaluation is provided in Table 6. A comparison of the accelerometer data for

tests KC-1 and KC-2 is shown in Appendix K. Similarly, a comparison of the rate transducer data for both tests is shown in Appendix L.

Table 6. Summary of Safety Performance Evaluation Results

Evaluation Factors	Evaluation Criteria	Test KC-1	Test KC-2
Structural Adequacy	A. Test article should contain and redirect the vehicle; the vehicle should not penetrate, underide, or override the installation although controlled lateral deflection of the test article is acceptable.	S	S
Occupant Risk	D. Detached elements, fragments or other debris from the test article should not penetrate or show potential for penetrating the occupant compartment, or present an undue hazard to other traffic, pedestrians, or personnel in a work zone. Deformations of, or intrusions into, the occupant compartment that could cause serious injuries should not be permitted.	S	S
	F. The vehicle should remain upright during and after collision although moderate roll, pitching, and yawing are acceptable.	S	U
Vehicle Trajectory	K. After collision it is preferable that the vehicle's trajectory not intrude into adjacent traffic lanes.	S	U
	L. The occupant impact velocity in the longitudinal direction should not exceed 12 m/sec, and the occupant ridedown acceleration in the longitudinal direction should not exceed 20 G's.	S	S
	M. The exit angle from the test article preferably should be less than 60 percent of test impact angle measured at time of vehicle loss of contact with test device.	M	S

S - Satisfactory
M - Marginal
U - Unsatisfactory
NA - Not Available

15 RECOMMENDATIONS

A strong-post, W-beam guardrail system for rigid attachment to the surface of low-fill concrete culverts was developed and successfully crash tested according to the criteria found in NCHRP Report No. 350 and is a suitable design for use on Federal-aid highways. The new guardrail system was configured with W152 x 13.4 steel posts spaced 952.5-mm on center and with the back side positioned 457 mm away from the front of the culvert's headwall.

From the results of tests KC-1 and KC-2, it was shown that a potential exists for vehicular instabilities or rollover to occur if the guardrail is placed too close to the culvert headwall. This phenomenon is the result of the system's posts being unable to rotate near the base due to contact with the top of the headwall, thus resulting in wheel snag on the posts, as seen in test KC-2. From an analysis of the KC-1 and KC-2 crash test results, it is recommended that the backside face of the steel posts can be positioned a minimum of 254 mm away from the front face of the culvert's headwall and still maintain acceptable barrier performance. However, any design modifications made to the guardrail system can only be verified through the use of full-scale crash testing.

Finally, it should be noted that the W-beam guardrail system was configured with the entire length installed tangent. However, in actual field installations, this guardrail system can be installed with either one or two ends flared away from the traveled way. For locations where a guardrail flare will be used, the flare rates should follow the recommended guidelines provided in AASHTO's *Roadside Design Guide* (8).

16 REFERENCES

1. Polivka, K.A., Bielenberg, B.W., Sicking, D.L., Faller, R.K., and Rohde, J.R., *Development of a 7.62-m Long Span Guardrail System*, Final Report to the Midwest State's Regional Pooled Fund Program, Transportation Report No. TRP-03-72-99, Project No. SPR-3(017)-Year 7, Midwest Roadside Safety Facility, University of Nebraska-Lincoln, April 6, 1999.
2. Polivka, K.A., Bielenberg, B.W., Sicking, D.L., Faller, R.K., Rohde, J.R., and Keller, E.A., *Development of a 7.62-m Long Span Guardrail System – Phase II*, Final Report to the Midwest State's Regional Pooled Fund Program, Transportation Report No. TRP-03-88-99, Project No. SPR-3(017)-Year 9, Midwest Roadside Safety Facility, University of Nebraska-Lincoln, August 13, 1999.
3. Faller, R.K., Sicking, D.L., Polivka, K.A., Rohde, J.R., and Bielenberg, R.W., *A Long-Span Guardrail System for Culvert Applications*, Transportation Research Record No. 1720, Transportation Research Board, National Research Council, Washington, D.C., 2000.
4. Hirsch, T.J., and Beggs, D., *Use of Guardrails on Low Fill Bridge Length Culverts*, Transportation Research Record No. 1198, Transportation Research Board, National Research Council, Washington, D.C., 1988.
5. Michie, J.D., *Recommended Procedures for the Safety Performance Evaluation of Highway Appurtenances*, National Cooperative Highway Research Program (NCHRP) Report No. 230, Transportation Research Board, Washington, D.C., March 1981.
6. Pfeifer, B.G., and Luedke, J.K., *Safety Performance Evaluation of a Nested W-Beam with Half-Post Spacing Over a Low-Fill Culvert*, Final Report to the Kansas Department of Transportation, Transportation Report No. TRP-03-36-92, Midwest Roadside Safety Facility, University of Nebraska-Lincoln, March 1993.
7. Ross, H.E., Sicking, D.L., Zimmer, R.A., and Michie, J.D., *Recommended Procedures for the Safety Performance Evaluation of Highway Features*, National Cooperative Research Program (NCHRP) Report No. 350, Transportation Research Board, Washington, D.C., 1993.
8. *Roadside Design Guide*, Third Edition, American Association of State Highway and Transportation Officials (AASHTO), Washington, D.C., 2002.
9. *Memorandum on W-Beam Guardrail over Low-Fill Culverts*, September 9, 1991, File Designation HNG-14, Federal Highway Administration (FHWA), Washington, D.C., 1991.
10. Mak, K.K., Bligh, R.P., Gripne, D.J., and McDevitt, C.F., *Long-Span Nested W-Beam Guardrails over Low-Fill Culverts*, Transportation Research Record No. 1367, Transportation Research Board, National Research Council, Washington, D.C., 1992.

11. Buth, C.E., Campise, W.L., Griffin, III, L.I., Love, M.L., and Sicking, D.L., *Performance Limits of Longitudinal Barrier Systems - Volume I - Summary Report*, Report No. FHWA/RD-86/153, Submitted to the Office of Safety and Traffic Operations, Federal Highway Administration, Performed by Texas Transportation Institute, May 1986.
12. Ivy, D.L., Robertson, R., and Buth, C.E., *Test and Evaluation of W-Beam and Thrie-Beam Guardrails*, Report No. FHWA/RD-82/071, Submitted to the Office of Research, Federal Highway Administration, Performed by Texas Transportation Institute, March 1986.
13. Ross, Jr., H.E., Perera, H.S., Sicking, D.L., and Bligh, R.P., *Roadside Safety Design for Small Vehicles*, National Cooperative Highway Research Program (NCHRP) Report No. 318, Transportation Research Board, Washington, D.C., May 1989.
14. Hinch, J., Yang, T.L., and Owings, R., *Guidance Systems for Vehicle Testing*, ENSCO, Inc., Springfield, VA 1986.
15. *Standard Specifications for Transportation Materials and Methods of Sampling and Testing*, American Association of State Highway and Transportation Officials (AASHTO), Part I Specifications, Seventeenth Edition, Washington, D.C., 1995.
16. Powell, G.H., *BARRIER VII: A Computer Program For Evaluation of Automobile Barrier Systems*, Prepared for: Federal Highway Administration, Report No. FHWA RD-73-51, April 1973.
17. *Vehicle Damage Scale for Traffic Investigators*, Second Edition, Technical Bulletin No. 1, Traffic Accident Data (TAD) Project, National Safety Council, Chicago, Illinois, 1971.
18. *Collision Deformation Classification - Recommended Practice J224 March 1980*, Handbook Volume 4, Society of Automotive Engineers (SAE), Warrendale, Pennsylvania, 1985.

17 APPENDICES

APPENDIX A

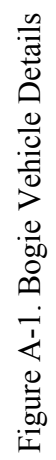
Bogie Vehicle Design and Fabrication Details

Figure A-1. Bogie Vehicle Details

Figure A-2. Bogie Vehicle Details

Figure A-3. Bogie Vehicle Tube Fabrication Details

Figure A-4. Bogie Vehicle Gusset Plate Details



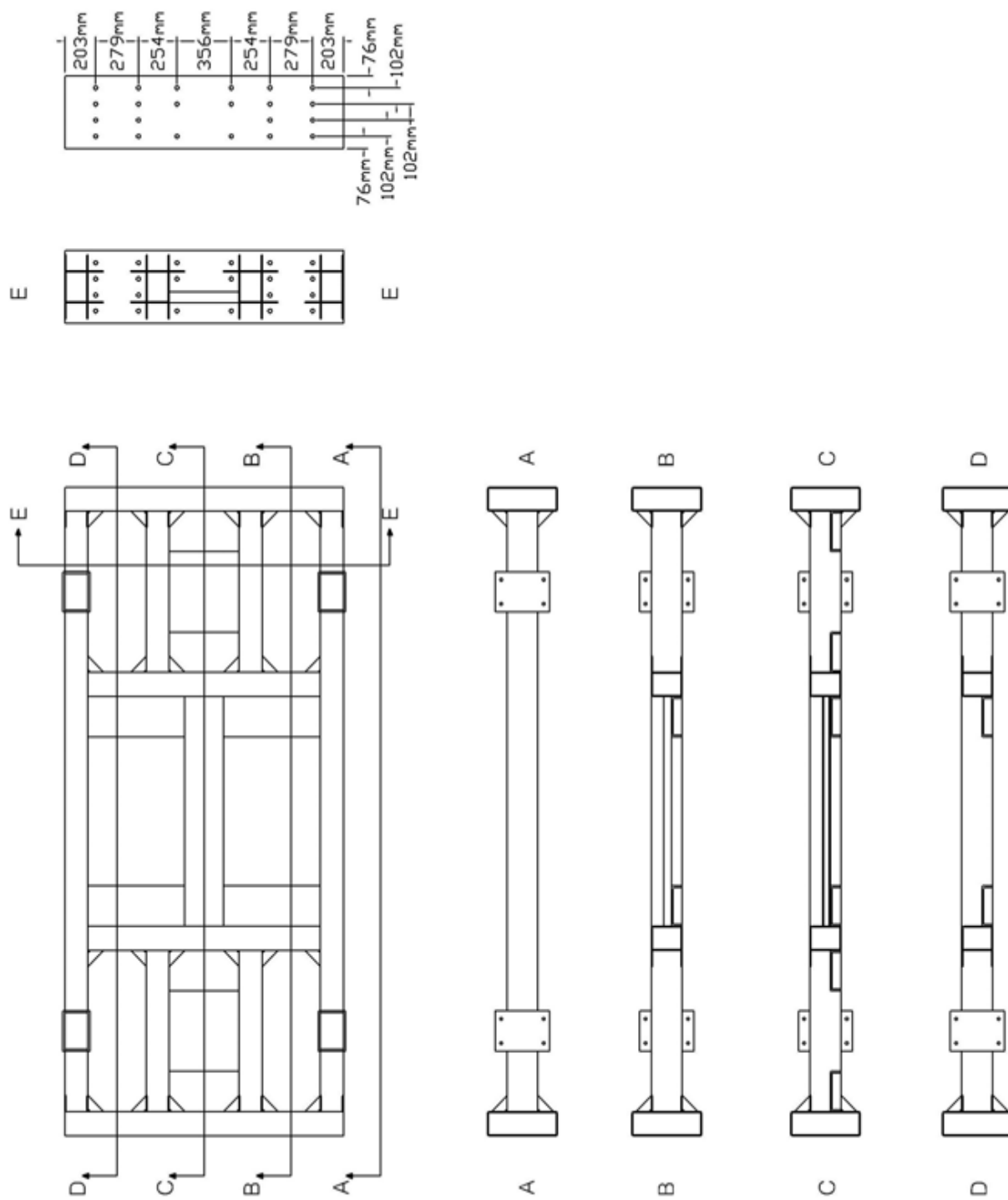


Figure A-2. Bogie Vehicle Details

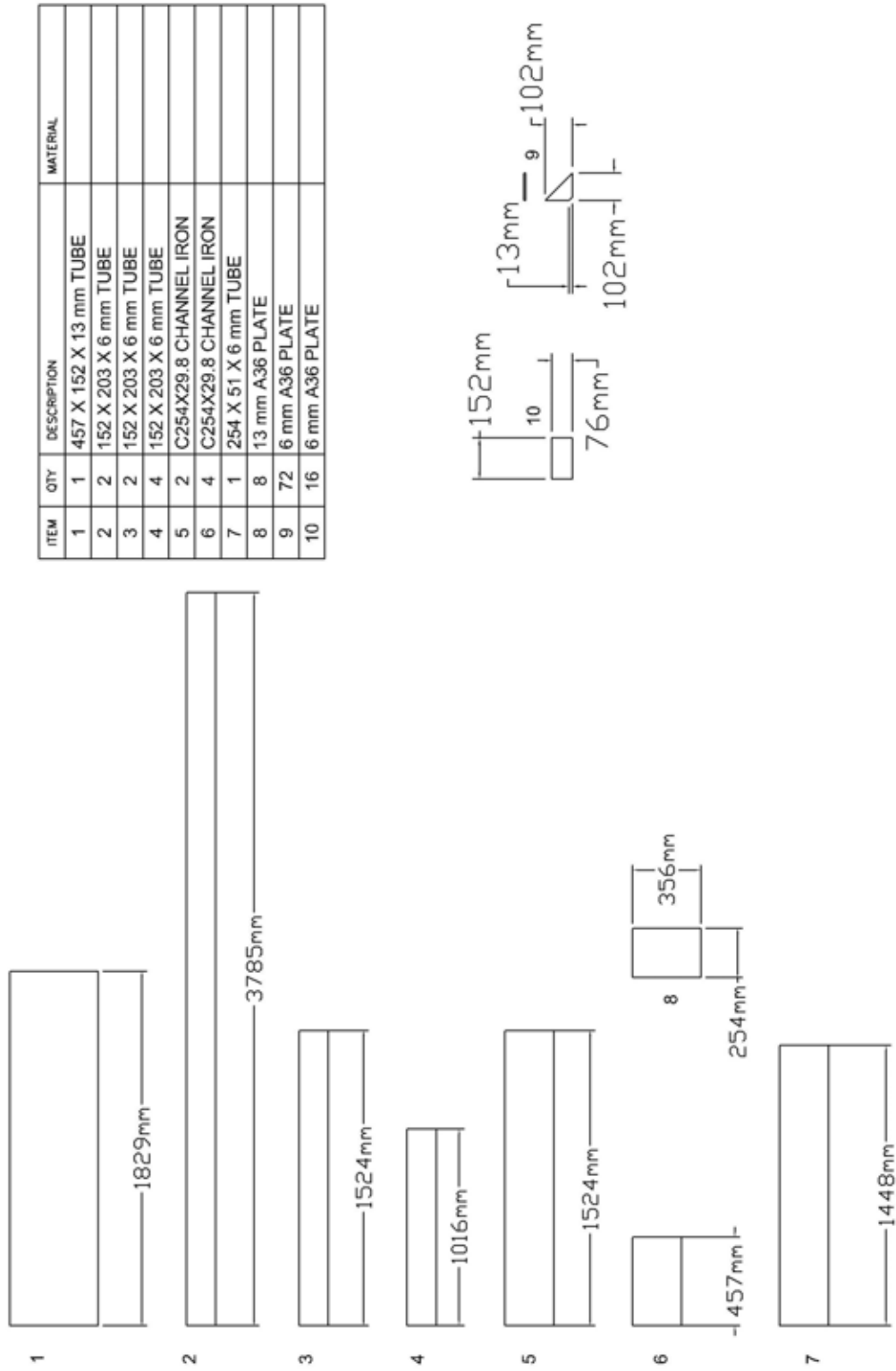


Figure A-3. Bogie Vehicle Tube Fabrication Details

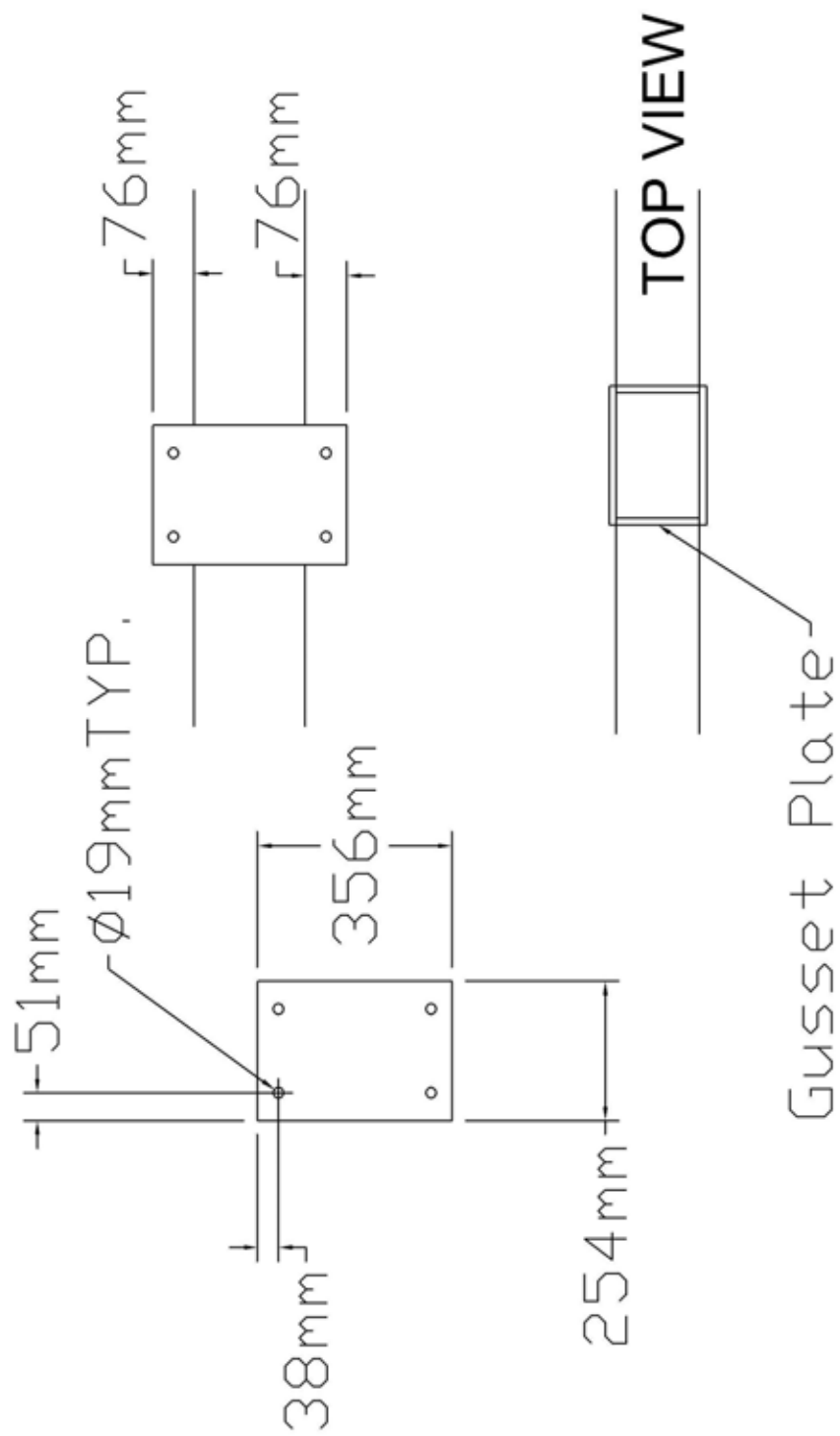


Figure A-4. Bogie Vehicle Gusset Plate Details

APPENDIX B

Force-Deflection Behavior of Bogie Tests

Figure B-1. Graph of Force-Deflection Behavior, Test KCB-1b

Figure B-2. Graph of Force-Deflection Behavior, Test KCB-2

Figure B-3. Graph of Force-Deflection Behavior, Test KCB-3

Figure B-4. Graph of Force-Deflection Behavior, Test KCB-4

Figure B-5. Graph of Force-Deflection Behavior, Test KCB-5

Figure B-6. Graph of Force-Deflection Behavior, Test KCB-6

Figure B-7. Graph of Force-Deflection Behavior, Test KCB-7

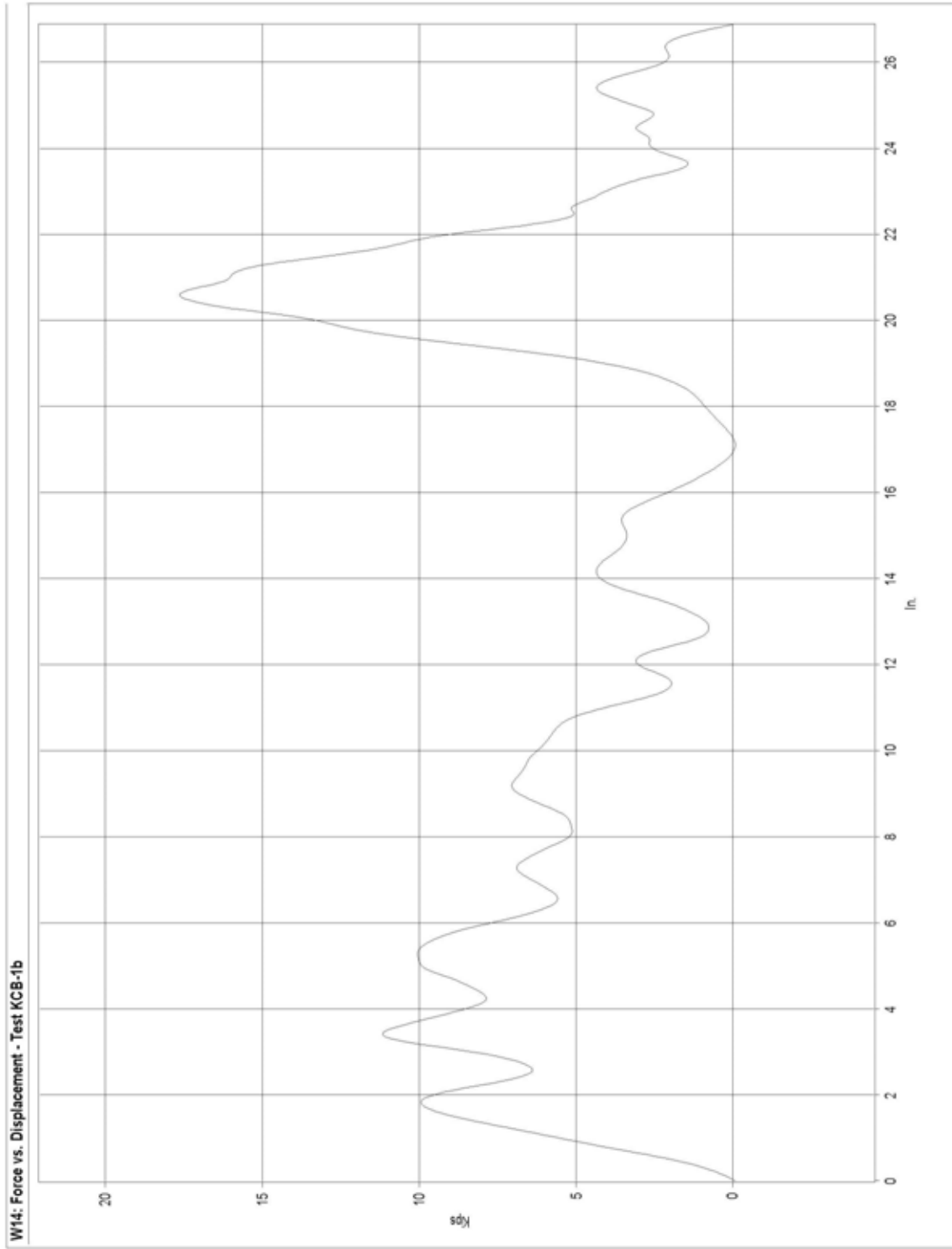


Figure B-1. Graph of Force-Deflection Behavior, Test KCB-1b

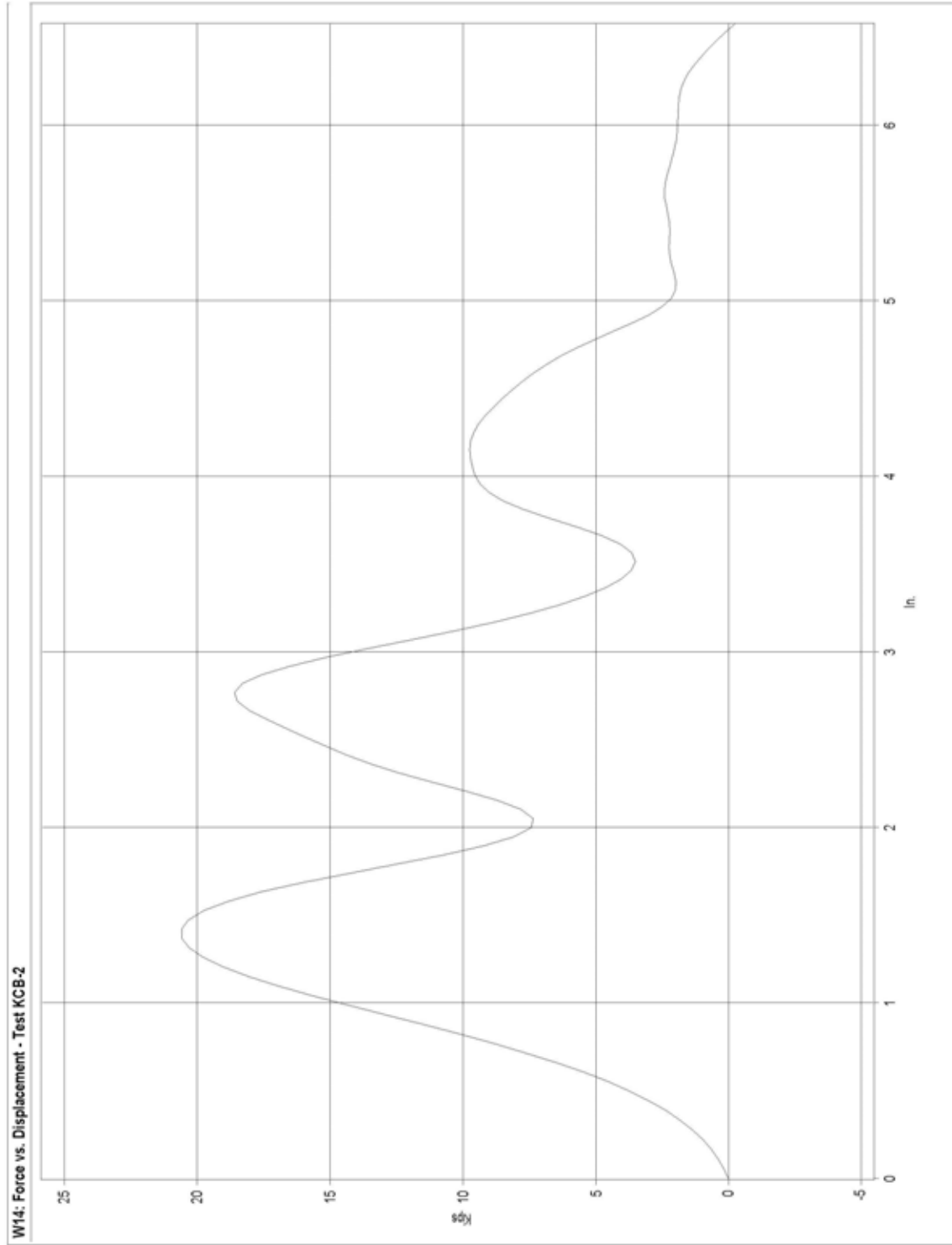


Figure B-2. Graph of Force-Deflection Behavior, Test KCB-2

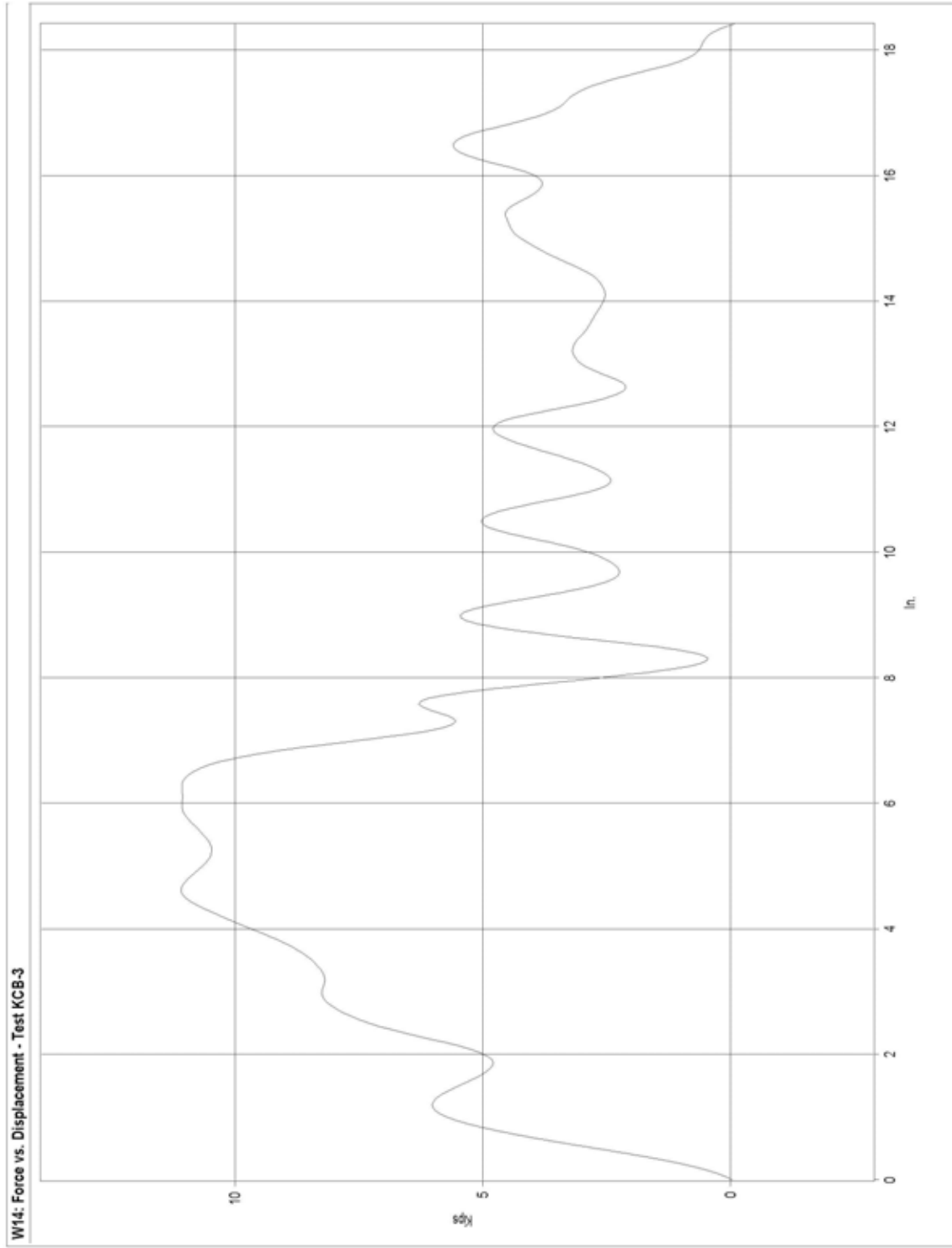


Figure B-3. Graph of Force-Deflection Behavior, Test KCB-3

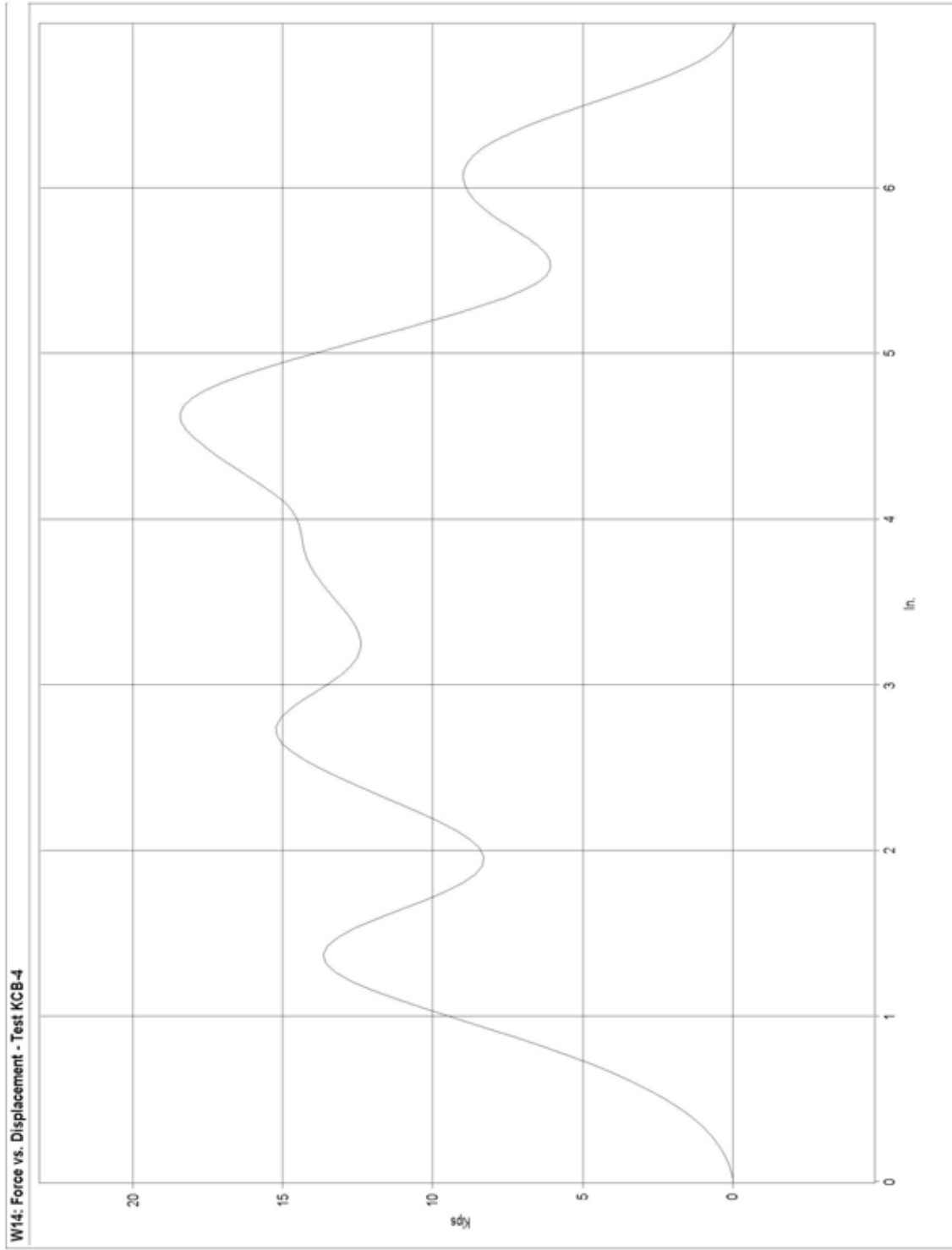


Figure B-4. Graph of Force-Deflection Behavior, Test KCB-4

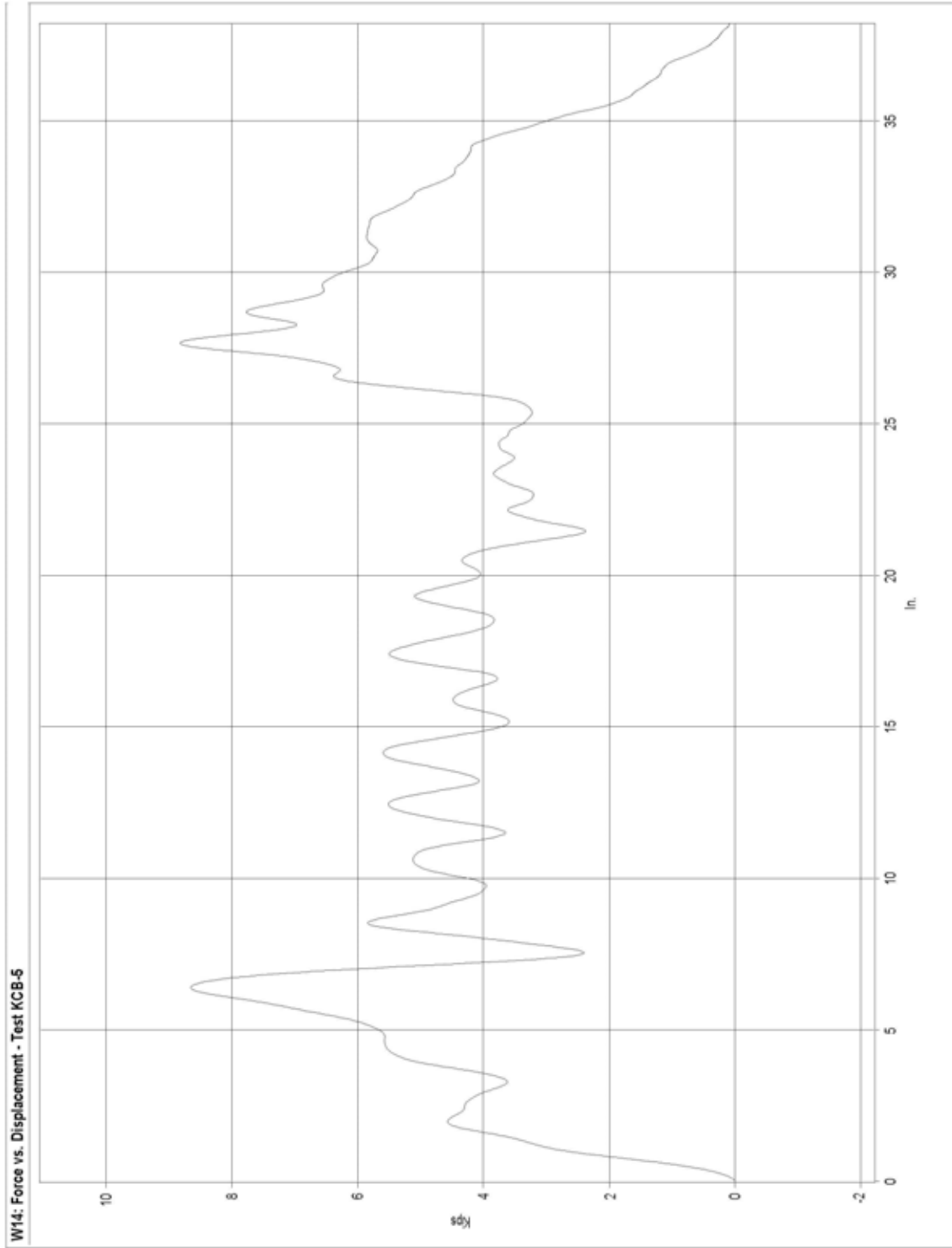


Figure B-5. Graph of Force-Deflection Behavior, Test KCB-5

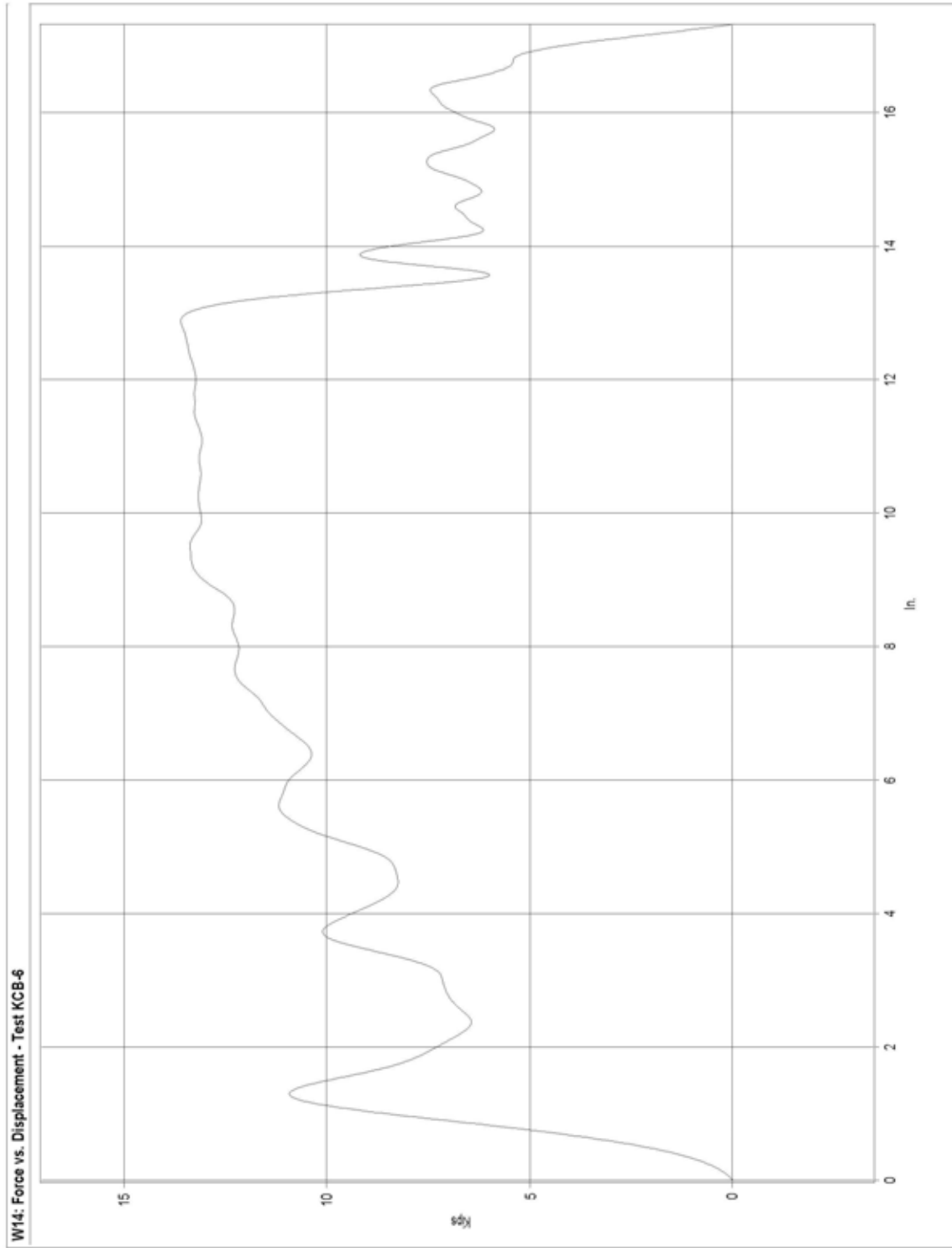


Figure B-6. Graph of Force-Deflection Behavior, Test KCB-6

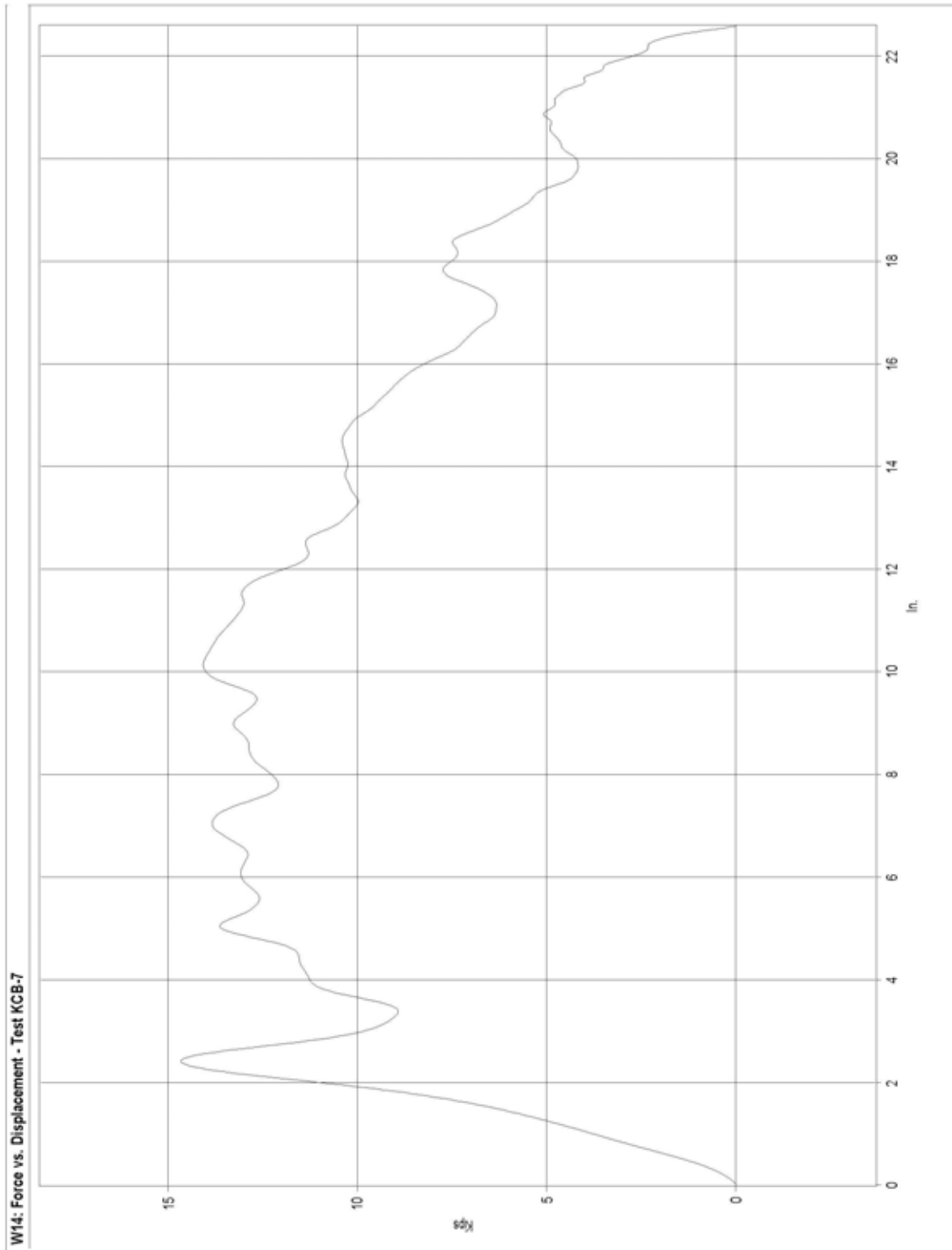


Figure B-7. Graph of Force-Deflection Behavior, Test KCB-7

APPENDIX C

BARRIER VII Computer Models

Figure C-1. Model of the Post-to-Culvert Guardrail System, Full-Post Spacing

Figure C-2. Model of the Post-to-Culvert Guardrail System, Half-Post Spacing

Figure C-3. Idealized Finite Element, 2 Dimensional Vehicle Model for the 1,996-kg Pickup Truck

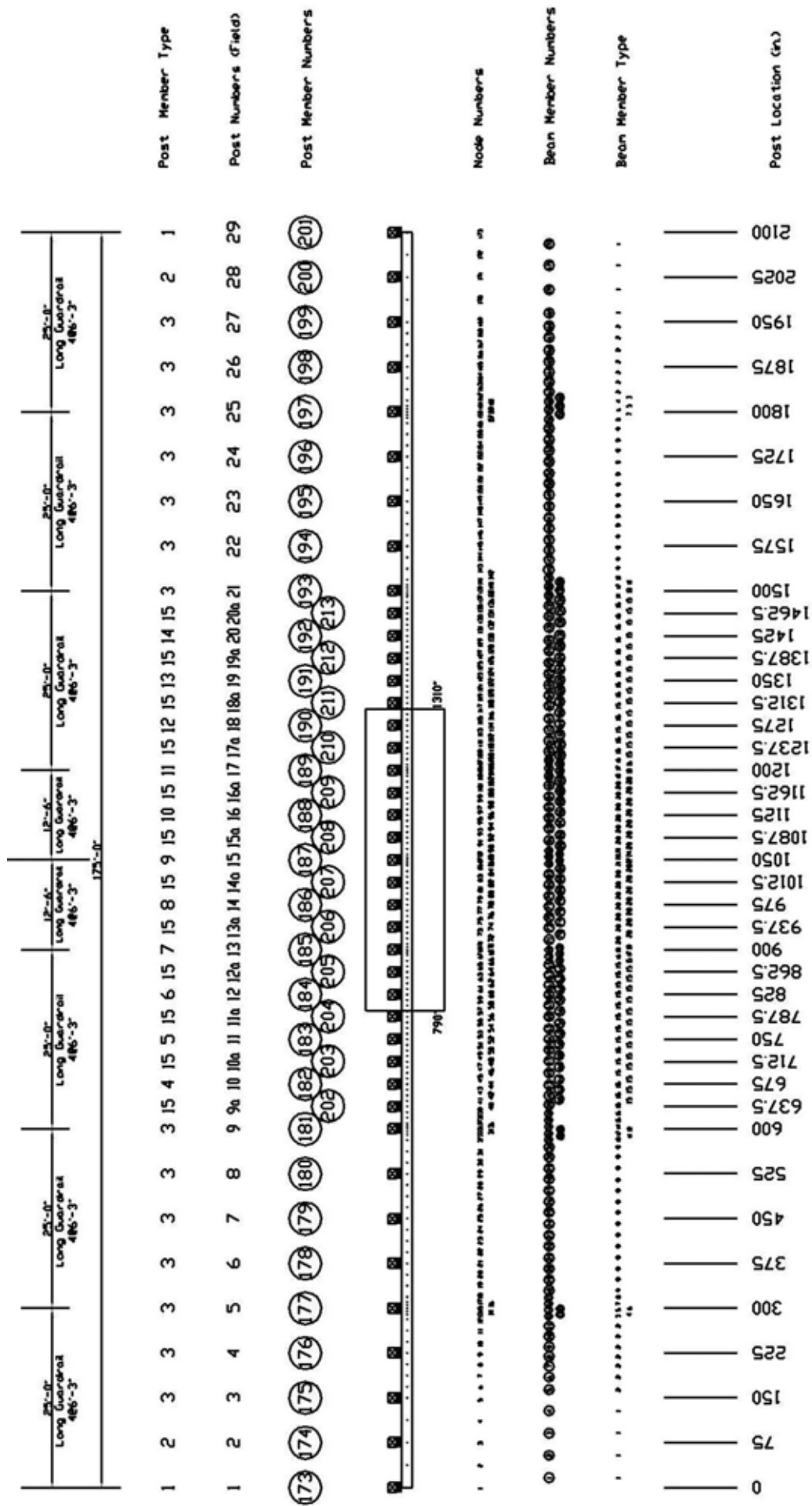


Figure C-2. Model of the Post-to-Culvert Guardrail System, Half-Post Spacing

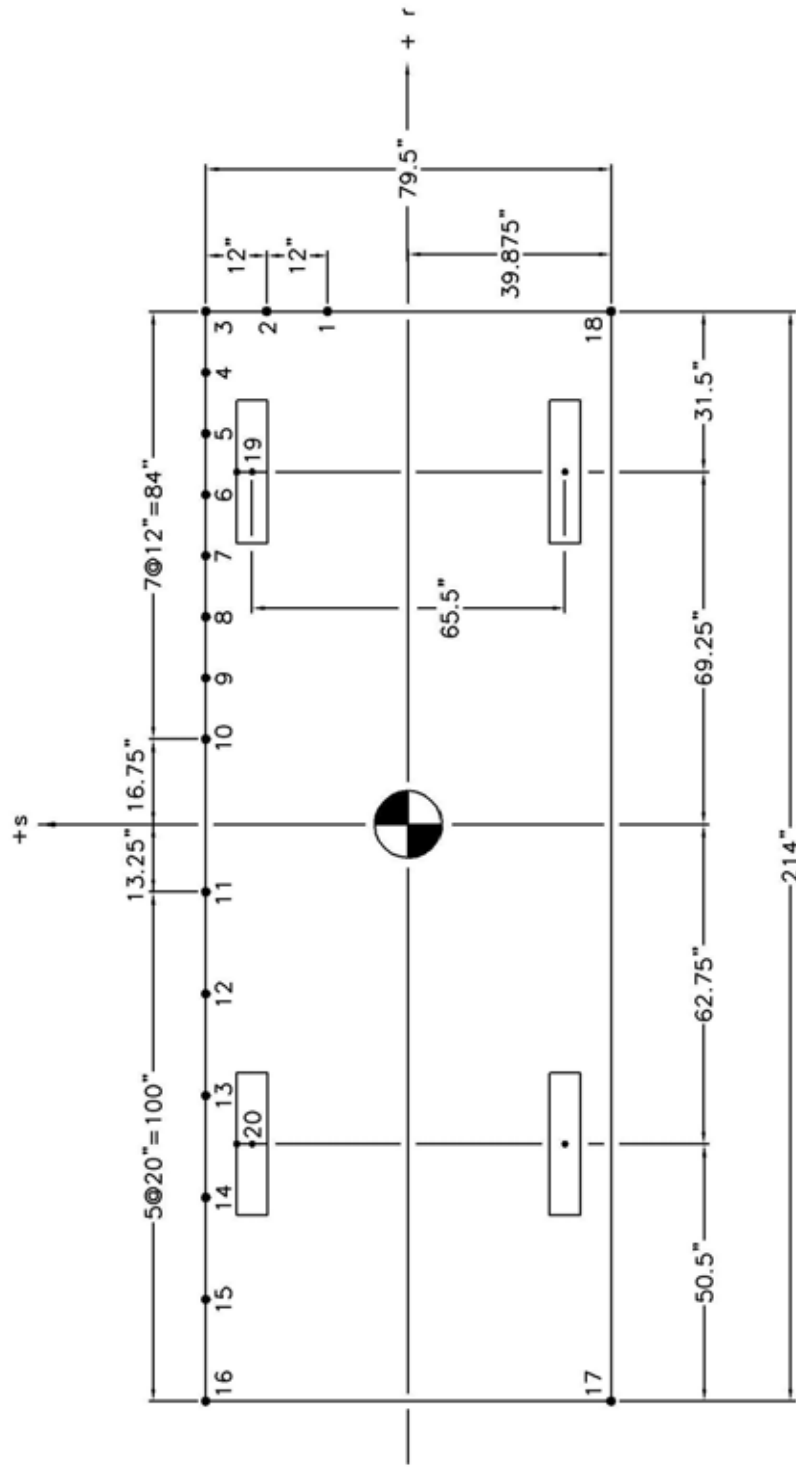


Figure C-3. Idealized Finite Element, 2 Dimensional Vehicle Model for the 1,996-kg Pickup Truck

APPENDIX D

Typical BARRIER VII Input File

Note that the example BARRIER VII input data files included in Appendix D corresponds with examples of the standard post spacing and half-post spacing, respectively.

Kansas Guardrail on Culvert (Standard Post Spacing) - RUN No. 9B - NODE 87

173	71	28	1	213	85	2	0			
	0.0001		0.0001		0.800	600	0	1.0	1	
1	5	5	5	5	5	1				
1		0.0		0.0						
3		75.00		0.0						
5		150.00		0.0						
9		225.00		0.0						
12		281.25		0.0						
13		290.625		0.0						
14		295.3125		0.0						
15		300.00		0.0						
16		304.6875		0.0						
17		309.375		0.0						
18		318.75		0.0						
21		375.00		0.0						
25		450.00		0.0						
29		525.00		0.0						
32		581.25		0.0						
33		590.625		0.0						
34		595.3125		0.0						
35		600.00		0.0						
36		604.6875		0.0						
37		609.375		0.0						
38		618.75		0.0						
44		675.00		0.0						
52		750.00		0.0						
60		825.00		0.0						
66		881.25		0.0						
67		890.625		0.0						
68		895.3125		0.0						
69		900.00		0.0						
70		904.6875		0.0						
71		909.375		0.0						
72		918.75		0.0						
78		975.00		0.0						
84		1031.25		0.0						
85		1040.625		0.0						
86		1045.3125		0.0						
87		1050.00		0.0						
88		1054.6875		0.0						
89		1059.375		0.0						
90		1068.75		0.0						
96		1125.00		0.0						
102		1181.25		0.0						
103		1190.625		0.0						
104		1195.3125		0.0						
105		1200.00		0.0						
106		1204.6875		0.0						
107		1209.375		0.0						
108		1218.75		0.0						
114		1275.00		0.0						
122		1350.00		0.0						
130		1425.00		0.0						
136		1481.25		0.0						
137		1490.625		0.0						
138		1495.3125		0.0						
139		1500.00		0.0						
140		1504.6875		0.0						
141		1509.375		0.0						
142		1518.75		0.0						
145		1575.00		0.0						
149		1650.00		0.0						
153		1725.00		0.0						
156		1781.25		0.0						
157		1790.625		0.0						
158		1795.3125		0.0						
159		1800.00		0.0						
160		1804.6875		0.0						
161		1809.375		0.0						
162		1818.75		0.0						
165		1875.00		0.0						

22	2.29	1.99	4.6875	30000.0	6.92	99.5	68.5	0.10	12-Gauge W-Beam
23	2.29	1.99	4.6875	30000.0	6.92	99.5	68.5	0.10	12-Gauge W-Beam
24	2.29	1.99	4.6875	30000.0	6.92	99.5	68.5	0.10	12-Gauge W-Beam
300	15								
1	21.65	0.00	4.0	4.0	100.0	250.0	250.0	0.10	Simulated Strong Anchor Post
100.0	100.0	100.0	10.0	10.0					
2	21.65	0.00	3.0	3.0	100.0	100.0	150.00	0.10	Second BCT Post
50.0	50.0		6.0	6.0					
3	21.65	0.0	4.00	4.00	54.0	92.88	270.62	0.10	W6x9 by 6' Long
6.0	15.0		16.0	16.0					
4	21.65	0.0	4.00	4.00	54.0	92.88	270.62	0.10	W6x9 by 6' Long
6.0	15.0		16.0	16.0					
5	21.65	0.0	4.00	4.00	54.0	92.88	270.62	0.10	W6x9 by 6' Long
6.0	15.0		16.0	16.0					
6	30.65	0.0	6.62	5.00	28.0	92.88	337.15	0.10	W6x9 Posts on Culvert
6.0	15.0		18.0	18.0					
7	30.65	0.0	6.62	5.00	28.0	92.88	337.15	0.10	W6x9 Posts on Culvert
6.0	15.0		18.0	18.0					
8	30.65	0.0	6.62	5.00	28.0	92.88	337.15	0.10	W6x9 Posts on Culvert
6.0	15.0		18.0	18.0					
9	30.65	0.0	6.62	5.00	28.0	92.88	337.15	0.10	W6x9 Posts on Culvert
6.0	15.0		18.0	18.0					
10	30.65	0.0	6.62	5.00	28.0	92.88	337.15	0.10	W6x9 Posts on Culvert
6.0	15.0		18.0	18.0					
11	30.65	0.0	6.62	5.00	28.0	92.88	337.15	0.10	W6x9 Posts on Culvert
6.0	15.0		18.0	18.0					
12	30.65	0.0	6.62	5.00	28.0	92.88	337.15	0.10	W6x9 Posts on Culvert
6.0	15.0		18.0	18.0					
13	30.65	0.0	6.62	5.00	28.0	92.88	337.15	0.10	W6x9 Posts on Culvert
6.0	15.0		18.0	18.0					
14	30.65	0.0	6.62	5.00	28.0	92.88	337.15	0.10	W6x9 Posts on Culvert
6.0	15.0		18.0	18.0					
15	30.65	0.0	1.00	1.00	28.0	1.00	1.00	0.10	W6x9 Posts on Culvert
(Removed)									
6.0	15.0		18.0	18.0					
1	1	2	4	1	101	0.0	0.0	0.0	
5	5	6	11	1	102	0.0	0.0	0.0	
12	12	13			103	0.0	0.0	0.0	
13	13	14			104	0.0	0.0	0.0	
14	14	15			105	0.0	0.0	0.0	
15	15	16			106	0.0	0.0	0.0	
16	16	17			107	0.0	0.0	0.0	
17	17	18			108	0.0	0.0	0.0	
18	18	19	31	1	109	0.0	0.0	0.0	
32	32	33			110	0.0	0.0	0.0	
33	33	34			111	0.0	0.0	0.0	
34	34	35			112	0.0	0.0	0.0	
35	35	36			113	0.0	0.0	0.0	
36	36	37			114	0.0	0.0	0.0	
37	37	38	66	1	115	0.0	0.0	0.0	
67	67	68			116	0.0	0.0	0.0	
68	68	69			117	0.0	0.0	0.0	
69	69	70			118	0.0	0.0	0.0	
70	70	71			119	0.0	0.0	0.0	
71	71	72	84	1	120	0.0	0.0	0.0	
85	85	86			121	0.0	0.0	0.0	
86	86	87			122	0.0	0.0	0.0	
87	87	88			123	0.0	0.0	0.0	
88	88	89			124	0.0	0.0	0.0	
89	89	90	102	1	120	0.0	0.0	0.0	
103	103	104			119	0.0	0.0	0.0	
104	104	105			118	0.0	0.0	0.0	
105	105	106			117	0.0	0.0	0.0	
106	106	107			116	0.0	0.0	0.0	
107	107	108	136	1	115	0.0	0.0	0.0	
137	137	138			114	0.0	0.0	0.0	
138	138	139			113	0.0	0.0	0.0	
139	139	140			112	0.0	0.0	0.0	
140	140	141			111	0.0	0.0	0.0	
141	141	142			110	0.0	0.0	0.0	
142	142	143	155	1	109	0.0	0.0	0.0	
156	156	157			108	0.0	0.0	0.0	

157	157	158			107	0.0	0.0	0.0		
158	158	159			106	0.0	0.0	0.0		
159	159	160			105	0.0	0.0	0.0		
160	160	161			104	0.0	0.0	0.0		
161	161	162			103	0.0	0.0	0.0		
162	162	163	168	1	102	0.0	0.0	0.0		
169	169	170	172	1	101	0.0	0.0	0.0		
173	1				301	0.0	0.0	0.0	0.0	0.0
174	3				302	0.0	0.0	0.0	0.0	0.0
175	5				303	0.0	0.0	0.0	0.0	0.0
176	9				303	0.0	0.0	0.0	0.0	0.0
177	15				303	0.0	0.0	0.0	0.0	0.0
178	21				303	0.0	0.0	0.0	0.0	0.0
179	25				303	0.0	0.0	0.0	0.0	0.0
180	29				303	0.0	0.0	0.0	0.0	0.0
181	35				303	0.0	0.0	0.0	0.0	0.0
182	44				304	0.0	0.0	0.0	0.0	0.0
183	52				305	0.0	0.0	0.0	0.0	0.0
184	60				306	0.0	0.0	0.0	0.0	0.0
185	69				307	0.0	0.0	0.0	0.0	0.0
186	78				308	0.0	0.0	0.0	0.0	0.0
187	87				309	0.0	0.0	0.0	0.0	0.0
188	96				310	0.0	0.0	0.0	0.0	0.0
189	105				311	0.0	0.0	0.0	0.0	0.0
190	114				312	0.0	0.0	0.0	0.0	0.0
191	122				313	0.0	0.0	0.0	0.0	0.0
192	130				314	0.0	0.0	0.0	0.0	0.0
193	139				303	0.0	0.0	0.0	0.0	0.0
194	145				303	0.0	0.0	0.0	0.0	0.0
195	149				303	0.0	0.0	0.0	0.0	0.0
196	153				303	0.0	0.0	0.0	0.0	0.0
197	159				303	0.0	0.0	0.0	0.0	0.0
198	165				303	0.0	0.0	0.0	0.0	0.0
199	169				303	0.0	0.0	0.0	0.0	0.0
200	171				302	0.0	0.0	0.0	0.0	0.0
201	173				301	0.0	0.0	0.0	0.0	0.0
202	40				315	0.0	0.0	0.0	0.0	0.0
203	48				315	0.0	0.0	0.0	0.0	0.0
204	56				315	0.0	0.0	0.0	0.0	0.0
205	64				315	0.0	0.0	0.0	0.0	0.0
206	74				315	0.0	0.0	0.0	0.0	0.0
207	82				315	0.0	0.0	0.0	0.0	0.0
208	92				315	0.0	0.0	0.0	0.0	0.0
209	100				315	0.0	0.0	0.0	0.0	0.0
210	110				315	0.0	0.0	0.0	0.0	0.0
211	118				315	0.0	0.0	0.0	0.0	0.0
212	126				315	0.0	0.0	0.0	0.0	0.0
213	134				315	0.0	0.0	0.0	0.0	0.0
4400.0	40000.0	20			6	4	0	1		
1	0.055	0.12			6.00	17.0				
2	0.057	0.15			7.00	18.0				
3	0.062	0.18			10.00	12.0				
4	0.110	0.35			12.00	6.0				
5	0.35	0.45			6.00	5.0				
6	1.45	1.50			15.00	1.0				
1	100.75	15.875	1		12.0	1	1	0	0	
2	100.75	27.875	1		12.0	1	1	0	0	
3	100.75	39.875	2		12.0	1	1	0	0	
4	88.75	39.875	2		12.0	1	1	0	0	
5	76.75	39.875	2		12.0	1	1	0	0	
6	64.75	39.875	2		12.0	1	1	0	0	
7	52.75	39.875	2		12.0	1	1	0	0	
8	40.75	39.875	2		12.0	1	1	0	0	
9	28.75	39.875	2		12.0	1	1	0	0	
10	16.75	39.875	2		12.0	1	1	0	0	
11	-13.25	39.875	3		12.0	1	1	0	0	
12	-33.25	39.875	3		12.0	1	1	0	0	
13	-53.25	39.875	3		12.0	1	1	0	0	
14	-73.25	39.875	3		12.0	1	1	0	0	
15	-93.25	39.875	3		12.0	1	1	0	0	
16	-113.25	39.875	4		12.0	1	1	0	0	
17	-113.25	-39.875	4		12.0	0	0	0	0	

18	100.75	-39.875	1	12.0	0	0	0	0
19	69.25	37.75	5	1.0	1	1	0	0
20	-62.75	37.75	6	1.0	1	1	0	0
1	69.25	32.75		0.0	608.			
2	69.25	-32.75		0.0	608.			
3	-62.75	32.75		0.0	492.			
4	-62.75	-32.75		0.0	492.			
1	0.0	0.0						
3	1050.00	0.0	25.0	62.14		0.0	0.0	1.0

Kansas Guardrail on Culvert (Half-Post Spacing) - RUN No. 9 - NODE 87

173	71	28	1	213	85	2	0		1.0	1
0.0001		0.0001			0.800	600	0			
1	5	5	5	5	5	1				
1		0.0		0.0						
3		75.00		0.0						
5		150.00		0.0						
9		225.00		0.0						
12		281.25		0.0						
13		290.625		0.0						
14		295.3125		0.0						
15		300.00		0.0						
16		304.6875		0.0						
17		309.375		0.0						
18		318.75		0.0						
21		375.00		0.0						
25		450.00		0.0						
29		525.00		0.0						
32		581.25		0.0						
33		590.625		0.0						
34		595.3125		0.0						
35		600.00		0.0						
36		604.6875		0.0						
37		609.375		0.0						
38		618.75		0.0						
44		675.00		0.0						
52		750.00		0.0						
60		825.00		0.0						
66		881.25		0.0						
67		890.625		0.0						
68		895.3125		0.0						
69		900.00		0.0						
70		904.6875		0.0						
71		909.375		0.0						
72		918.75		0.0						
78		975.00		0.0						
84		1031.25		0.0						
85		1040.625		0.0						
86		1045.3125		0.0						
87		1050.00		0.0						
88		1054.6875		0.0						
89		1059.375		0.0						
90		1068.75		0.0						
96		1125.00		0.0						
102		1181.25		0.0						
103		1190.625		0.0						
104		1195.3125		0.0						
105		1200.00		0.0						
106		1204.6875		0.0						
107		1209.375		0.0						
108		1218.75		0.0						
114		1275.00		0.0						
122		1350.00		0.0						
130		1425.00		0.0						
136		1481.25		0.0						
137		1490.625		0.0						
138		1495.3125		0.0						
139		1500.00		0.0						
140		1504.6875		0.0						
141		1509.375		0.0						
142		1518.75		0.0						
145		1575.00		0.0						
149		1650.00		0.0						
153		1725.00		0.0						
156		1781.25		0.0						
157		1790.625		0.0						
158		1795.3125		0.0						
159		1800.00		0.0						
160		1804.6875		0.0						
161		1809.375		0.0						
162		1818.75		0.0						
165		1875.00		0.0						

22	2.29	1.99	4.6875	30000.0	6.92	99.5	68.5	0.10	12-Gauge W-Beam
23	2.29	1.99	4.6875	30000.0	6.92	99.5	68.5	0.10	12-Gauge W-Beam
24	2.29	1.99	4.6875	30000.0	6.92	99.5	68.5	0.10	12-Gauge W-Beam
300	15								
1	21.65	0.00	4.0	4.0	100.0	250.0	250.0	0.10	Simulated Strong Anchor Post
2	21.65	0.00	3.0	3.0	100.0	100.0	150.00	0.10	Second BCT Post
3	21.65	0.0	4.00	4.00	54.0	92.88	270.62	0.10	W6x9 by 6' Long
4	21.65	0.0	4.00	4.00	54.0	92.88	270.62	0.10	W6x9 by 6' Long
5	21.65	0.0	4.00	4.00	54.0	92.88	270.62	0.10	W6x9 by 6' Long
6	30.65	0.0	6.62	5.00	28.0	92.88	337.15	0.10	W6x9 Posts on Culvert
7	30.65	0.0	6.62	5.00	28.0	92.88	337.15	0.10	W6x9 Posts on Culvert
8	30.65	0.0	6.62	5.00	28.0	92.88	337.15	0.10	W6x9 Posts on Culvert
9	30.65	0.0	6.62	5.00	28.0	92.88	337.15	0.10	W6x9 Posts on Culvert
10	30.65	0.0	6.62	5.00	28.0	92.88	337.15	0.10	W6x9 Posts on Culvert
11	30.65	0.0	6.62	5.00	28.0	92.88	337.15	0.10	W6x9 Posts on Culvert
12	30.65	0.0	6.62	5.00	28.0	92.88	337.15	0.10	W6x9 Posts on Culvert
13	30.65	0.0	6.62	5.00	28.0	92.88	337.15	0.10	W6x9 Posts on Culvert
14	30.65	0.0	6.62	5.00	28.0	92.88	337.15	0.10	W6x9 Posts on Culvert
15	30.65	0.0	6.62	5.00	28.0	92.88	337.15	0.10	W6x9 Posts on Culvert
1	1	2	4	1	101	0.0	0.0	0.0	
5	5	6	11	1	102	0.0	0.0	0.0	
12	12	13			103	0.0	0.0	0.0	
13	13	14			104	0.0	0.0	0.0	
14	14	15			105	0.0	0.0	0.0	
15	15	16			106	0.0	0.0	0.0	
16	16	17			107	0.0	0.0	0.0	
17	17	18			108	0.0	0.0	0.0	
18	18	19	31	1	109	0.0	0.0	0.0	
32	32	33			110	0.0	0.0	0.0	
33	33	34			111	0.0	0.0	0.0	
34	34	35			112	0.0	0.0	0.0	
35	35	36			113	0.0	0.0	0.0	
36	36	37			114	0.0	0.0	0.0	
37	37	38	66	1	115	0.0	0.0	0.0	
67	67	68			116	0.0	0.0	0.0	
68	68	69			117	0.0	0.0	0.0	
69	69	70			118	0.0	0.0	0.0	
70	70	71			119	0.0	0.0	0.0	
71	71	72	84	1	120	0.0	0.0	0.0	
85	85	86			121	0.0	0.0	0.0	
86	86	87			122	0.0	0.0	0.0	
87	87	88			123	0.0	0.0	0.0	
88	88	89			124	0.0	0.0	0.0	
89	89	90	102	1	120	0.0	0.0	0.0	
103	103	104			119	0.0	0.0	0.0	
104	104	105			118	0.0	0.0	0.0	
105	105	106			117	0.0	0.0	0.0	
106	106	107			116	0.0	0.0	0.0	
107	107	108	136	1	115	0.0	0.0	0.0	
137	137	138			114	0.0	0.0	0.0	
138	138	139			113	0.0	0.0	0.0	
139	139	140			112	0.0	0.0	0.0	
140	140	141			111	0.0	0.0	0.0	
141	141	142			110	0.0	0.0	0.0	
142	142	143	155	1	109	0.0	0.0	0.0	
156	156	157			108	0.0	0.0	0.0	
157	157	158			107	0.0	0.0	0.0	

158	158	159			106	0.0	0.0	0.0		
159	159	160			105	0.0	0.0	0.0		
160	160	161			104	0.0	0.0	0.0		
161	161	162			103	0.0	0.0	0.0		
162	162	163	168	1	102	0.0	0.0	0.0		
169	169	170	172	1	101	0.0	0.0	0.0		
173	1				301	0.0	0.0	0.0	0.0	0.0
174	3				302	0.0	0.0	0.0	0.0	0.0
175	5				303	0.0	0.0	0.0	0.0	0.0
176	9				303	0.0	0.0	0.0	0.0	0.0
177	15				303	0.0	0.0	0.0	0.0	0.0
178	21				303	0.0	0.0	0.0	0.0	0.0
179	25				303	0.0	0.0	0.0	0.0	0.0
180	29				303	0.0	0.0	0.0	0.0	0.0
181	35				303	0.0	0.0	0.0	0.0	0.0
182	44				304	0.0	0.0	0.0	0.0	0.0
183	52				305	0.0	0.0	0.0	0.0	0.0
184	60				306	0.0	0.0	0.0	0.0	0.0
185	69				307	0.0	0.0	0.0	0.0	0.0
186	78				308	0.0	0.0	0.0	0.0	0.0
187	87				309	0.0	0.0	0.0	0.0	0.0
188	96				310	0.0	0.0	0.0	0.0	0.0
189	105				311	0.0	0.0	0.0	0.0	0.0
190	114				312	0.0	0.0	0.0	0.0	0.0
191	122				313	0.0	0.0	0.0	0.0	0.0
192	130				314	0.0	0.0	0.0	0.0	0.0
193	139				303	0.0	0.0	0.0	0.0	0.0
194	145				303	0.0	0.0	0.0	0.0	0.0
195	149				303	0.0	0.0	0.0	0.0	0.0
196	153				303	0.0	0.0	0.0	0.0	0.0
197	159				303	0.0	0.0	0.0	0.0	0.0
198	165				303	0.0	0.0	0.0	0.0	0.0
199	169				303	0.0	0.0	0.0	0.0	0.0
200	171				302	0.0	0.0	0.0	0.0	0.0
201	173				301	0.0	0.0	0.0	0.0	0.0
202	40				315	0.0	0.0	0.0	0.0	0.0
203	48				315	0.0	0.0	0.0	0.0	0.0
204	56				315	0.0	0.0	0.0	0.0	0.0
205	64				315	0.0	0.0	0.0	0.0	0.0
206	74				315	0.0	0.0	0.0	0.0	0.0
207	82				315	0.0	0.0	0.0	0.0	0.0
208	92				315	0.0	0.0	0.0	0.0	0.0
209	100				315	0.0	0.0	0.0	0.0	0.0
210	110				315	0.0	0.0	0.0	0.0	0.0
211	118				315	0.0	0.0	0.0	0.0	0.0
212	126				315	0.0	0.0	0.0	0.0	0.0
213	134				315	0.0	0.0	0.0	0.0	0.0
4400.0						40000.0	20	6	4	0
1	0.055	0.12				6.00	17.0			
2	0.057	0.15				7.00	18.0			
3	0.062	0.18				10.00	12.0			
4	0.110	0.35				12.00	6.0			
5	0.35	0.45				6.00	5.0			
6	1.45	1.50				15.00	1.0			
1	100.75	15.875	1		12.0	1	1	0	0	
2	100.75	27.875	1		12.0	1	1	0	0	
3	100.75	39.875	2		12.0	1	1	0	0	
4	88.75	39.875	2		12.0	1	1	0	0	
5	76.75	39.875	2		12.0	1	1	0	0	
6	64.75	39.875	2		12.0	1	1	0	0	
7	52.75	39.875	2		12.0	1	1	0	0	
8	40.75	39.875	2		12.0	1	1	0	0	
9	28.75	39.875	2		12.0	1	1	0	0	
10	16.75	39.875	2		12.0	1	1	0	0	
11	-13.25	39.875	3		12.0	1	1	0	0	
12	-33.25	39.875	3		12.0	1	1	0	0	
13	-53.25	39.875	3		12.0	1	1	0	0	
14	-73.25	39.875	3		12.0	1	1	0	0	
15	-93.25	39.875	3		12.0	1	1	0	0	
16	-113.25	39.875	4		12.0	1	1	0	0	
17	-113.25	-39.875	4		12.0	0	0	0	0	
18	100.75	-39.875	1		12.0	0	0	0	0	

19	69.25	37.75	5	1.0	1	1	0	0
20	-62.75	37.75	6	1.0	1	1	0	0
1	69.25	32.75		0.0	608.			
2	69.25	-32.75		0.0	608.			
3	-62.75	32.75		0.0	492.			
4	-62.75	-32.75		0.0	492.			
1	0.0	0.0						
3	1050.00	0.0	25.0	62.14		0.0	0.0	1.0

APPENDIX E

Occupant Compartment Deformation Data, Test KC-1

Figure E-1. Occupant Compartment Deformation Data, Test KC-1

VEHICLE PRE/POST CRUSH INFO

TEST: KC-1
VEHICLE: 1994 GMC 2500

POINT	X	Y	Z	X'	Y'	Z'	DEL X	DEL Y	DEL Z
1	4.25	53.25	2.5	4.25	53	6	0	-0.25	3.5
2	8.25	54.25	1.5	8	54.5	4.5	-0.25	0.25	3
3	12.5	56.5	-0.25	11.25	56.25	3	-1.25	-0.25	3.25
4	16.5	58.5	-0.25	15.25	58.5	1.75	-1.25	0	2
5	24.75	58.25	0.5	22.75	57.5	2.25	-2	-0.75	1.75
6	3.75	49	0	3.75	48.75	3.25	0	-0.25	3.25
7	7.5	49.25	0	7.5	49	3.25	0	-0.25	3.25
8	10	49.5	-3.75	9	49.5	-0.75	-1	0	3
9	14	53	-4.75	12.75	52.75	-2.25	-1.25	-0.25	2.5
10	20.25	53	-4	19	52.5	-2.25	-1.25	-0.5	1.75
11	26.75	52.25	-3.5	26	52.25	-3	-0.75	0	0.5
12	4.5	42.75	-0.5	4.25	42.25	2.25	-0.25	-0.5	2.75
13	7.125	44	-0.5	7	43.75	2.75	-0.125	-0.25	3.25
14	10.25	44.5	-5.25	9.25	44.25	-2.5	-1	-0.25	2.75
15	15.25	46	-5.75	14.25	46	-3	-1	0	2.75
16	21	46	-5.25	20.25	46.25	-4	-0.75	0.25	1.25
17	27.25	44.5	-5	27	45.25	-1.5	-0.25	0.75	3.5
18	4.75	36.375	-1	4.5	36	1.5	-0.25	-0.375	2.5
19	9.75	37.75	-4.25	8.75	37.5	-1.5	-1	-0.25	2.75
20	14.75	39.25	-5.75	13.75	39	-3.25	-1	-0.25	2.5
21	23.75	39.5	-5.25	23.75	39.25	-3.25	0	-0.25	2
22	28.25	39.75	-5.75	27.375	39.5	-3.5	-0.875	-0.25	2.25
23	5.75	31.75	-1.5	5.5	32.5	-1.25	-0.25	0.75	0.25
24	16.75	34.5	-6	15.75	34.25	-3	-1	-0.25	3
25	27	33.5	-6	27	38.5	-3.5	0	5	2.5
26	13.25	30.75	-5.75	12.25	30.5	-3	-1	-0.25	2.75
27	19.5	30.25	-5.5	19.25	30.5	-3.25	-0.25	0.25	2.25
28	32.25	31	2	31.75	30.5	2.25	-0.5	-0.5	0.25
29	2	48	22.25	2	48.5	24.75	0	0.5	2.5
30	15.25	48.5	22.5	15.25	48.5	19.25	0	0	-3.25

ORIENTATION AND REFERENCE INFO

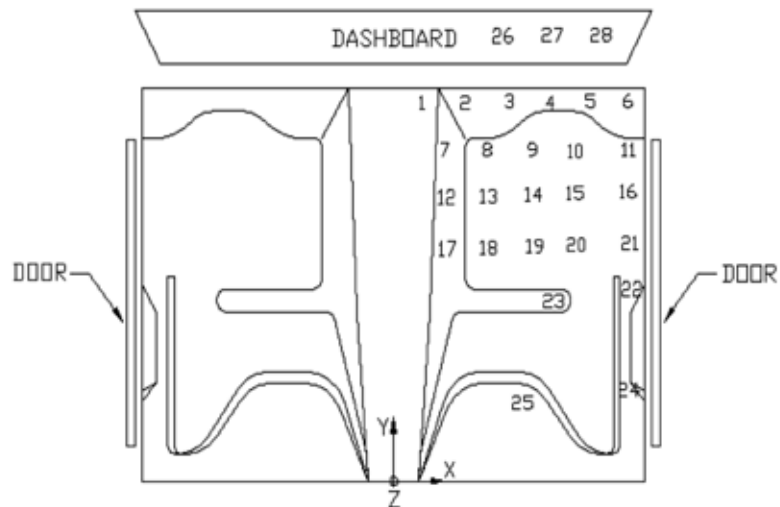


Figure E-1. Occupant Compartment Deformation Data, Test KC-1

APPENDIX F

Accelerometer Data Analysis, Test KC-1

Figure F-1. Graph of Longitudinal Deceleration, Test KC-1

Figure F-2. Graph of Longitudinal Occupant Impact Velocity, Test KC-1

Figure F-3. Graph of Longitudinal Occupant Displacement, Test KC-1

Figure F-4. Graph of Lateral Deceleration, Test KC-1

Figure F-5. Graph of Lateral Occupant Impact Velocity, Test KC-1

Figure F-6. Graph of Lateral Occupant Displacement, Test KC-1

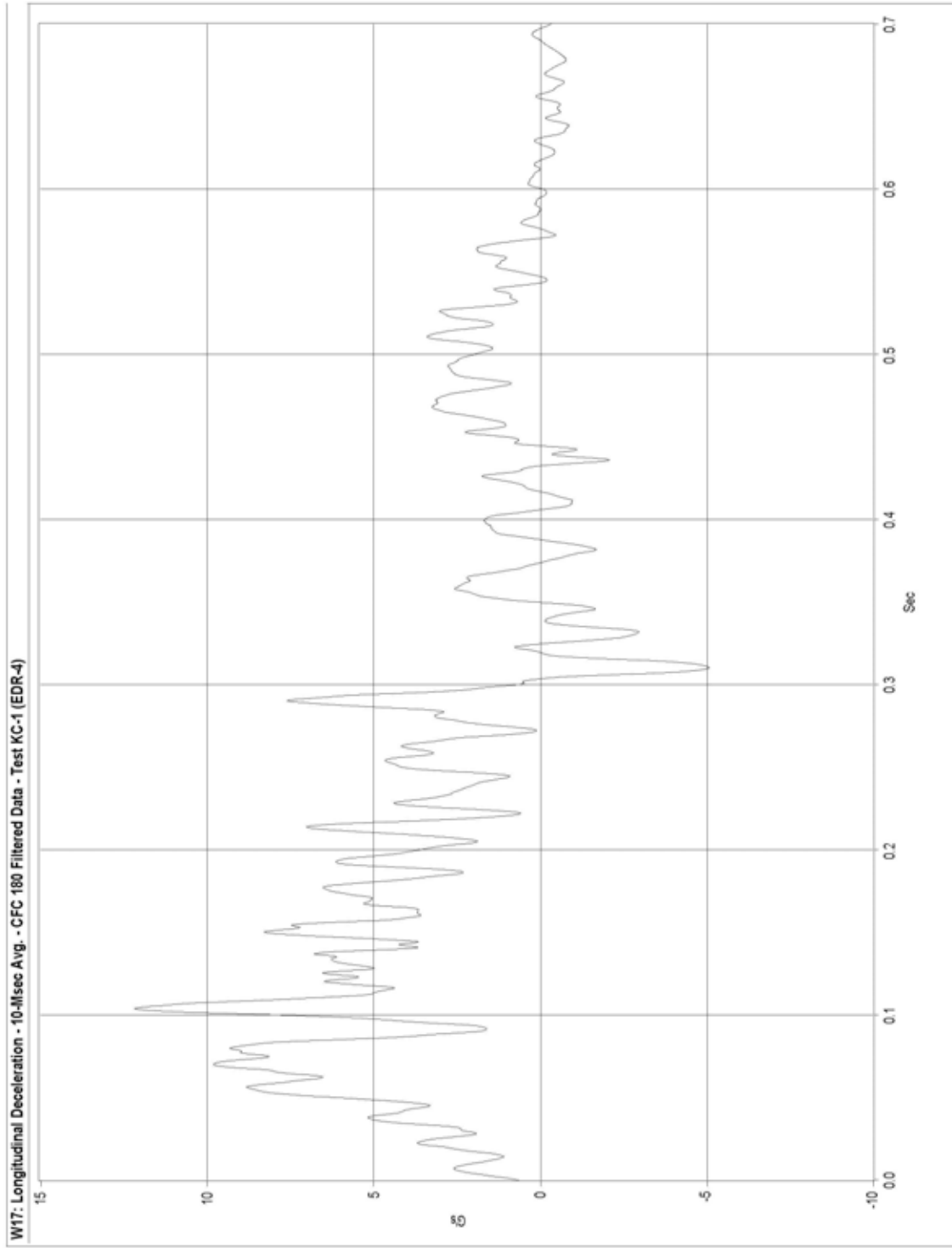


Figure F-1. Graph of Longitudinal Deceleration Test KC-1

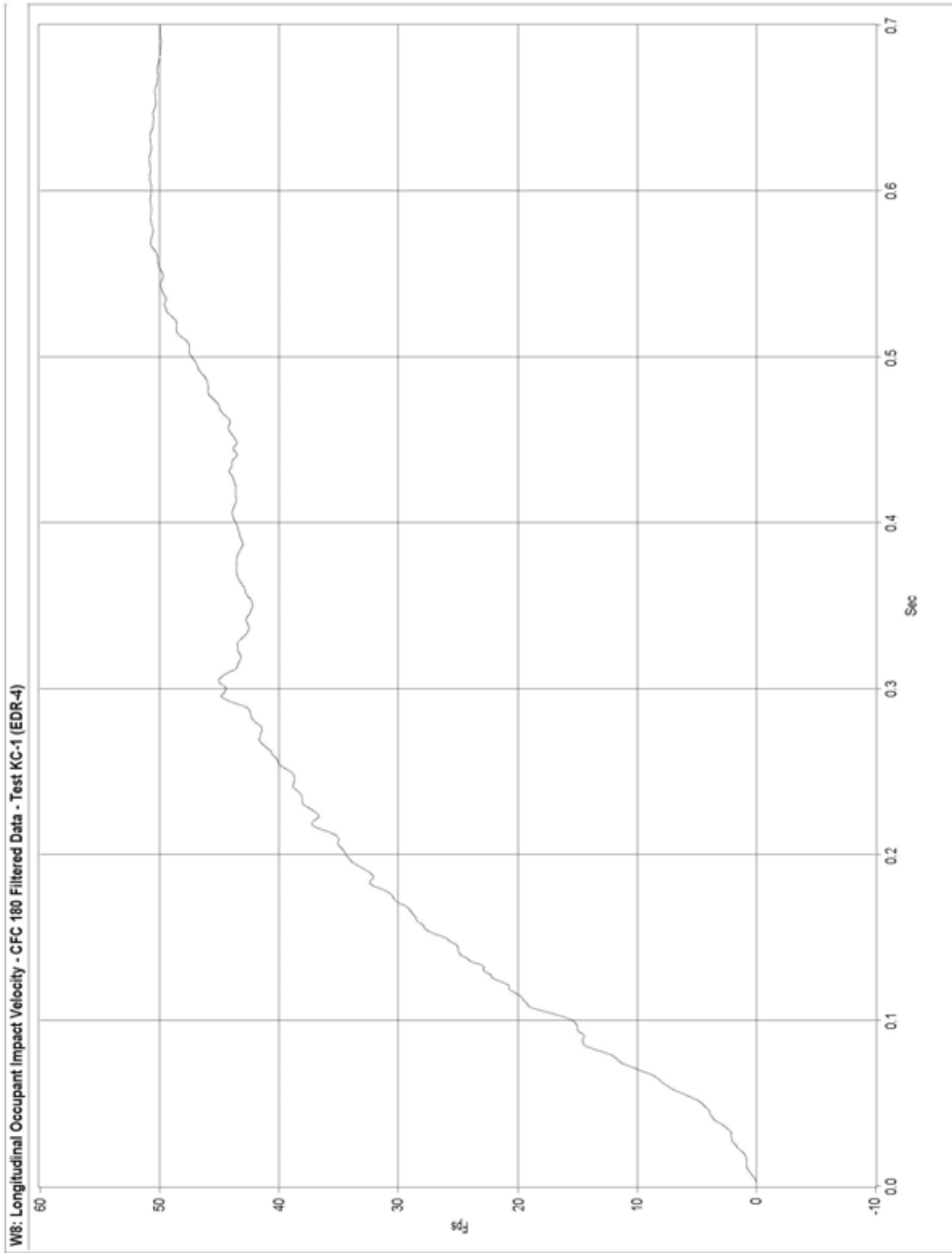


Figure F-2. Graph of Longitudinal Occupant Impact Velocity, Test KC-1

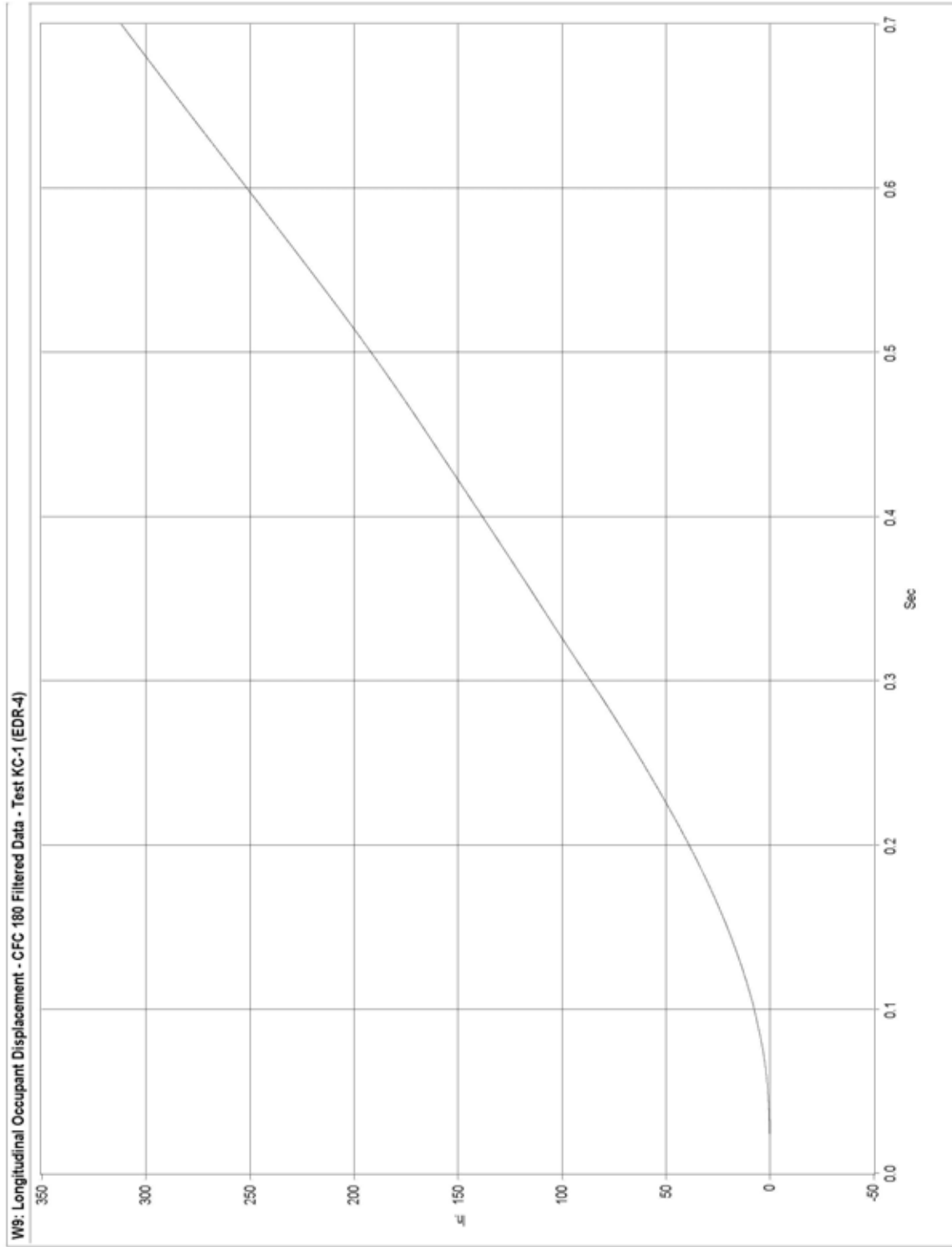


Figure F-3. Graph of Longitudinal Occupant Displacement, Test KC-1

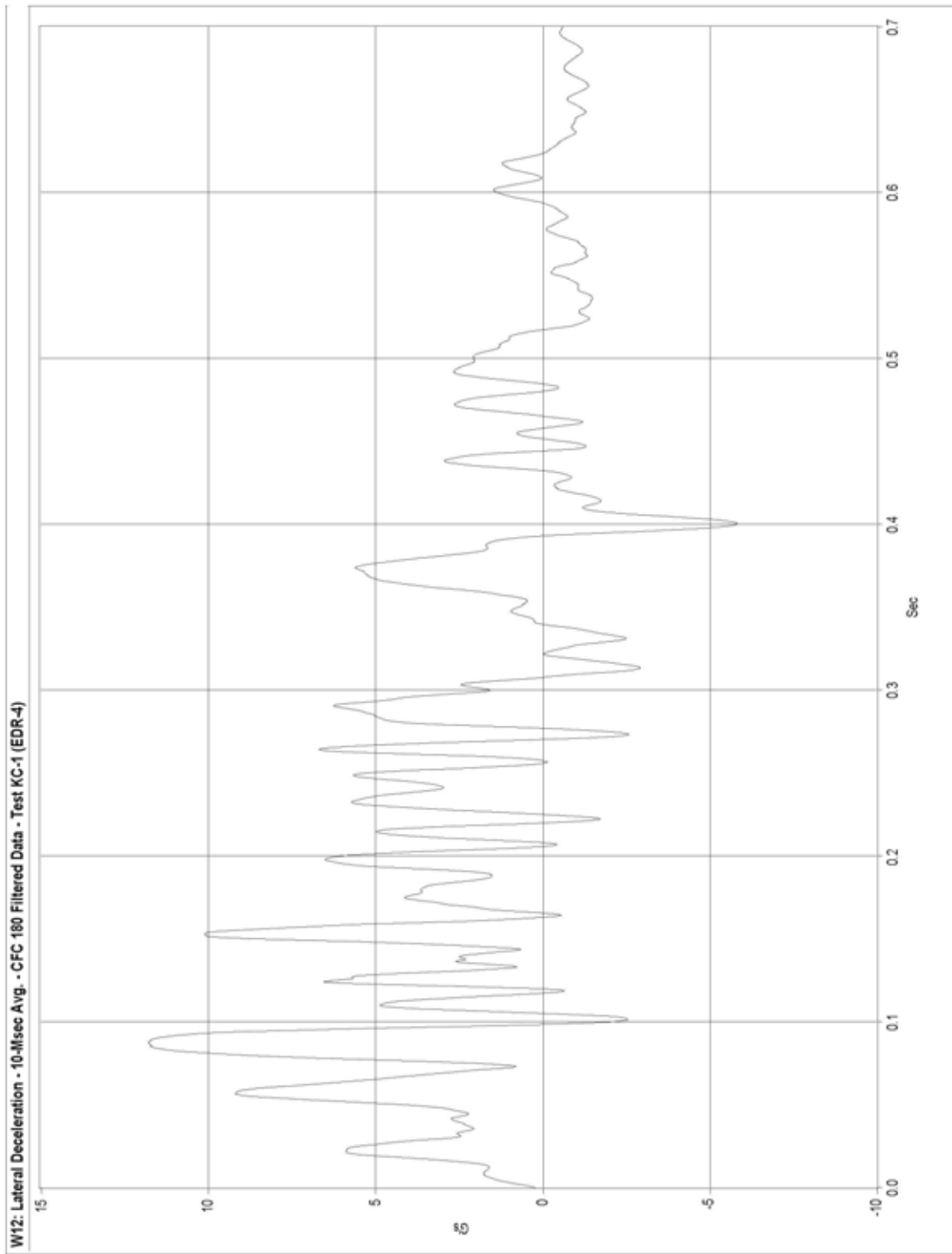


Figure F-4. Graph of Lateral Deceleration, Test KC-1



Figure F-5. Graph of Lateral Occupant Impact Velocity, Test KC-1

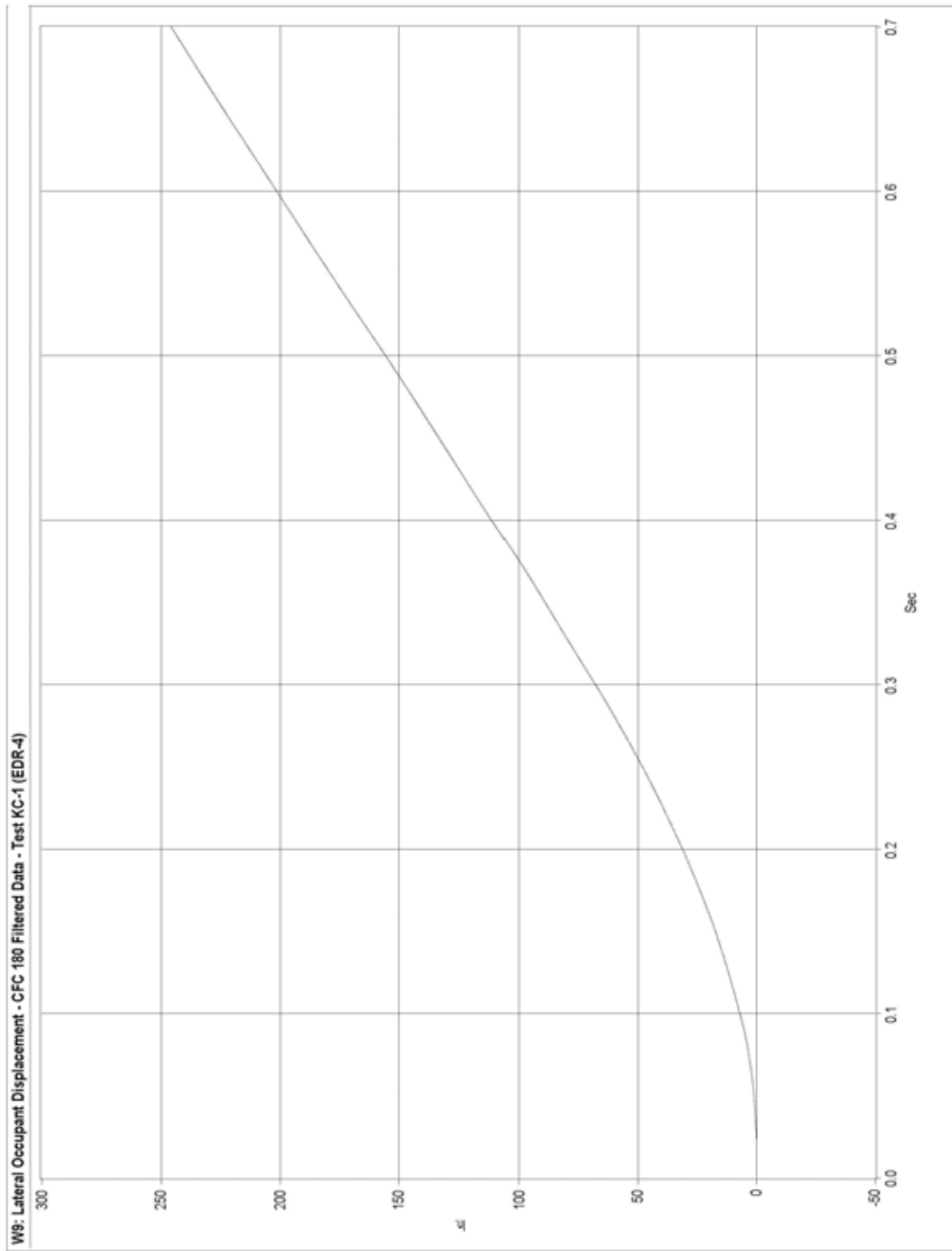


Figure F-6. Graph of Lateral Occupant Displacement, Test KC-1

APPENDIX G

Rate Transducer Data Analysis, Test KC-1

Figure G-1. Graph of Roll, Pitch, and Yaw Angular Displacements, Test KC-1

TEST: KC-1, UNCOUPLED ANGULAR DISPLACEMENTS

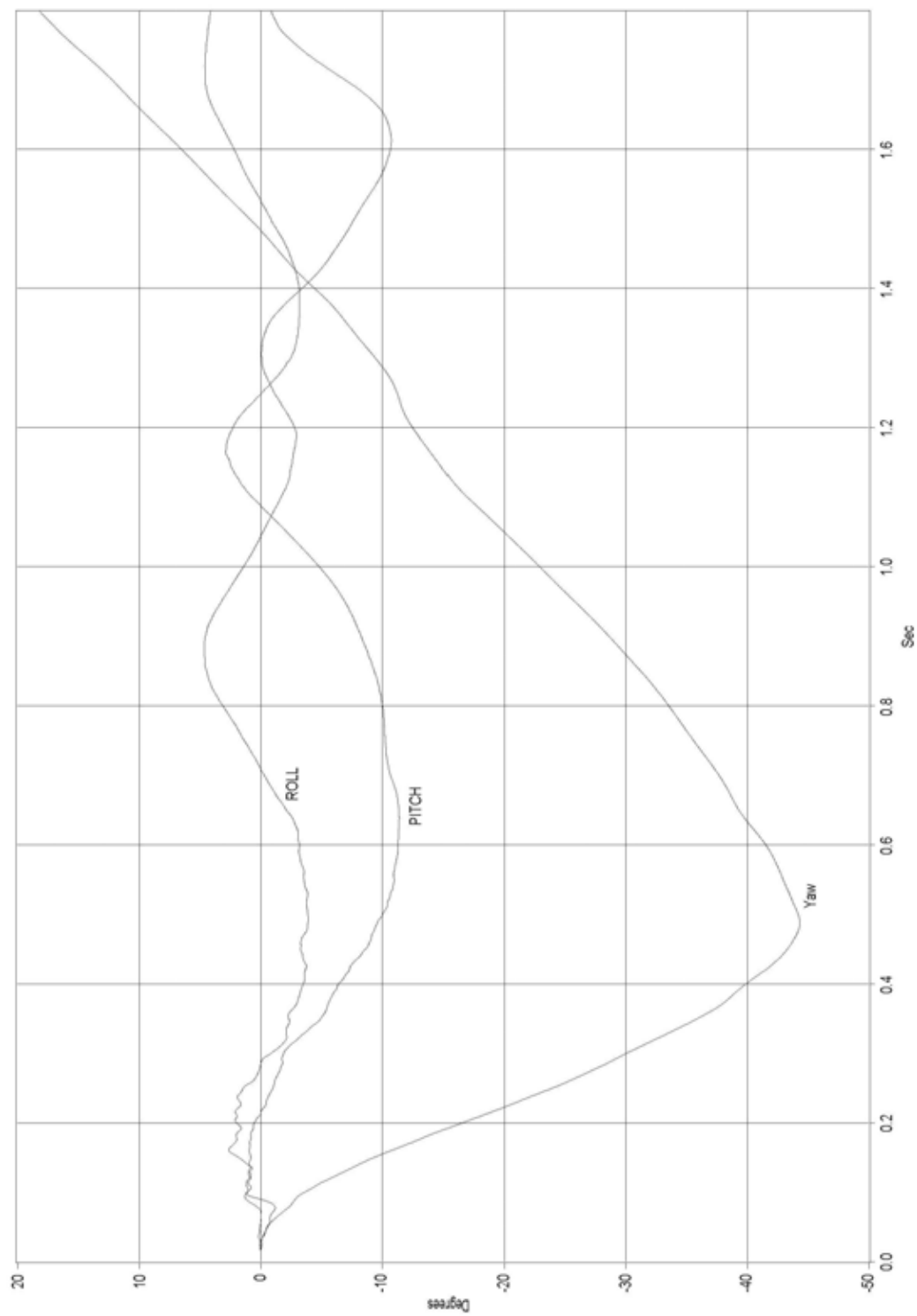


Figure G-1. Graph of Roll, Pitch, and Yaw Angular Displacements, Test KC-1

APPENDIX H

Occupant Compartment Deformation Data, Test KC-2

Figure H-1. Occupant Compartment Deformation Data, Test KC-2

VEHICLE PRE/POST CRUSH INFO

TEST: KC-2
VEHICLE: 1994/CHEVY/2500/WHITE

POINT	X	Y	Z	X'	Y'	Z'	DEL X	DEL Y	DEL Z
1	2	54.25	3	2	54	5	0	-0.25	2
2	9	56.5	1.5	8.75	56.25	4	-0.25	-0.25	2.5
3	14.25	58.25	1	14	57	3	-0.25	-1.25	2
4	19.75	60.75	0	18.25	59.75	1.5	-1.5	-1	1.5
5	24.25	59.25	0.75	22.75	56.75	2	-1.5	-2.5	1.25
6	29.75	58	1.5	28	56.5	2.75	-1.75	-1.5	1.25
7	4.25	49.5	-0.625	4.25	49.25	2	0	-0.25	2.625
8	10	53.25	-3.75	9.25	52.5	-1.25	-0.75	-0.75	2.5
9	15.5	53.75	-5	14.5	53.25	-3	-1	-0.5	2
10	21.5	55.5	-4	20.75	54.75	-2.5	-0.75	-0.75	1.5
11	29	54	-4.75	27.75	52.5	-2.75	-1.25	-1.5	2
12	0.5	41.5	-1	0.5	41.5	-1.5	0	0	-0.5
13	7.5	42.75	-1.5	7.75	42.5	-1.25	0.25	-0.25	0.25
14	13.5	45.5	-6.75	13	45.25	-4.5	-0.5	-0.25	2.25
15	23.25	45.75	-6.75	22.75	45.75	-5.75	-0.5	0	1
16	30.75	46.25	-7.75	30	45.75	-7.75	-0.75	-0.5	0
17	1	34.75	-1.5	1	34.5	-1	0	-0.25	0.5
18	9.25	36.5	-5	9.25	36	-2.5	0	-0.5	2.5
19	16.75	36.75	-6.5	16.25	36	-4.5	-0.5	-0.75	2
20	24.75	35.75	-6.75	24.75	35.75	-6	0	0	0.75
21	30.75	34.75	-8.5	30.5	34.5	-8.25	-0.25	-0.25	0.25
22	5	26.5	-2.125	4.75	26.25	0	-0.25	-0.25	2.125
23	17.25	26.5	-5.75	17.5	26.5	-4	0.25	0	1.75
24	22.5	31	1	32.5	29.75	2	10	-1.25	1
25	15	18.5	-6	15	18.25	-4.5	0	-0.25	1.5
26	3	49	22.5	3	47	23.5	0	-2	1
27	12	48.75	22.25	12	47	23	0	-1.75	0.75
28	24.25	46.75	21.5	24.5	45	22.75	0.25	-1.75	1.25
29									
30									

ORIENTATION AND REFERENCE INFO

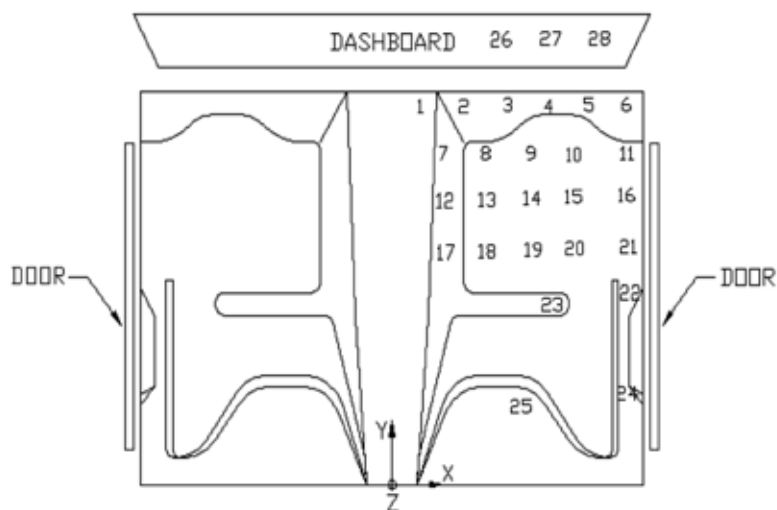


Figure H-1. Occupant Compartment Deformation Data, Test KC-2

APPENDIX I

Accelerometer Data Analysis, Test KC-2

Figure I-1. Graph of Longitudinal Deceleration, Test KC-2

Figure I-2. Graph of Longitudinal Occupant Impact Velocity, Test KC-2

Figure I-3. Graph of Longitudinal Occupant Displacement, Test KC-2

Figure I-4. Graph of Lateral Deceleration, Test KC-2

Figure I-5. Graph of Lateral Occupant Impact Velocity, Test KC-2

Figure I-6. Graph of Lateral Occupant Displacement, Test KC-2

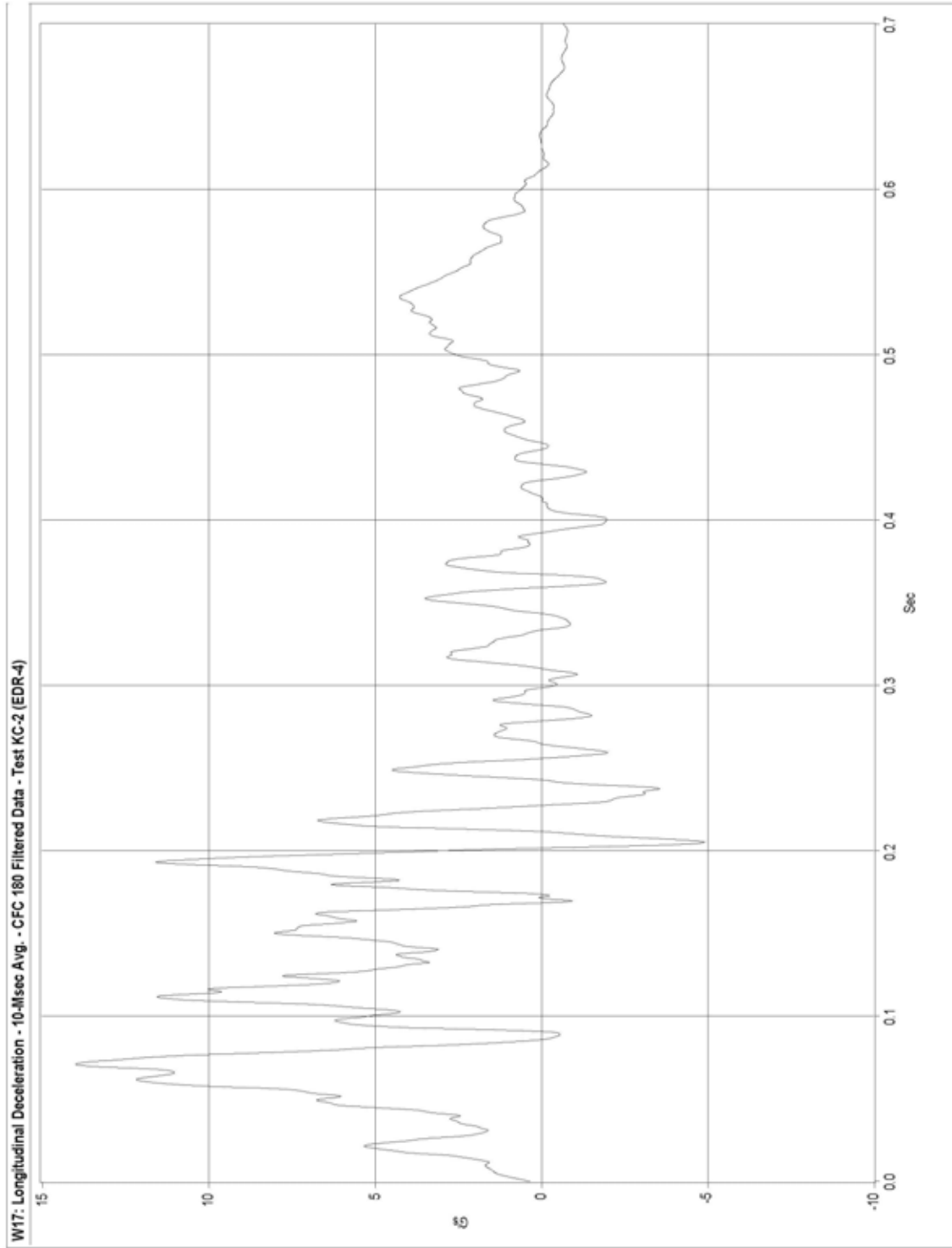


Figure I-1. Graph of Longitudinal Deceleration, Test KC-2

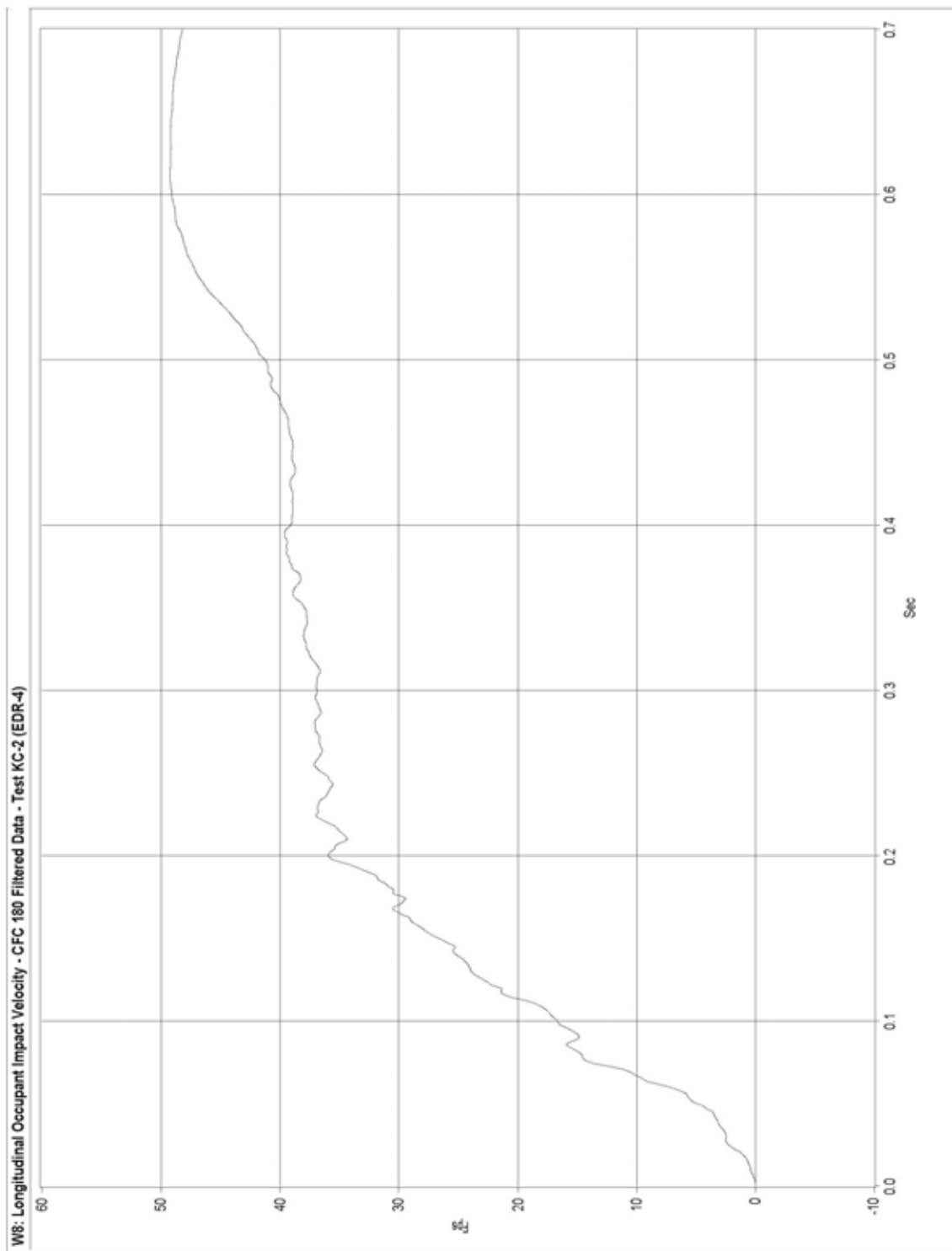


Figure I-2. Graph of Longitudinal Occupant Impact Velocity, Test KC-2

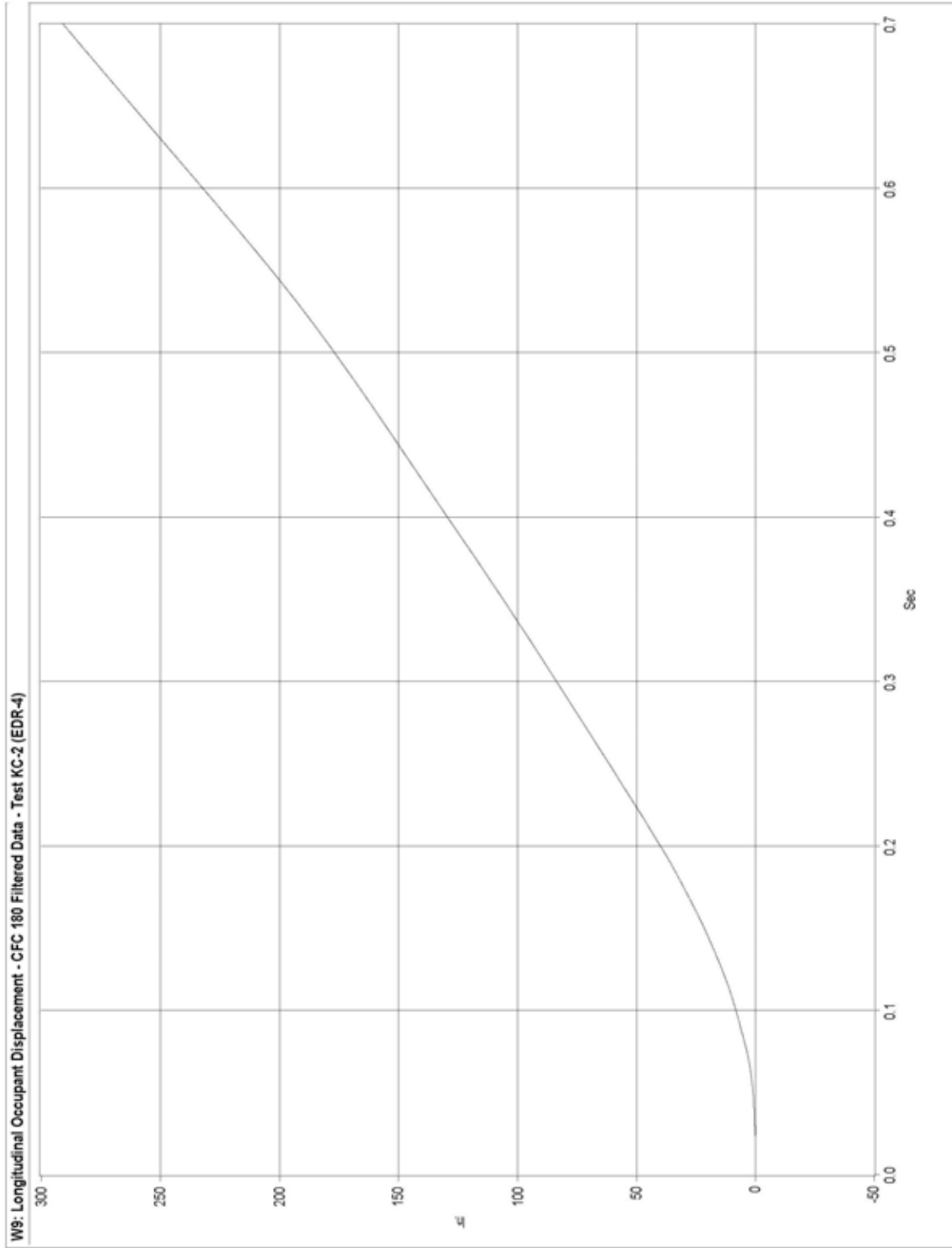


Figure I-3. Graph of Longitudinal Occupant Displacement, Test KC-2

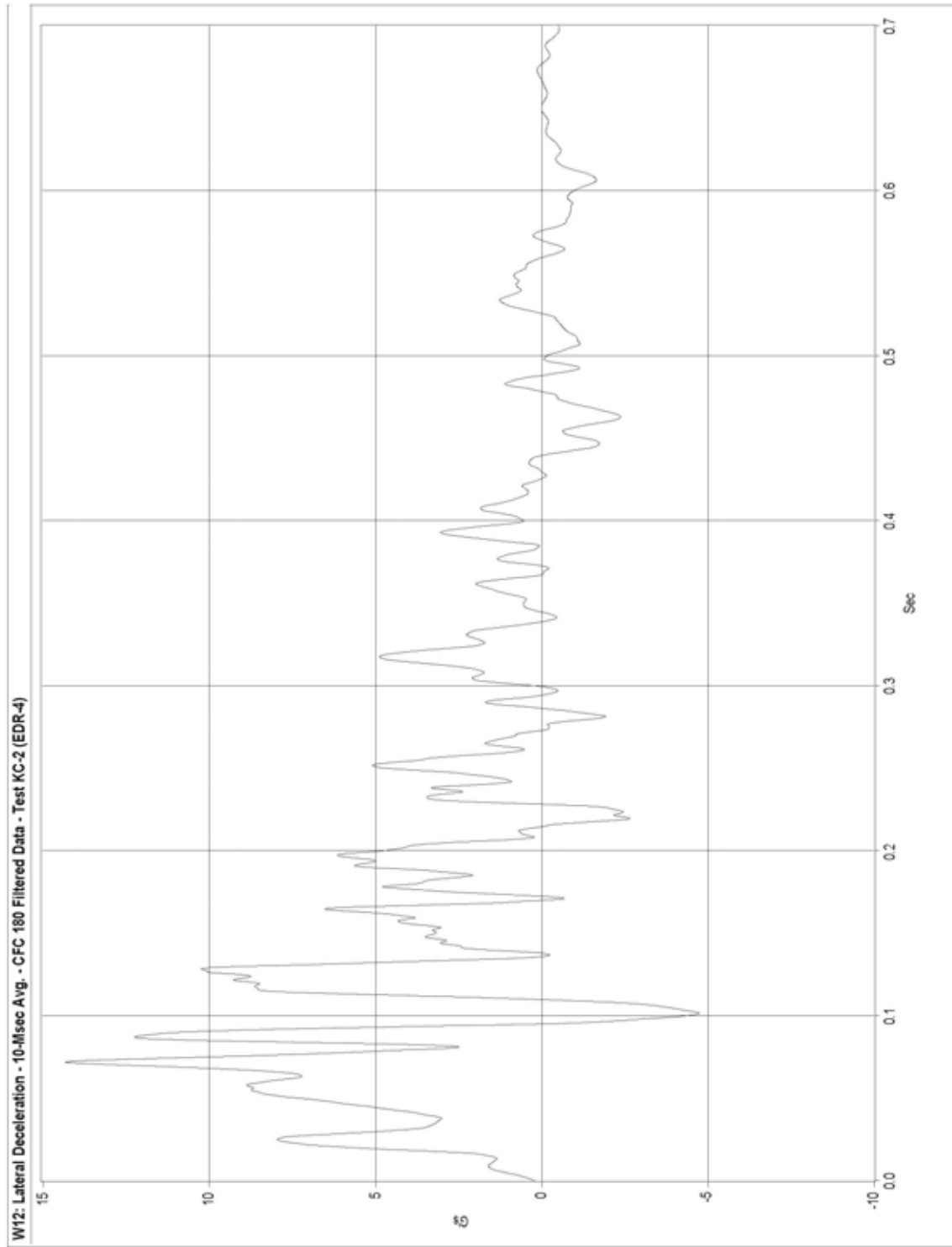


Figure I-4. Graph of Lateral Deceleration, Test KC-2

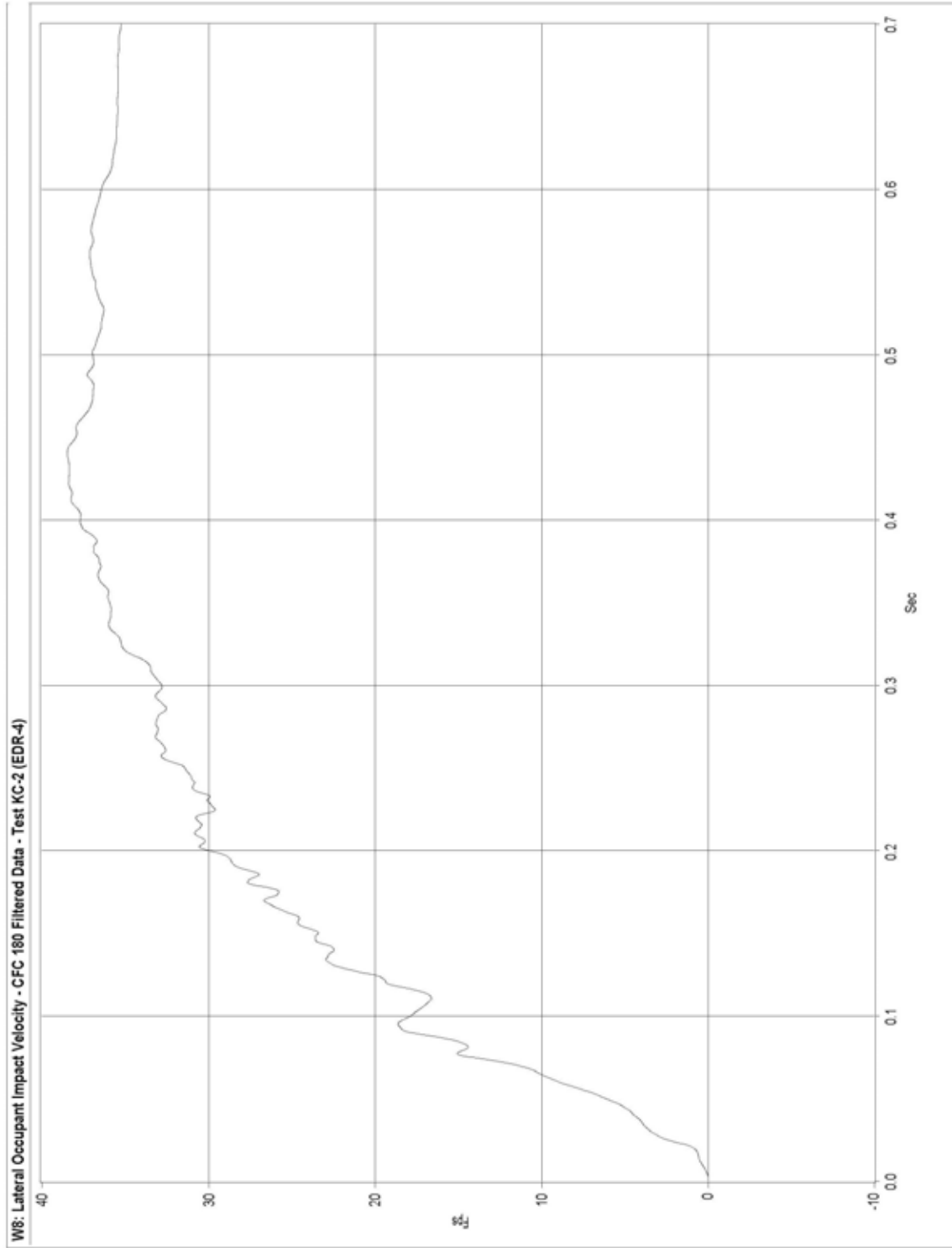


Figure I-5. Graph of Lateral Occupant Impact Velocity, Test KC-2

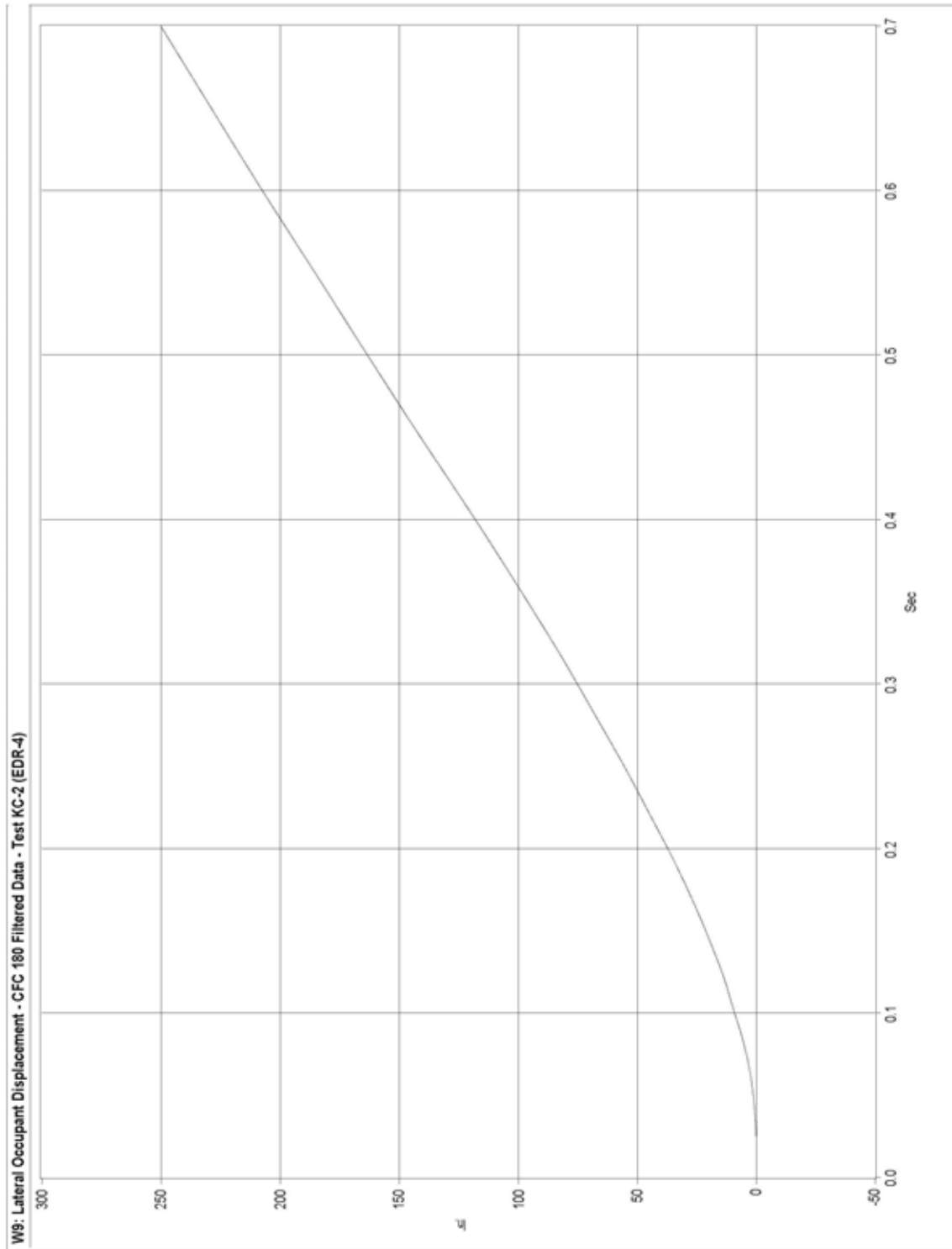


Figure I-6. Graph of Lateral Occupant Displacement, Test KC-2

APPENDIX J

Rate Transducer Data Analysis, Test KC-2

Figure J-1. Graph of Roll, Pitch, and Yaw Angular Displacements, Test KC-2

TEST: KC-2, UNCOUPLED ANGULAR DISPLACEMENTS

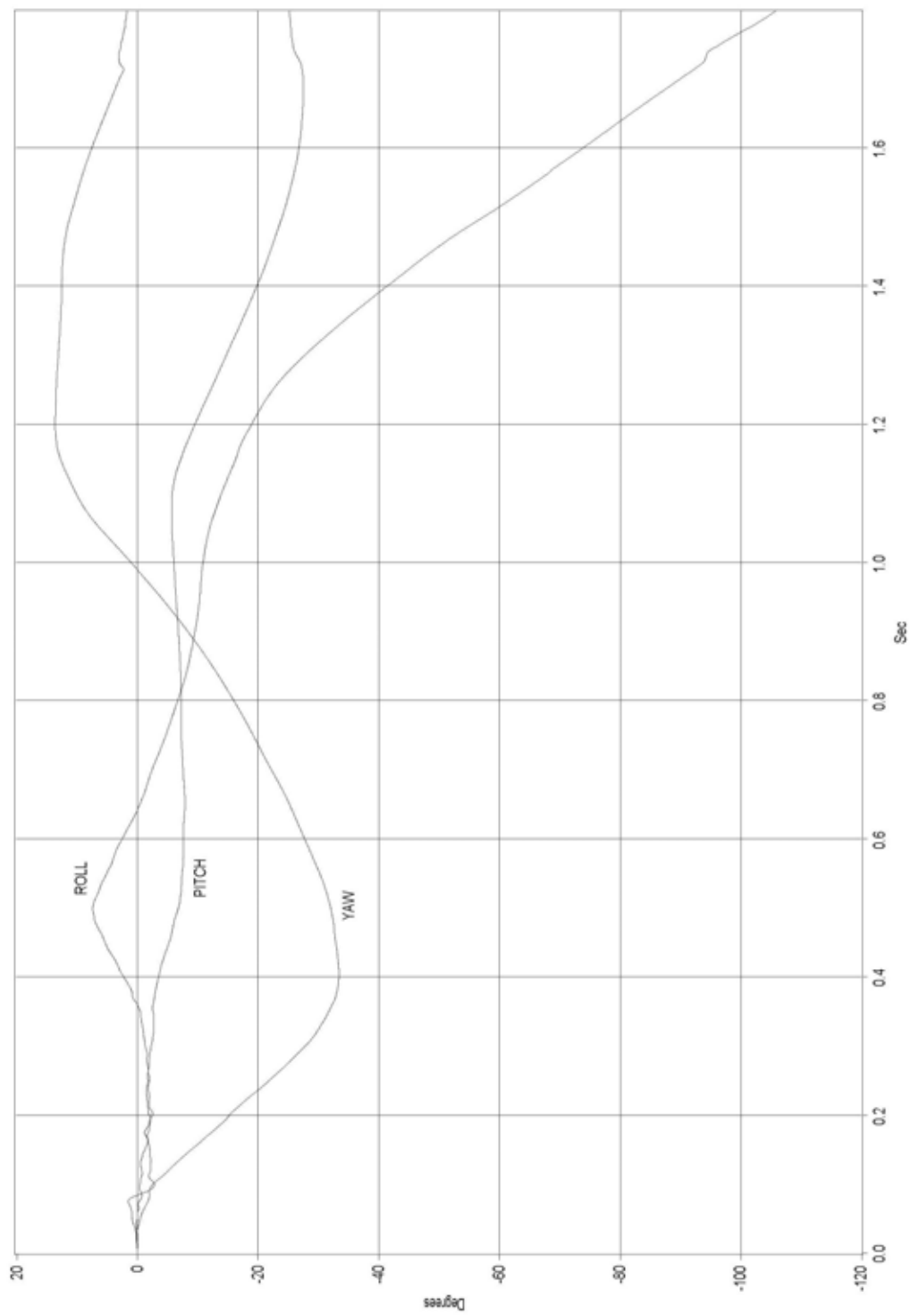


Figure J-1. Graph of Roll, Pitch, and Yaw Angular Displacements, Test KC-2

APPENDIX K

Accelerometer Data Analysis Comparison, Tests KC-1 and KC-2

Figure K-1. Comparison Graph of Longitudinal Decelerations, Tests KC-1 and KC-2

Figure K-2. Comparison Graph of Lateral Decelerations, Tests KC-1 and KC-2

Figure K-3. Comparison Graph of Vertical Decelerations, Tests KC-1 and KC-2

Figure K-4. Comparison Graph of Resultant Decelerations, Tests KC-1 and KC-2

Figure K-5. Comparison Graph of Longitudinal Velocity Change, Tests KC-1 and KC-2

Figure K-6. Comparison Graph of Lateral Velocity Change, Tests KC-1 and KC-2

Figure K-7. Comparison Graph of Vertical Velocity Change, Tests KC-1 and KC-2

Longitudinal Decelerations

SAE CFC 60 (100 Hz) Filter

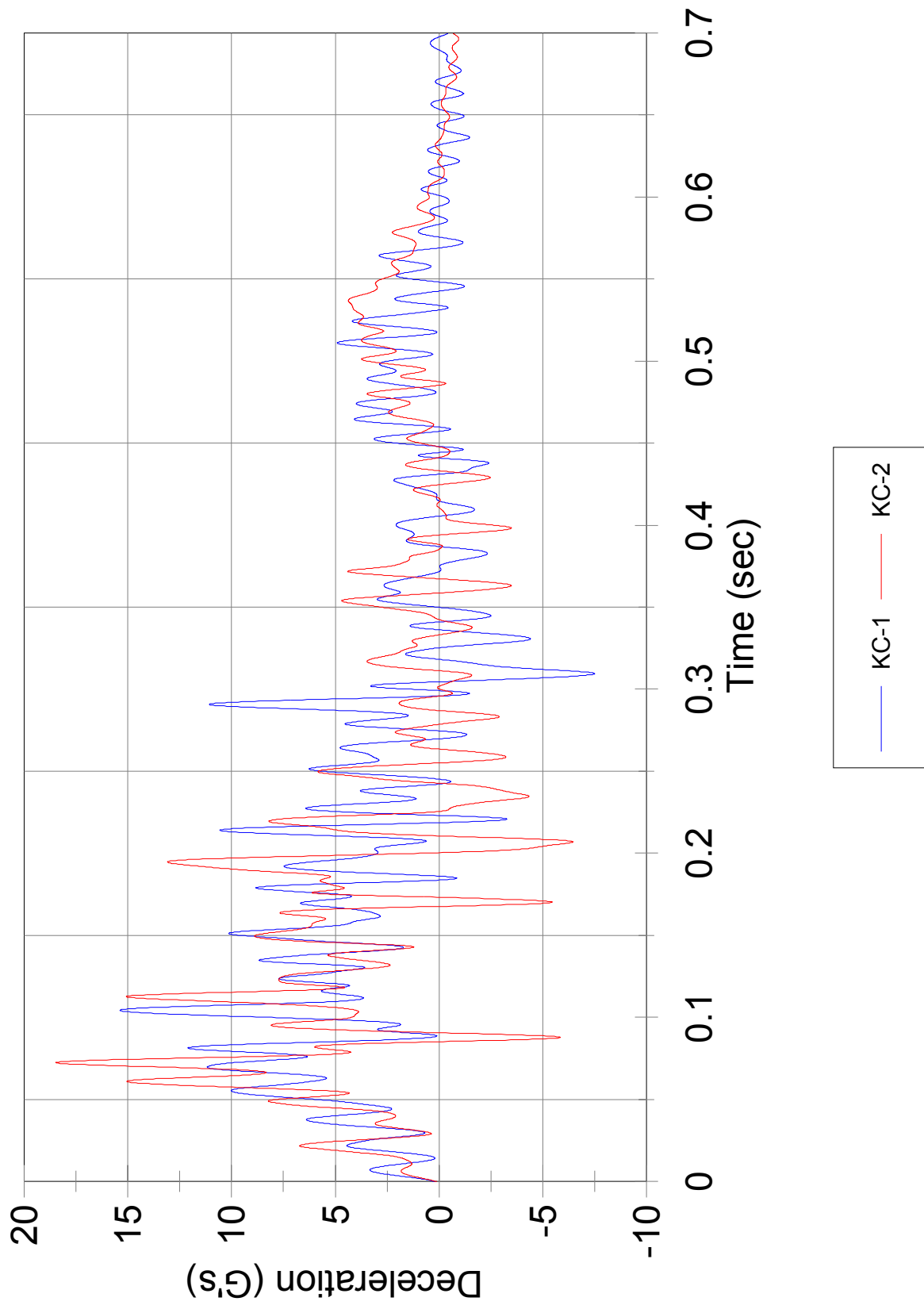


Figure K-1. Comparison Graph of Longitudinal Decelerations, Tests KC-1 and KC-2

Lateral Decelerations SAE CFC 60 (100 Hz) Filter

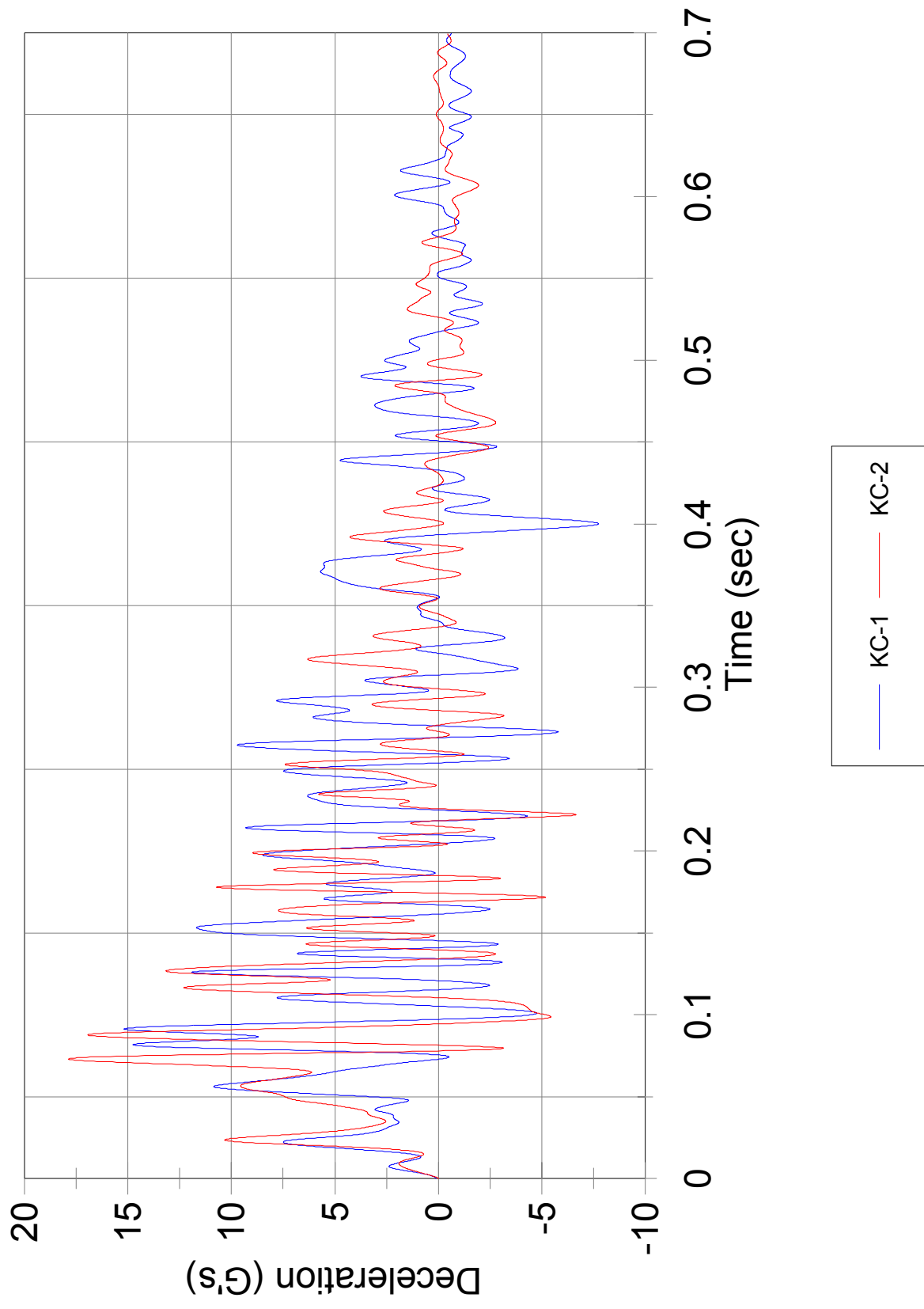


Figure K-2. Comparison Graph of Lateral Decelerations, Tests KC-1 and KC-2

Vertical Decelerations SAE CFC 60 (100 Hz) Filter

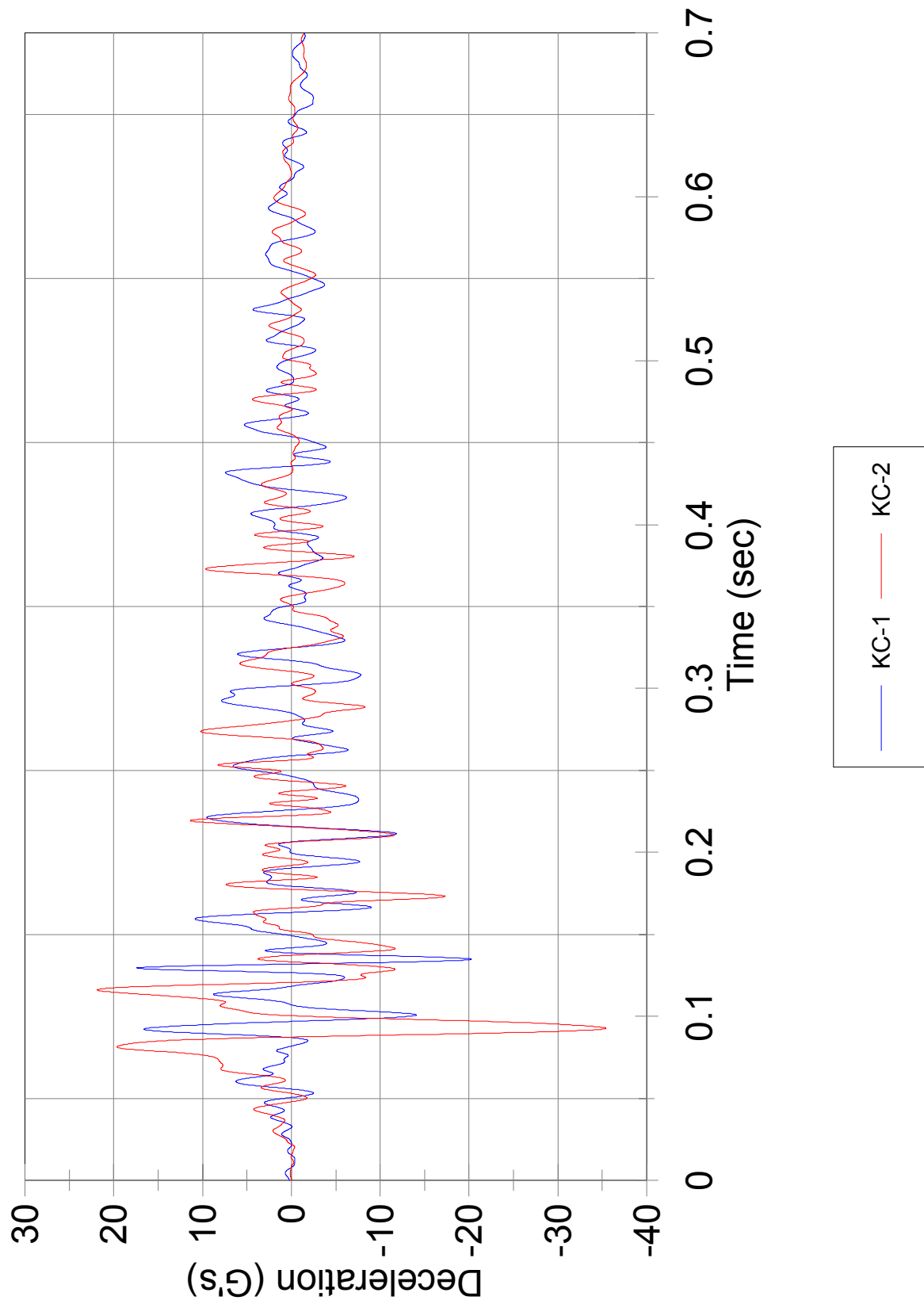


Figure K-3. Comparison Graph of Vertical Decelerations, Tests KC-1 and KC-2

Resultant Decelerations SAE CFC 60 (100 Hz) Filter

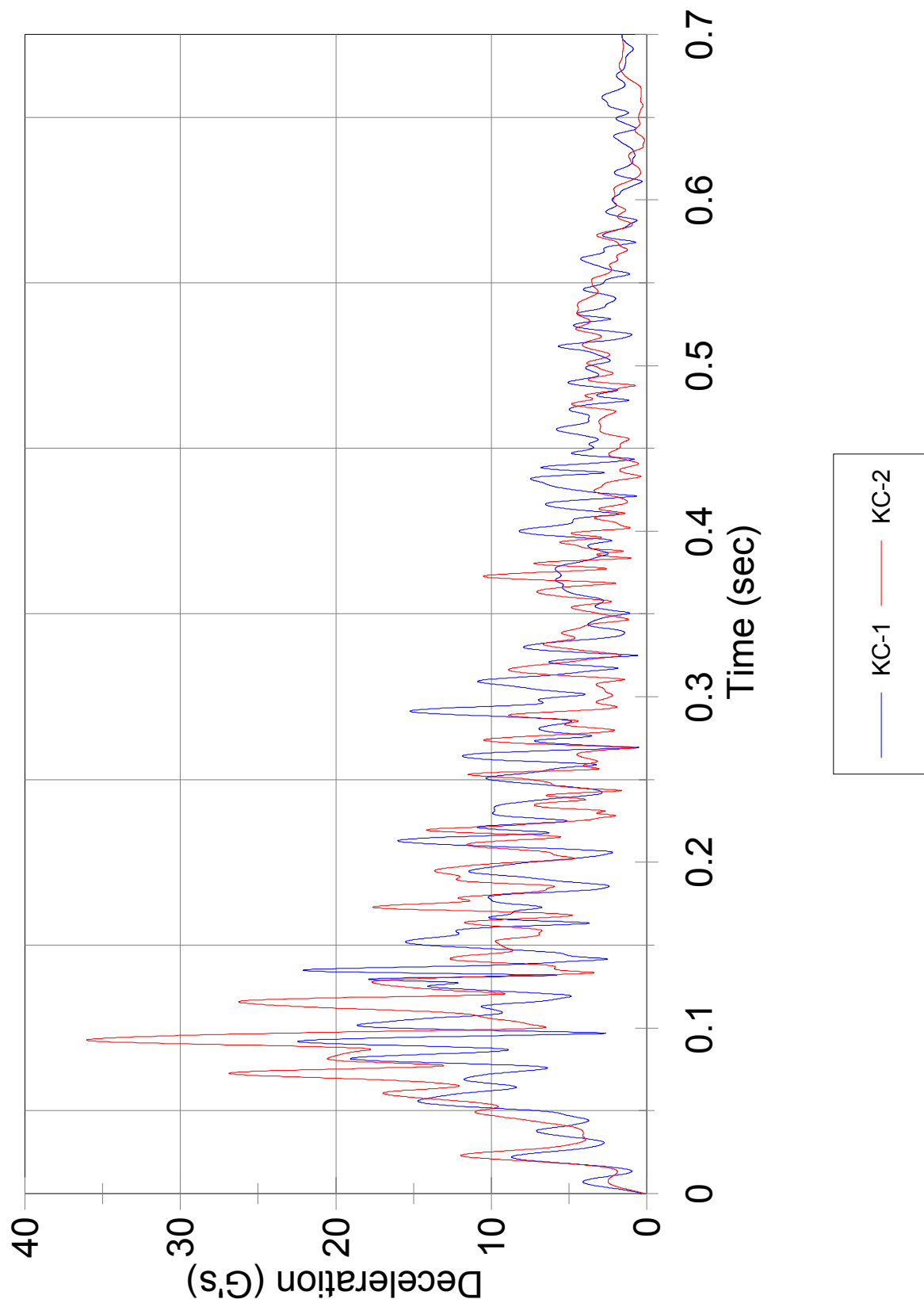


Figure K-4. Comparison Graph of Resultant Decelerations, Tests KC-1 and KC-2

Longitudinal Velocity Change SAE CFC 180 (300 Hz) Filter

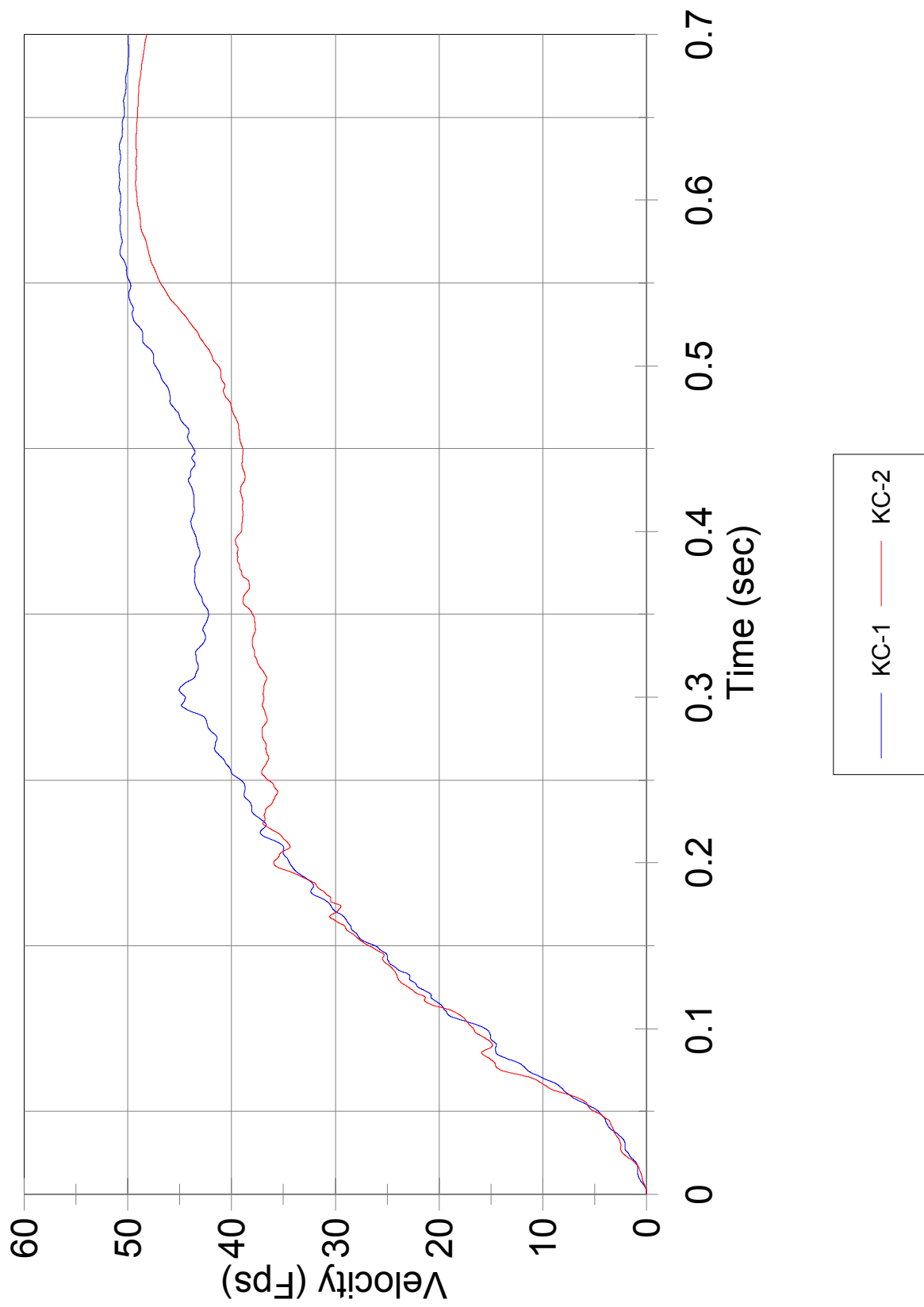


Figure K-5. Comparison Graph of Longitudinal Velocity Change, Tests KC-1 and KC-2

Lateral Velocity Change SAE CFC 180 (300 Hz) Filter

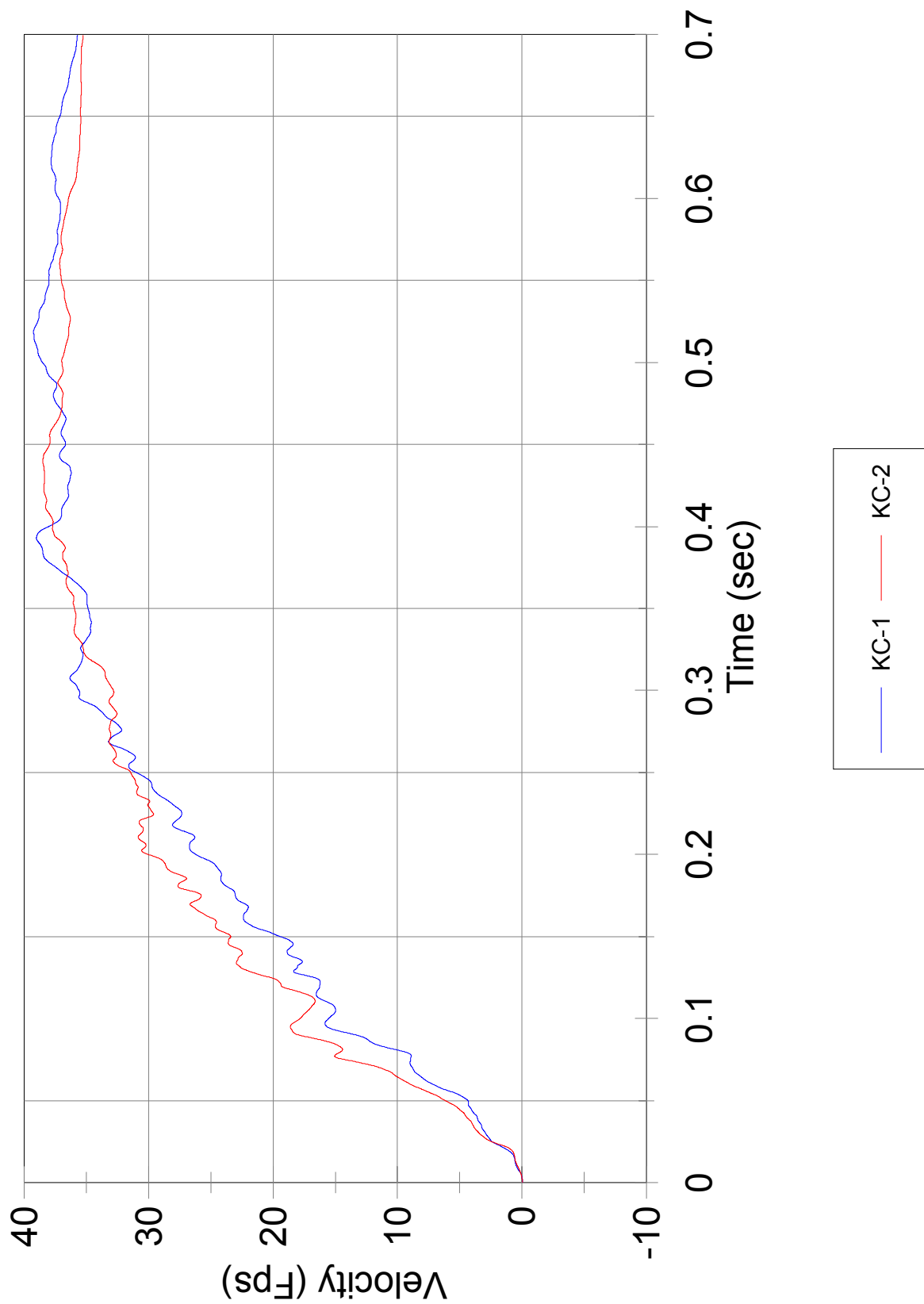


Figure K-6. Comparison Graph of Lateral Velocity Change, Tests KC-1 and KC-2

Vertical Velocity Change SAE CFC 180 (300 Hz) Filter

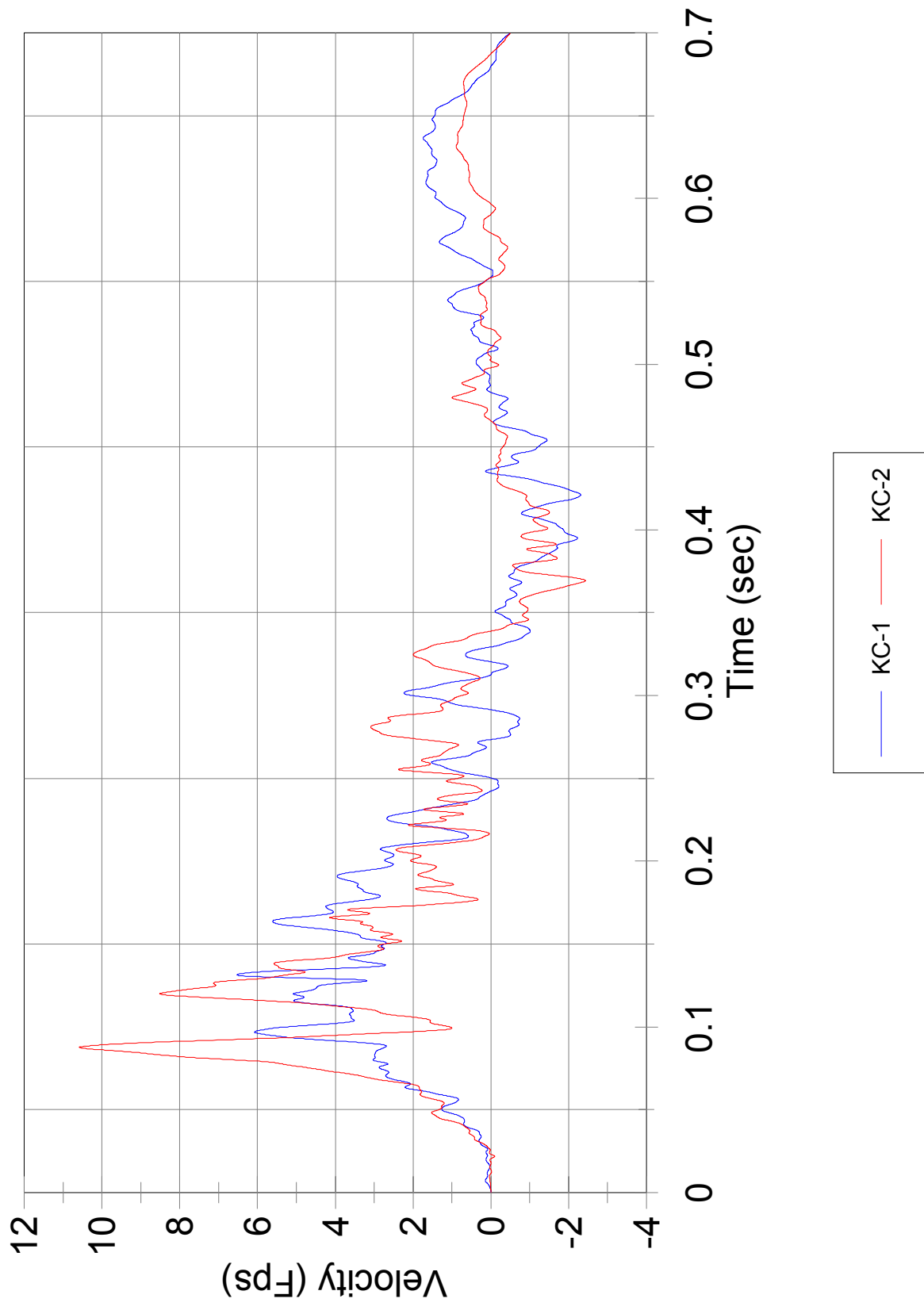


Figure K-7. Comparison Graph of Vertical Velocity Change, Tests KC-1 and KC-2

APPENDIX L

Rate Transducer Data Analysis Comparison, Tests KC-1 and KC-2

Figure L-1. Comparison Graph of Roll, Pitch, and Yaw Angular Displacements,
Tests KC-1 and KC-2

TEST: KC COMPARISON, UNCOUPLED ANGULAR DISPLACEMENTS

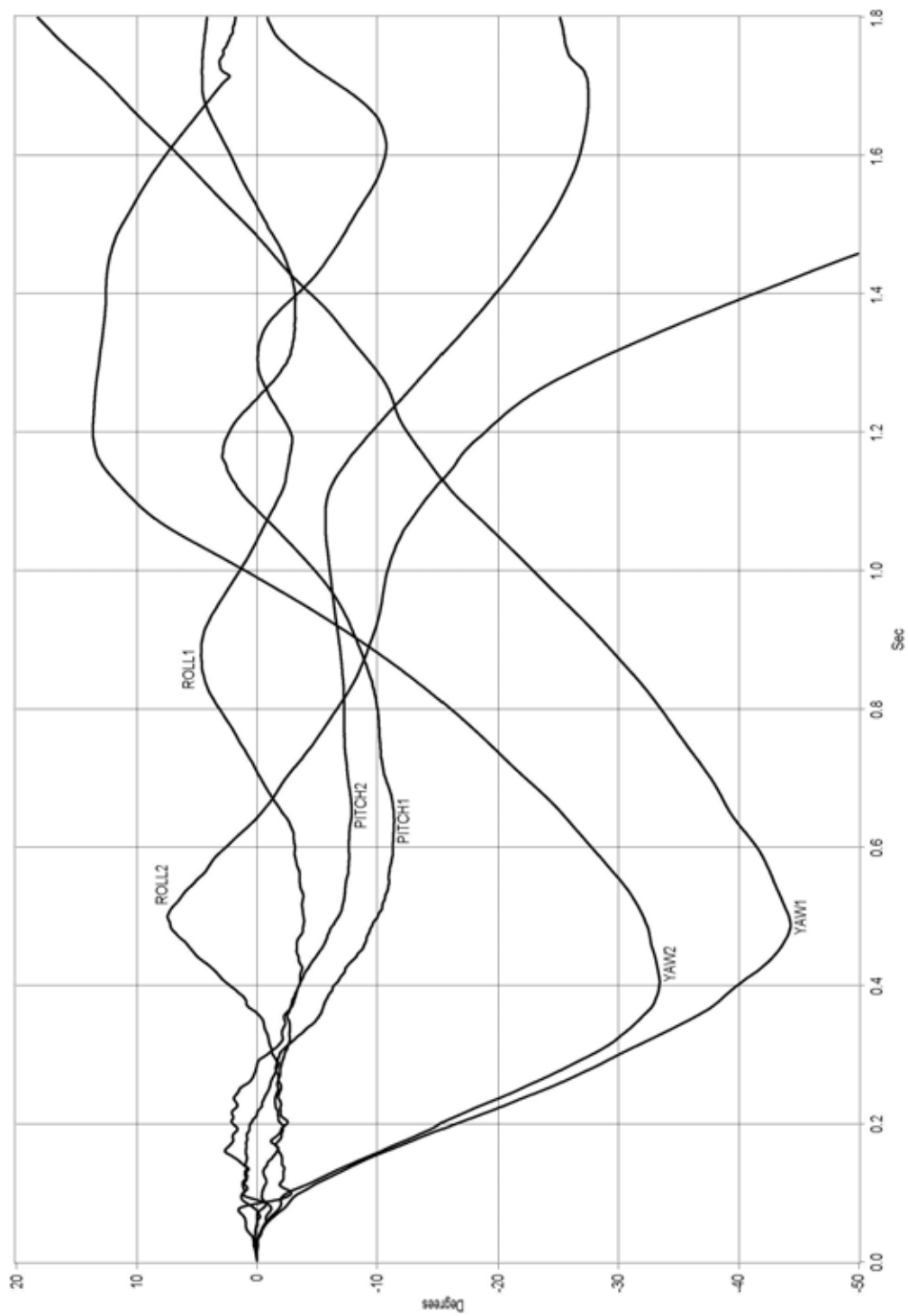


Figure L-1. Comparison Graph of Roll, Pitch, and Yaw Angular Displacements, Tests KC-1 and KC-2